

**Charles University in Prague,
Faculty of Medicine in Hradec Králové**



**10th INTERNATIONAL MEDICAL
POSTGRADUATE CONFERENCE**

New Frontiers in the Research of PhD Students
Conference of Medical Schools

21-22 November, 2013

Organized by
Charles University in Prague, Faculty of Medicine in Hradec Králové

Supported by
Specific Research Projekt 266905/2013

Under the auspices of his Magnificence,
Rector of the Charles University in Prague
Prof. RNDr. Václav Hampl, DrSc.

Hradec Králové
Educational Centre of the Faculty of Medicine,
location: University Hospital

Table of content

General Information	5
Dean's Welcome	6
Programme Overview	7
Scientific Programme	8
Evaluation Committee	11
Presentations	12
Author's Index	115

Organizing committee

Prof. MUDr. RNDr. Miroslav Červinka, CSc.
Prof. MUDr. Vladimír Palička, CSc., dr. h. c.
Ing. Miloslava Paterová

Editor:
prof. MUDr. RNDr. Miroslav Červinka, CSc.

Technical assistance:
Ing. Miloslava Paterová

The publication has undergone neither linguistic editing nor proof reading.
It is printed from the author's e-mail correspondence.

GENERAL INFORMATION

Venue:

Educational Centre (Výukové centrum)
Charles University, Faculty of Medicine
University Hospital (Fakultní nemocnice)
Hradec Králové

Conference office:

The conference office is to be set up for information
and registration at the Educational Centre
in the University Hospital at the following opening hours:

Thursday, 21 November 9.30 - 17.00
Friday, 22 November 8.00 - 14.00

Official language:

English

Presentation time:

Lecture 15 min
Discussion 5 min

Accommodation of participants:

Hotel Nové Adalbertinum
Velké náměstí 32
500 03 Hradec Králové 2

WELCOME



Dear friends and colleagues,

I would like to welcome you to the 10th International Medical Postgraduate Conference in Hradec Králové. The conference has been progressing well since its inception, and over the years it has turned into a real international meeting. We are proud to welcome participants not only from the Czech and Slovak Republics, but also from Austria, Croatia, Georgia, Germany, Hungary, Poland, Portugal and the United Kingdom. I personally believe that the position of this conference is well established and it is a standard part of our activities.

The first obvious reason for this conference is the opportunity to compare achieved results, to present one's own data and learn from others. Nevertheless, we consider this particular meeting of postgraduate students in biomedicine also very important for the international harmonization of PhD studies in the European area. This harmonization is currently one of the most important goals of several international organisations, with ORPHEUS (Organisation for PhD Education in Biomedicine Health Sciences in the European System) being one of the dominant players in this area. We are proud to be an active partner in this endeavor.

Another important reason for organizing this meeting is the opportunity for direct personal contacts. Nowadays, the electronic world is overloaded with information. You can find all the latest news, the latest publications, hypotheses and scientific results at various websites. However, this also means that an essential human quality of scientific communication is disappearing. Actually, each piece of information is more valuable if it is accompanied by a personal point of view, a direct contact or a personal acquaintance. Personal contacts open the world not only to electronic data but also to direct statements, open discussions and publications filled with personal experience.

Dear participants, take advantage of this occasion not only to learn the news in other medical fields but also to think about the bits of knowledge in other medical areas which can be valuable for you and your postgraduate work. Though there is only "one medicine", the mutual overlapping of its disciplines can result in great benefits for all.

Those of you evaluated as the best by an expert panel of judges will receive a financial award, yet this should be considered secondary. I am convinced that the idea of our meeting is similar to the idea behind the Olympic Games – winning is not the most important thing. Taking part, learning scientific news, and above all meeting new colleagues and friends is of the utmost importance. If we succeed in this, the conference has fulfilled its purpose.

I wish you all the best!

Prof. MUDr. RNDr. Miroslav Červinka, CSc.
Dean, Faculty of Medicine in Hradec Králové
Charles University in Prague

PROGRAMME OVERVIEW

Thursday - November 21, 2013

10.00-10.40	Meeting of the Evaluation Committee	Seminar room 4
10.40-11.00	Opening of the Conference	Main lecture hall
11.00-12.40	Presentations I (1-5)	Main lecture hall
12.40-13.40	Lunch	Seminar room 1
13.40-15.20	Presentations II (6-10)	Main lecture hall
15.20-15.40	Coffee break	Seminar room 1
15.40-17.20	Presentations III (11-15)	Main lecture hall
20.00	Social dinner	

Friday - November 22, 2013

9.00-10.40	Presentations IV (16-20)	Main lecture hall
10.40-11.00	Coffee break	Seminar room 1
11.00-12.40	Presentations V (21-25)	Main lecture hall
12.40-13.40	Lunch	Seminar room 1
13.40-15.20	Presentations VI (26-30)	Main lecture hall
15.20-16.20	Meeting of the Evaluation Committee	Seminar room 4
19.30-23.00	Social evening, Awards, Closing ceremony	Medical Library - Portico hall

SCIENTIFIC PROGRAMME

THURSDAY, 21 NOVEMBER

Part I

Chair: Doc. MUDr. Martina Řezáčová, Ph.D.

- 11.00 M. Blekić (Zagreb): POLYMORPHISMS IN 17q12-21 ARE ASSOCIATED WITH ASTHMA EXACERBATION AND LUNG FUNCTION IN ASTHMATIC CHILDREN
- 11.20 I. Erjavec (Zagreb): EFFECT OF BLOOD SEROTONIN LEVELS ON FOUR MONTHS OLD FEMALE RAT SKELETON
- 11.40 A. Farkašová (Martin): DETECTION OF ALK GENE REARRANGEMENT IN NON-SMALL CELL LUNG CARCINOMA BY FLUORESCENCE IN SITU HYBRIDIZATION
- 12.00 J. Fontana (Praha): DO GLUCAGON-LIKE PEPTIDE - 1 ANALOGUES AFFECT EARLY PHASE OF LIVER REGENERATION AFTER PARTIAL HEPATECTOMY IN RATS?
- 12.20 I. Heřmanová (Praha) A NOVEL INSIGHT INTO THE EFFECT OF L-ASPARAGINASE ON LEUKAEMIC CELLS

Part II

Chair: Prof. MUDr. Zuzana Červinková, CSc.

- 13.40 G. Horváth (Pécs): THE EFFECTS OF ENRICHED ENVIRONMENT ON THE NEUROBEHAVIORAL DEFICITS INDUCED BY GLUTAMATE TOXICITY IN RATS
- 14.00 E. Janoušová (Brno): A NOVEL METHOD FOR COMPUTER AIDED DIAGNOSTICS OF SCHIZOPHRENIA BASED ON MAGNETIC RESONANCE BRAIN IMAGES
- 14.20 L. Jedličková (Košice): CHARACTERISTICS OF PATIENTS WITH CARDIORENAL SYNDROME ADMITTED TO OUR DEPARTMENT
- 14.40 H. Kratochvílová (Praha) MITOCHONDRIAL MEMBRANE ASSEMBLY AND MULTIPLE FORMS OF TMEM70 PROTEIN
- 15.00 J. Křivánek (Brno): DIFFERENTIATION OF NEURAL CREST CELLS FROM HUMAN EMBRYONIC STEM CELLS AND THEIR ODONTOGENIC INDUCTION

SCIENTIFIC PROGRAMME

Part III

Chair: Prof. MUDr. Milan Bayer, CSc.

- 15.40 T. Kupsa (Hradec Králové): EVALUATION OF SERUM LEVELS OF MULTIPLE CYTOKINES AND ADHESION MOLECULES IN PATIENTS TREATED FOR ACUTE MYELOID LEUKEMIA
- 16.00 L. Láníková (Olomouc): NOVEL INSIGHTS INTO THE MOLECULAR MECHANISMS OF ACQUIRED AND CONGENITAL POLYCYTHEMIAS
- 16.20 V. Mezera (Hradec Králové): EFFECT OF INCB018424, A JAK1 AND JAK2 INHIBITOR, ON SENEESCENCE PHENOTYPE IN OLD MICE
- 16.40 P. Paulů (Praha): RESISTANCE TO CLOPIDOGREL – ETIOLOGY, MEASUREMENT AND IMPACT ON THE PROGNOSIS OF PATIENTS WITH CORONARY ARTERY DISEASE
- 17.00 D. Pawlica-Gosiewska (Kraków): THE USE OF THE PLASMA LEUCOCYTE ELASTASE, CALPROTECTIN, LACTOFERIN, INTESTINAL FATTY ACID BINDING PROTEIN (I-FABP) AND NEOPTERIN CONCENTRATION IN THE DIAGNOSIS AND ASSESSMENT THE CLINICAL ACTIVITY OF CROHN'S DISEASE AND ULCERATIVE COLITIS

FRIDAY, 22 NOVEMBER

Part IV

Chair: Prof. RNDr. Jan Krejsek, CSc.

- 9.00 J. Pejchal (Hradec Králové): NON-SPECIFIC CHANGES AFTER SOMAN POISONING
- 9.20 B. Pereira (Porto): REGULATION OF CDX2 AND INTESTINAL DIFFERENTIATION IN HOMEOSTASIS AND CARCINOGENESIS: UNVEILING THE ROLE OF THE RNA-BINDING PROTEIN MEX3A
- 9.40 A. Pöpperlová (Plzeň): LOW GDP PERITONEAL DIALYSIS REGIMEN HAS A BENEFICIAL EFFECT ON PLASMA LEVELS OF PROINFLAMMATORY LIGANDS OF RECEPTOR FOR ADVANCED GLYCATION END PRODUCTS
- 10.00 S. Richardson (Liverpool): RESVERATROL, CURCUMIN AND METABOLITES CAN MODULATE CYTOKINE RELEASE BY JURKAT T-LYMPHOCYTES
- 10.20 B. Šalovská (Hradec Králové): RADIO-SENSITIZATION OF HUMAN LEUKEMIC CELLS HL-60 BY ATR-KINASE INHIBITOR (VE-821): PHOSPHOPROTEOMIC ANALYSIS

SCIENTIFIC PROGRAMME

Part V

Chair: Doc. MUDr. RNDr. Milan Kaška, Ph.D.

- 11.00 T. Shatirishvili (Tbilisi): SHORT-TERM OUTCOME OF CONVULSIVE STATUS EPILEPTICUS (CSE) IN CHILDREN: HOSPITAL BASED PROSPECTIVE STUDY
- 11.20 M. Scharffenberg (Dresden): EFFECTS AND MECHANISMS OF INTRINSIC AND EXTRINSIC VARIABLE ASSISTED MECHANICAL VENTILATION IN THE EXPERIMENTAL ACUTE RESPIRATORY DISTRESS SYNDROME (ARDS)
- 11.40 H. Schneider (Dresden): THE IMPACT OF NEUROPILIN-2 ON THE CXCR4/CXCL12 AXIS IN THE FORMATION OF LYMPH NODE METASTASIS IN COLON CANCER
- 12.00 M. M. Sousa (Porto): ELECTROPHYSIOLOGICAL PROPERTIES OF THE PRONOCICEPTIVE DORSAL RETICULAR NUCLEUS
- 12.20 U. Thiem (Vienna): VITAMIN D DEFICIENCY AND ITS POTENTIAL IMPLICATIONS IN RENAL TRANSPLANTATION

Part VI

Chair: Prof. MUDr. Jan Čáp, CSc.

- 13.40 P. Vickerton (Liverpool): TRANSLATION OF BIOMECHANICAL STIMULI IN TO MORPHOLOGICAL AND MICROSCOPIC RESPONSE IN THE RAT TIBIA
- 14.00 O. Vyčítal (Plzeň): TUMOR INFILTRATING LYMPHOCYTES AS PROGNOSTIC FACTOR OF EARLY RECCURENCE AND POOR PROGNOSIS OF COLORECTAL CANCER AFTER RADICAL SURGICAL TREATMENT
- 14.20 K. Agrawal (Olomouc): EPIGENETIC STUDY OF 5-AZACYTIDINE NUCLEOSIDES AND THEIR DERIVATIVES
- 14.40 J. Warszawska (Vienna): LIPOCALIN-2 DEACTIVATES MACROPHAGES AND WORSENS PNEUMOCOCCAL PNEUMONIA OUTCOMES
- 15.00 G. L. Woth (Pécs): PLATELET AND PLATELET-DERIVED MICROPARTICLE STUDIES IN SEVERE SEPSIS

EVALUATION COMMITTEE

Chairperson: **Professor Vladimír Palička**

Vice-Dean for International Relations
Charles University, Faculty of Medicine
Hradec Králové, Czech Republic

Members: **Professor Margarethe Geiger**

Institut of Vascular Biology and Thrombosis Research
Medical University of Vienna
Vienna, Austria

Professor David Gordon

President, Association of Medical Schools in Europe
Faculty of Health Sciences, University of Copenhagen
Copenhagen, Denmark

Professor Zdravko Lacković

Assistant to the dean for doctoral studies, President, ORPHEUS
School of Medicine, University of Zagreb
Zagreb, Croatia

Dr. Thorsten Liebers

Coordinator of scientific large-scale projects
Faculty of Medicine C. G. Carus, University of Technology
Dresden, Germany

Professor Alan Shenkin

Emeritus Professor of Clinical Chemistry
Faculty of Health and Life Sciences, University of Liverpool
Liverpool, Great Britain

Professor Peter Soeters

Emeritus Professor of Surgery
Faculty of Health, Medicine and Life Sciences,
University of Maastricht
Maastricht, the Netherlands

Dr. Andrea Tamás

Department of Anatomy
Medical School, University of Pécs,
Pécs, Hungary

EPIGENETIC STUDY OF 5-AZACYTIDINE NUCLEOSIDES AND THEIR DERIVATIVES

Khushboo Agrawal

E-mail: khushboograwal86@gmail.com

Institute of Molecular and Translational Medicine, Faculty of Medicine and Dentistry,
Palacky University in Olomouc, Czech Republic,
Institute of Organic Chemistry and Biochemistry,
Academy of Sciences of the Czech Republic, Prague

Co-authors: P. Džubák, I. Frydrych, D. Holub, M. Krečmerová, M. Otmar, M. Hajdúch
Tutor: doc. MUDr. Marián Hajdúch, Ph.D.

Introduction

Existence of aberrant DNA methylation remains the major hallmark of cancer. Hypermethylation of gene promoter sequences resulting in transcriptional silencing of tumor suppressor genes has long been explored as a therapeutic target in cancer. Despite significant results *in vitro*, 2'-deoxy-5-azacytidine, an experimental and well characterized drug that has been approved for the treatment of myelodysplastic syndromes develops resistance *in vivo*¹. In the quest for more potent drugs targeting methylation, we have developed a fluorescence based detection system to test the series of compounds for hypomethylation activity with the main focus on 5-azacytidine nucleosides and their derivatives. Furthermore, in the present study, we have taken into account, 2'-deoxy-5-azacytidine (decitabine) to study the mechanism of resistance in human colon cancer cell line.

Methods

Cell culture: The human colon cancer cell line, HCT116, was purchased from American Type Culture Collection and cultured in McCoy's 5A supplemented with 10% fetal bovine serum, 50 µg/ml streptomycin, 100 U/ml penicillin and 3 mM L-glutamine at 37°C and 5% CO₂.

Screening of new epigenetic drugs for hypomethylation activity:

Development of the fluorescence reporter system

To generate the reporter cell line, a targeting vector was constructed where a part of exon 3 of the FLJ32130 gene was replaced by the fusion of IRES, Hygromycin and EGFP². HCT116 cells were transfected with the linearized vector using electroporation and stable transfectants were generated by selection with 500 µg/ml neomycin. To obtain a sensitive detection system, numerous neomycin resistant clones were screened by flow cytometry for the EGFP fluorescence before and after the addition of decitabine. Finally, one clone with expected homologous recombination was isolated and anticipated green fluorescence was confirmed after treatment with 0.5 µM decitabine and no EGFP expression was examined before treatment. To facilitate the high content cellular imaging and continuous visualization of chromosomal degradation in response to the drug, reporter cell line was further transduced with the TagRFP fused with histone H2B using lentiviral system.

High throughput screening

To test the potential candidates for demethylation, the reporter cell line (HCT116-pFLJ-H2B) was seeded at the density of 1.5×10^3 cells per well in 96 well plates. After 24 h, drugs were added. Following the treatment with the drugs, images were captured at every 24 h intervals for 5 days under appropriate wavelengths for EGFP (excitation/emission: 458 nm/525 nm) and RFP (excitation/emission: 555 nm/584 nm) using high content imaging system (Operetta, PerkinElmer). Images were then analyzed using image analysis software (Columbus, PerkinElmer). To monitor the cytotoxic response of the drugs, numbers of cells were counted in each well with the help of TagRFP fused with

histone H2B in the cell nucleus. However, hypomethylation activity of the drugs was analyzed by quantifying the intensity of EGFP fluorescence in each well.

Molecular characterization of HCT116 cells resistant to 5-aza-2'-deoxycytidine:

Development of decitabine resistant HCT116 cells

Early passage HCT116 cells were seeded into two petridishes (A and B) at a density of 1×10^6 cells/10 cm dish. The cells in dish A were initially treated with decitabine at $1x IC_{50}$ concentration (0.28 μ M) which was gradually increased up to $10x IC_{50}$. Cells in dish B were directly exposed to $5x IC_{50}$ concentration, which was further doubled to $10x IC_{50}$. After long term exposure to the drug, three resistant clones were derived from each dish³. MTT based proliferation assay was performed⁴ to confirm the resistance to decitabine and all the six clones thus analyzed exhibited high resistance ($>100x IC_{50}$).

Flow cytometry

Flow cytometry based cellular assays were performed on the HCT116 parental and the resistant clones. To distinguish the cells at different phases of the cell cycle Phospho-Histone H3 staining was done⁵. BrdU and BrU cell proliferation assays were performed subsequently to analyze the cells actively synthesizing DNA and RNA respectively⁶. Furthermore, to investigate the phenomenon of multi-drug resistance, P-glycoprotein (Pgp) expression was analyzed by flow cytometry⁷.

Proteomic analysis

Stable isotope labeling by amino acids in cell culture (SILAC)⁸ was used for the proteome wide analysis. HCT116 parental cells were labeled with heavy Lys-¹³C₆ and Arg-¹³C₆ and mixed with each of the non-labeled resistant cell lines in 1:1 ratio followed by cellular lysis. Each of the SILAC samples were then separated by the preparative gel electrophoresis and subjected to enzymatic digestion. Mass spectrometric analysis was done to quantify the expression of various differentially expressed proteins and the commonly affected pathways were analyzed.

Results

Screening of the new epigenetic drugs: After screening 76 new epigenetic drugs, LEM-789 was identified as the potential candidate for demethylation. Fig.1 show the cytotoxicity and demethylation profile of LEM-789 for 5 days in comparison with decitabine, alpha-DAC and Vidaza available commercially. Moreover, the demethylation activity of LEM-789 was found to be nearly constant from day 1 to day 5 indicating towards the stability of the drug during the treatment.

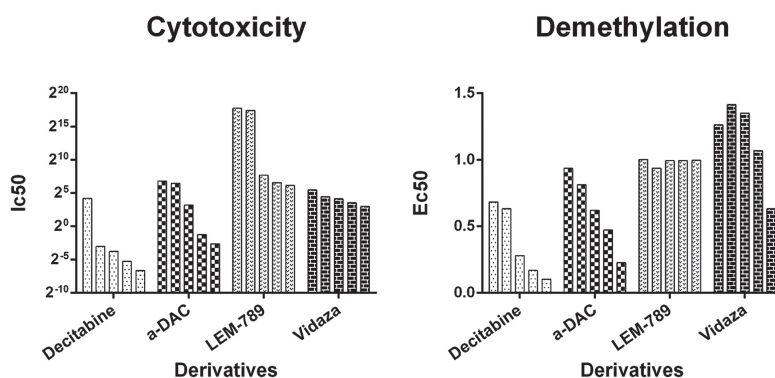


Figure 1. Cytotoxicity and Demethylation profile of epigenetic drugs

Flow cytometric analysis: No significant changes were observed in the distribution of cells at different phases within the cell cycle. However, cell proliferation assays revealed the significant up-regulation of DNA and RNA synthesis in each of the resistant cell lines. In addition, no reproducible changes were observed in the P-glycoprotein (Pgp) expression on comparing parental and the resistant cell lines.

Proteome wide analysis: Mass spectrometry based proteomic analysis identified a total of 4344 proteins with significant reproducible changes. This extensive proteome coverage enabled analysis of a broad range of processes and functions.

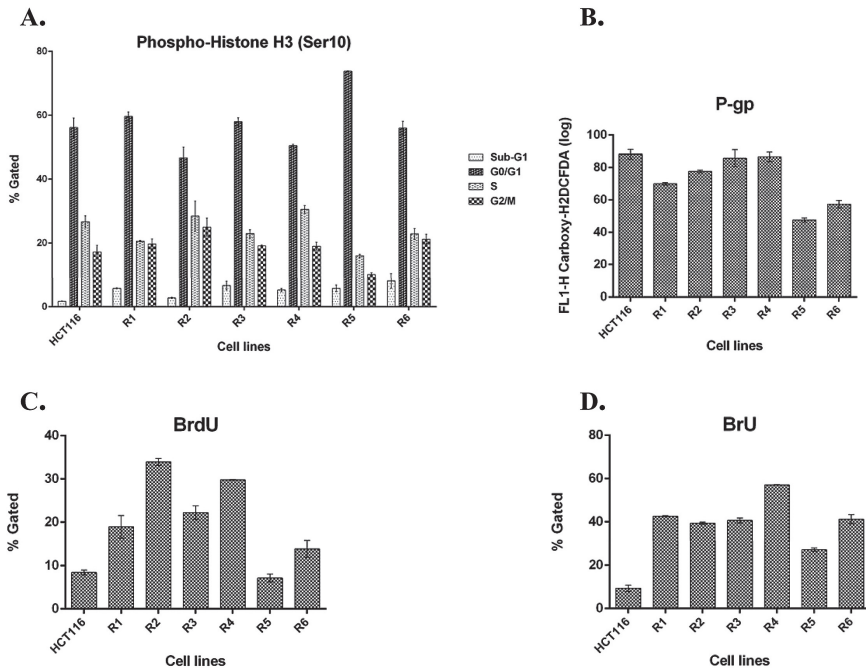


Figure 2. Flow cytometry data for parental (HCT116) and derived resistant (R1-R6) cell lines. (A) Cell cycle analysis (B) P-gp analysis (C) DNA synthesis (D) RNA synthesis

Discussions

Characterization of mechanisms leading to the development of drug resistance in cancer therapy is crucial for identification of targets for novel anti-cancer drugs, which may selectively eliminate the cell resistance and avoid potential therapy failure.

Conclusions

The present study will aid further understanding of the molecular basis of acquired tumor resistance to 2'-deoxy-5-azacytidine and help in predicting the clinical response to the same. It will also facilitate the introduction of novel therapeutics targeting methylation.

Summary

The cytosine analogues, 5-azacytidine and 2'-deoxy-5-azacytidine, function as DNA methyltransferase inhibitors and are currently most advanced drugs for epigenetic cancer therapies. Despite encouraging

results, mechanisms of *in vivo* resistance to these nucleoside analogues remain unresolved limiting their clinical application. This emphasizes the need for more potent drugs targeting methylation. To characterize the hypomethylation activity of wide range of methylation inhibitors, we successfully established a fluorescence detection system with high sensitivity, suitable for screening by robust high content cellular imaging techniques. LEM-789, the epigenetic drug discovered and developed by the Institute of Organic Chemistry and Biochemistry, Czech Republic, showed significant demethylation activity in preclinical studies. In addition, we also developed several HCT116 p53 wild-type cell clones resistant towards 2'-deoxy-5-azacytidine to investigate the mechanisms of resistance and here we also present the preliminary data characterizing the resistant clones. In MTT cytotoxicity assay, all clones showed a high degree of resistance. Flow cytometry based studies revealed significant up-regulation of DNA and RNA synthesis. In addition, there was no change in P-glycoprotein expression between parental and the resistant clones. Furthermore, proteome wide analysis of the resistant clones using mass spectrometry unveiled different sets of proteins with varying expression suggesting different mechanisms of resistance towards the studied methylation inhibitor. The molecular profiling of resistant clones at transcriptomics level including target mutation analyses and other gene expression studies together with the search for more potent methylation inhibitors is ongoing.

References

1. Taichun Q, Ryan C, Samih EA, Jaroslav J, Xiaodan W, Jiali S, Jingmin S, Rong H, Nianxiang Z, Woonbok C, Hagop MK, Jean-Pierre JI: Mechanisms of Resistance to Decitabine in the Myelodysplastic Syndrome. PLoS ONE 2011; 6(8), e23372.
2. Takada EO, Ichimura S, Kaneda A, Sugimura T, Ushijima T: Establishment of a detection system for demethylating agents using an endogenous promoter CpG island. Mutation Research 2004; 568, 187-194.
3. Crowley-Weber CL, Payne CM, Gleason-Guzman M, Watts GS, Futscher B, Waltmire CN, Crowley C, Dvorakova K, Bernstein C, Craven M, Garewal H, Bernstein H: Development and molecular characterization of HCT-116 cell lines resistant to the tumor promoter and multiple stress-inducer, deoxycholate. Carcinogenesis 2002; 23(12), 2063-2080.
4. Dzubak P, Hajduch M, Gazak R, Svobodova A, Psotova J, Walterova D, Sedmera P, Kren V: New derivatives of silybin and 2,3-dehydrosilybin and their cytotoxic and P-glycoprotein modulatory activity. Bioorg. Med. Chem. 2006; 14(11), 3793-3810.
5. Fabienne H, Stefan D: Histone H3 phosphorylation and cell division. Oncogene 2001; 20, 3021-3027.
6. Rothausler K, Baumgarth N: Assessment of Cell Proliferation by 5-Bromodeoxyuridine (BrdU) Labeling for Multicolor Flow Cytometry. Current Protocols in Cytometry 2001, 7-31.
7. Bradley G, Naik M, Ling V: P-Glycoprotein Expression in Multidrug-resistant Human Ovarian Carcinoma Cell Lines. Cancer Research 1989; 49, 2790-2796.
8. Shao-En O, Blagoev B, Kratchmarova I, Foster LJ, Andersen JS, Mann M: Stable isotope labeling by amino acids in cell culture for quantitative proteomics. Quantitative Proteomics by Mass Spectrometry 2007, 37-52.

Acknowledgment

This work was supported by internal grant of Palacky University (LF_2013_016), BIOMEDREG (CZ.1.05/2.1.00/01.0030) and Ministry of Industry and Trade of the Czech Republic (FR-TI4/625).

POLYMORPHISMS IN 17q12-21 ARE ASSOCIATED WITH ASTHMA EXACERBATION AND LUNG FUNCTION IN ASTHMATIC CHILDREN

Mario Blekic

E-mail: blekic1978@yahoo.com

General Hospital "Dr Josip Bencevic" Slavonski Brod, University of Osijek, Croatia
The University of Manchester, Manchester Academic Health Science Centre,
University Hospital of South Manchester NHS Foundation Trust, Manchester, UK

Co-authors: Blazenka Kljaic Bukvic MD, Neda Aberle MD, PhD, Susana Marinho MD, PhD,
Jenny Hankinson, Adnan Custovic MD, PhD, Angela Simpson MD, PhD
Tutor: Professor Neda Aberle MD, PhD

Introduction

Asthma is common chronic illness with the moderate prevalence among Croatian schoolchildren¹. It has an important genetic component confirmed by twin studies but no clear pattern of inheritance². Hundreds of genetic association studies have investigated associations between more than hundred genes and asthma and allergy phenotypes. Few have been successfully replicated in multiple populations, and often the replication is not precise, with different SNPs implicated in different studies³. The rapid increase in asthma prevalence that occurred in last decades⁴ in developed societies suggests a role for environmental exposures in the aetiology of allergic disease. Exposure to environmental tobacco smoke (ETS) in early life has been associated with the development of asthma⁵. Maternal smoking during pregnancy affects the neonatal immune system development, lung structure, and lung function in offspring⁶. Studies on different genes confirmed that exposure to tobacco smoke in early life modifies genetic susceptibility for asthma⁷. More than 15 studies associated genetic variants in 17q21 region with asthma.

We aimed to investigate whether amongst Croatian asthmatic children, genetic variants in this region are associated with asthma severity and exacerbation. We then investigated whether there were interactions between early life ETS exposure in relation to asthma severity.

Methods

We recruited 423 children aged 6-18 years with asthma from the paediatric asthma clinic. All had a physician diagnosis of asthma and were currently taking asthma medications and had had two or more asthma symptoms (wheezing, coughing, and both) in the last 12 month. Information on hospital admission with asthma exacerbations was retrieved from medical records. Data on wheeze frequency and environmental tobacco smoke (ETS) exposure was collected using validated questionnaire. Lung function (FEV1%predicted) was measured using spirometry. We selected Haplotype-tagging SNPs with a minor allele frequency (MAF) $\geq 5\%$ in the 17q12-21 chromosomal region including GSDMA, GSDMB, ORMDL3, IKZF3, ZPBP2, TOP2A. We included relevant SNPs reported in the literature.

Result

Of the 51 SNPs originally selected for genotyping, 3 failed genotyping, one was monomorphic and one was not in Hardy-Weinberg equilibrium. For the remaining 46 SNPs, we applied linkage disequilibrium (LD) filtering algorithm to identify tagging SNPs, whilst keeping key SNPs reported in other published studies. This resulted in 35 SNPs being used in the analysis. We found significant associations between 4 SNPs and hospital admissions (rs12150079, rs7212938, rs2290400, rs8067378). For example, G allele homozygotes in rs12150079 were at higher risk of being admitted to hospital than carriers of A allele (aOR 1.85, 95%CI 1.26-2.72, $p=0.002$); this SNP was also associated with current wheezing.

Six SNPs were associated with lung function (rs9635726, rs921651, rs9900538, rs3169572, rs4795403, rs471692). We observed significant interactions between 3 SNPs (rs8079416, rs4795408, rs7212938) and early life ETS exposure in relation to hospital admissions with acute asthma exacerbation. In addition, we observed significant interaction between 3 SNPs (rs12603332, rs8067378, rs9303277) and *in utero* ETS exposure in relation to lung function ($p < 0.04$), in that amongst children of mothers who smoked during pregnancy, major allele homozygotes had lower FEV1% predicted than minor allele carriers, but amongst non-exposed children there was no difference in lung function between different genotype groups.

Discussion

Amongst asthmatic children we observed several associations between SNPs in 17q12-q21 region and hospital admission with asthma exacerbation, some of which were only seen if children were exposed to tobacco smoke in early life. Others have looked for associations between 17q12-q21 and other indicators of exacerbations or severity. Two studies in children, in which exacerbations were generally defined as the use of oral corticosteroids showed association between T allele of rs7216389 and asthma exacerbations. Two studies carried out in adults observed an association between same allele and greater asthma severity among early-onset asthma cases. However these studies investigated only the single SNP rs7216389. In our study we found a trend for association with exacerbations and rs7216389 ($p = 0.09$). We investigated a much broader panel of SNPs, and found the strongest associations to be with SNPs rs8067378 and rs2290400, both of which also lie within ORMDL3 in the same LD block as rs7216389. To date, few studies have investigated the associations between polymorphisms in 17q12-21 region and asthma with respect of smoking during childhood. Bouzigon⁸ reported associations between 11 SNPs in 17q12-21 region and early-onset of asthma only amongst those that had been exposed to ETS in early life, but not in the unexposed subgroup of children. Flory⁹ et al investigated influences between exposure to smoking during childhood, gene variants in 17q12-21 and asthma in two populations (but not for African American subjects) and reported modifying effects for nine 17q12-21 SNPs. Associations between these nine SNPs and asthma were stronger in the group exposed to ETS. Data from two independent prospective cohort studies from foetal life onwards in the Netherlands associated rs2305480 with asthma-like symptoms in preschool children, and this association was modified by smoke exposure already during foetal life, and in infancy¹⁰. To the best of our knowledge, our study is the first to demonstrate the interaction between polymorphisms in the 17q12-q21 region, ETS exposure and hospital admission for severe exacerbation of asthma, suggesting a possible role of early life ETS exposure on developing more severe asthma.

We have also identified a significant interaction between genetic variants and *in utero* tobacco smoke exposure, with lung function being diminished in specific genotypes, but only amongst children exposed to ETS.

Conclusion

Among Croatian schoolchildren with asthma variants in *17q12-21 region* are associated with disease severity.

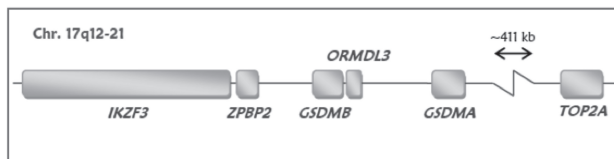
Acknowledgements

I would like to thank Professor Adnan Custovic and colleges from School of Translational Medicine, University of Manchester, Manchester, UK, my mentor Professor Neda Aberle and other colleges from General Hospital iDr Josip Benčević Slavonski Brod for all support and EAACI for a short-term Fellowship.

MeSH / Keywords: Asthma, Child, Croatia, 17q, Polymorphism, Single Nucleotide, Smoking

References

1. Banac S, Tomulić KL, Ahel V, et al. Prevalence of asthma and allergic diseases in Croatian children is increasing: survey study. *Croat Med J.* 2004; 45: 721-726.
2. Duffy DL, Martin NG, Battistutta D, Hopper JL, Mathews JD. Genetics of asthma and hay fever in Australian twins. *Am Rev Respir Dis.* 1990; 142: 1351-1358.
3. Pinto LA, Stein RT, Kabesch M. Impact of genetics in childhood asthma. *J Pediatr (Rio J).* 2008; 84(4 Suppl): S68-S75.
4. Asher MI, Montefort S, Björkstén B, et al. Worldwide time trends in the prevalence of symptoms of asthma, allergic rhinoconjunctivitis, and eczema in childhood: ISAAC Phases One and Three repeat multicountry cross-sectional surveys. *Lancet* 2006; 368: 733-743.
5. Hofhuis W, De Jongste JC, Merkus P. Adverse health effects of prenatal and postnatal tobacco smoke exposure on children. *Arch Dis Child.* 2003; 88: 1086-90.
6. Hanrahan JP, Tager IB, Segal MR, et al. The effect of maternal smoking during pregnancy on early infant lung function. *Am Rev Respir Dis.* 1992; 145: 1129-35.
7. Dizier MH, Bouzigon E, Guilloud-Bataille M, et al. Evidence for gene× smoking exposure interactions in a genome-wide linkage screen of asthma and bronchial hyper-responsiveness in EGEA families. *Eur J Hum Genet.* 2007; 15: 810-815.
8. Bouzigon E, Corda E, Aschard H, et al. Effect of 17q21 variants and smoking exposure in early-onset asthma. *N Engl J Med.* 2008; 359: 1985-1994.
9. Flory JH, Sleiman PM, Christie JD, et al. 17q12-21 variants interact with smoke exposure as a risk factor for pediatric asthma but are equally associated with early-onset versus late-onset asthma in North Americans of European ancestry. *J Allergy Clin Immunol.* 2009; 124: 605-7.
10. van der Valk RJ, Duijts L, Kerkhof M, et al. Interaction of a 17q12 variant with both fetal and infant smoke exposure in the development of childhood asthma-like symptoms. *Allergy.* 2012; 67: 767-774.



Tab. 1. Genes selected in the Chr. 17q12-21 region

SNP	Gene	Allele*	p-Value	FDR	Genetic Model	aOR	95%CI	
							Lower	Upper
rs number								
rs12150079	ZPBP2	G /A	0.02	0.75	AA+AG vs.GG	0.61	0.40	0.93
rs8067378	GSDMB	A/ G	0.04	0.43	GG vs.GA+AA	0.56	0.32	0.99
rs2290400	GSDMB	T /C	0.03	0.91	CC vs.TC+TT	0.52	0.28	0.95
rs7212938	GSDMA	T/ G	0.04	0.69	GG+GT vs.TT	1.71	1.01	2.88

Tab. 2. Association between genetic variants in the region 17q12-21 and admission to hospital with acute asthma exacerbation

*common allele is first, risk allele is in bold

Highlighted SNPs are in high LD ($r^2 > 0.90$).

Gene	Allele*	p-value	FDR	FEV1% predicted				
				Genetic Model	mean	95%CI		
						lower	upper	
rs9900538	<i>IKZF3</i>	T/C	0.04	0.35	CC+CT	102.30	98.04	106.57
					TT	97.43	95.77	99.09
rs9635726	<i>IKZF3</i>	C/T	<0.01	0.01	TT	86.01	79.23	92.79
					CT+CC	98.63	97.06	100.20
rs3169572	<i>ORMDL3</i>	G/A	0.02	0.20	AA+AG	102.80	98.74	106.85
					GG	97.41	95.75	99.06
rs4795403	<i>ORMDL3</i>	C/T	0.04	0.33	TT+TC	100.93	97.84	104.01
					CC	97.27	95.50	99.04
rs921651	<i>GSDMA</i>	A/G	0.04	0.29	GG+GA	95.83	93.11	98.54
					AA	99.20	97.32	101.09
rs471692	<i>TOP2A</i>	G/A	0.04	0.31	AA	107.94	98.66	117.22
					AG+GG	97.84	96.28	99.41

Tab. 3. Genetic variants in the region 17q12-21 and lung-function measures
*common allele is listed first, risk allele is in bold

SNP					Exposed to smoke				Non exposed to smoke			
					FEV ₁ % pred		95% CI		FEV ₁ % pred		95% CI	
					Mean	n	L	U	Mean	n	L	U
rs9303277	<i>IKZF3</i>	C/T	TT+TC	0.03	101.67	61	97.59	105.76	97.42	185	95.15	99.7
			CC	0.03	92.7	20	85.57	99.83	98.16	108	95.19	101.13
rs8067378	<i>GSDMB</i>	A/G	GG+GA	0.03	101.86	63	97.8	105.92	97.51	199	95.34	99.68
			AA	0.03	92.96	21	85.92	100	97.95	112	95.06	100.85
rs12603332	<i>ORMDL3</i>	C/T	TT+TC	0.04	101.76	64	97.75	105.77	97.82	198	95.66	99.99
			CC	0.04	92.96	21	85.96	99.97	97.73	118	94.93	100.54

Tab. 4. Significant interaction between 3 SNPs and in utero ETS exposure in relation to lung function ($p_{int} < 0.04$)

EFFECT OF BLOOD SEROTONIN LEVELS ON FOUR MONTHS OLD FEMALE RAT SKELETON

Igor Erjavec

E-mail: igor.erjavec@mef.hr

Department of Anatomy, Center for Translational and Clinical Research,
Laboratory for Mineralized Tissue, School of Medicine, University of Zagreb, Croatia

Co-authors: L. Grgurević, L. Čičin-Šain, D. Ježek, S. Vukičević

Tutor: Associate Professor Lovorka Grgurević, MD, PhD

Introduction

Serotonin or 5-hydroxytryptamine (5HT) is an important neurotransmitter in the central nervous system (CNS) and has a major role in vasoconstriction, peristaltic bowel movement and blood clotting on the periphery. The main production of 5HT in the body happens in the gut and in the CNS, where blood-brain barrier completely blocks traverse of the 5HT between these two systems. Latest discoveries imply serotonin effects on bone, where 5HT exerts direct effect on bone cells (Yadav et al. 2008, Cui et al. 2011, Chabbi-Achengli et al. 2012).

Aims

To test the effect of serotonin (5HT) on bone quality in an animal model of altered blood serotonin level.

Methods

To examine serotonin effect on bone we used well described animal model with altered blood serotonin levels. Animals were developed by selective breeding to create two distinct animal sublines, high-5HT and low-5HT (Jernej and Cicin-Sain, 1990). Four months old female Wistar-Zagreb 5HT (WZ-5HT) rats were used in this experiment. Trabecular and cortical bone structure and quality were investigated in distal part of femur, while only trabecular parameters were analyzed in the body of third lumbar vertebrae. Animals were weighed on a digital scale and femur length was measured using a caliper. Bone structure was analyzed *ex vivo* using a SkyScan 1076 micro CT system while bone quality was assessed by biomechanical testing using a Texture analyzer TA.HD Plus. In the biomechanical testing femurs were subjected to three point bending test for cortical bone analysis and an indentation test for trabecular bone analysis. Obtained data were tested for normal distribution and further statistical analysis was completed using the Student's t-test with the level of significance set at $P < 0,05$.

Results

Animals with high serotonin level had increased weight, femur length and bone tissue volume revealing an effect of 5HT on growth and development (Figure 1).

When analyzing cortical bone, no difference in cortical bone volume and thickness was observed between the two sublines, while high-5HT animals had increased endosteal volume due to larger bones. Biomechanical testing confirmed results from micro CT analysis with no difference in parameters between the high-5HT and low-5HT subline (Figure 2).

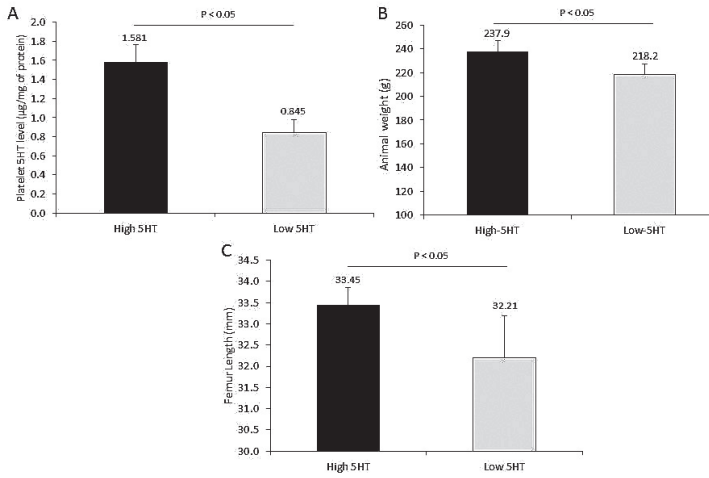


Figure 1. Phenotype difference between the WZ-5HT rat sublimes. Platelet 5HT content (A), body weight (B) and bone length (C) was higher in high-5HT subline, all reaching statistical significance ($P < 0,05$).

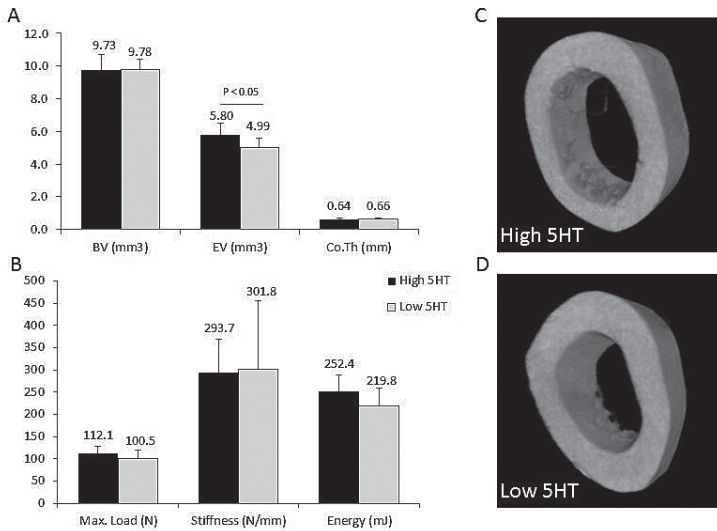


Figure 2. Cortical bone testing. Micro CT data analysis revealed no difference in bone volume (BV) and cortical thickness (Co.Th) while, due to larger bones, endosteal volume (EV) was greater in high-5HT rats (A). Biomechanical testing confirmed no difference in cortical bone quality between the sublimes (B). 3D model of the cortical bone from high-5HT (C) and low-5HT (D) animals.

No difference in trabecular bone parameters between high-5HT and low-5HT animals was observed on periphery, while in axial skeleton trabecular parameters were significantly better in animals with low serotonin level. Indentation test revealed no difference between the two sublines in force parameters of the trabecular bone in femur (Figure 3).

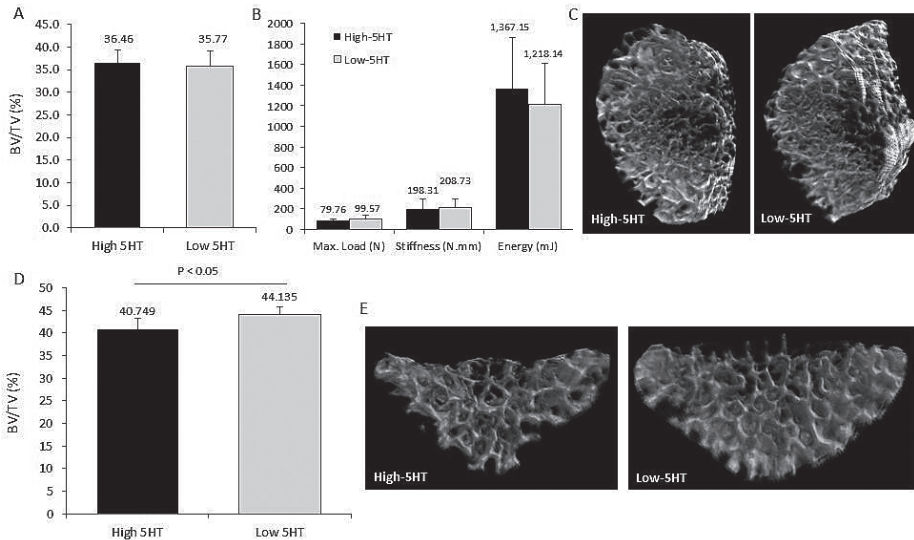


Figure 3. Trabecular bone analysis. No difference in femur trabecular bone was observed between the sublines. Micro CT measurements of the bone volume (A) were confirmed by biomechanical testing (B). No difference in femur trabecular bone is also noticeable on the 3D model of the trabecular bone form the femur (C). Analysis of the spine trabecular bone revealed lower quality bone in the high-5HT rats (D). 3D model of the spine trabecular bone visualizes the difference in trabecular bone (E).

Discussion

In four months old female rats, effect of 5HT on bone was only evident at axial skeleton in the site of lumbar spine. These effects, where only axial skeleton is affected by the change in the physiological serotonin concentration, could be caused by the fact that there are two separated systems of 5HT production in the body.

Conclusions

In four months old animals, serotonin effect on development and growth was evident due to difference in weight and bone length. 5HT showed no effect on femur bone parameters, while on spine a negative effect of increased 5HT was observed. Our findings point out that serotonin has a distinct negative effect on trabecular bone properties in axial skeleton, while it has no effect on cortical or trabecular bone in peripheral skeleton in four months old females.

Summary

Serotonin affected development and growth in WZ-5HT rats due to difference in size between the sublines. No effect on cortical and trabecular bone was noticed at the site of distal femur, while negative effect of higher 5HT level was observed at the site of lumbar spine.

Keywords: serotonin, 5-hydroxytryptamine, bone remodeling, micro CT, trabecular bone, cortical bone, biomechanical testing

References

1. Chabbi-Achengli Y, Coudert AE, Callebert J, Geoffroy V, Côté F, Collet C, de Vernejoul MC. Decreased osteoclastogenesis in serotonin-deficient mice. *Proc Natl Acad Sci U S A*. 2012;109(7): 2567-72.
2. Cui Y, Niziolek PJ, MacDonald BT, Zylstra CR, Alenina N, Robinson DR, Zhong Z, Matthes S, Jacobsen CM, Conlon RA, Brommage R, Liu Q, Mseeh F, Powell DR, Yang QM, Zambrowicz B, Gerrits H, Gossen JA, He X, Bader M, Williams BO, Warman ML, Gobling AG. Lrp5 functions in bone to regulate bone mass. *Nat. Med.*: 2011; 17: 684-691
3. Jernej B, Cicin-Sain L. Platelet serotonin level in rats is under genetic control. *Psychiat Res*. 1990; 32: 167-174
4. Yadav VK, Ryu JH, Suda N, Tanaka KF, Gingrich JA, Schütz G, Glorieux FH, Chiang CY, Zajac JD, Insogna KL, Mann JJ, Hen R, Ducy P, Karsenty G. Lrp5 controls bone formation by inhibiting serotonin synthesis in the duodenum. *Cell.*; 2008; 135(5): 825-37

DETECTION OF *ALK* GENE REARRANGEMENT IN NON-SMALL CELL LUNG CARCINOMA BY FLUORESCENCE IN SITU HYBRIDIZATION

Anna Farkašová

E-mail: farkasova.anka@gmail.com

Department of Pathology, Jessenius Medical Faculty, Comenius University, Martin and Martin Biopsy Center Ltd., Martin, Slovak republic

Co-authors: M. Barthová, T. Balhárek, E. Janáková, Z. Kviatkovská

Tutor: L. Plank

Introduction

Non-small cell lung carcinoma (NSCLC) accounts for approximately 80% to 85% of all cases of lung cancers. One of its main subtypes - adenocarcinoma (AC), is characterized by various genetic changes of tumor cells, which identification is essential in relation to the indication of the targeted therapy. In cases of NSCLC without *EGFR* gene mutations it is now important to define further molecular subgroup with *ALK* gene rearrangement. Currently there are several approaches to detect rearrangement in the *ALK* gene and/or to detect EML4/*ALK* fusion protein.

Methods

Paraffin-embedded tissue sections of 281 NSCLC cases, which were negative for *EGFR* gene mutations were analyzed by the method of fluorescence in situ hybridization (FISH) using two probes produced by Zytovision and Vysis/Abbott, with the purpose of detecting the presence of *ALK* gene rearrangement and/or translocation of *EML4/ALK*. Moreover, 91/281 cases were simultaneously analyzed by immunohistochemistry (IHC) method, using an anti-*ALK* antibody (clone D5F3) produced by Ventana on BenchMark GX platform.

Results

a) 37/281 cases were positive for the rearrangement of the *ALK* gene. 34/37 cases were positive also by using a probe *EML4/ALK*. Remaining 3/37 cases were not tested due to lack of material, b) 237/281 cases were negative for *ALK* gene rearrangement, c) 7/281 cases were not evaluable due to technical limitations, d) all FISH negative cases, that were also tested by IHC (104/281), didn't express *ALK* protein, e) 17/22 FISH positive cases expressed the *ALK* protein and f) 5/22 FISH positive cases didn't express *ALK* protein positivity.

Conclusions

The aim of this project was to compare the two different break-apart probes from the Zytovision and Vysis/Abbott to determine an algorithm for the analyses of cases with lung adenocarcinoma. Our results show that in the case of detection of rearrangement in the *ALK* gene it is preferable to use a break-apart probe for the gene, because the *ALK* gene (although rarely) may form fusions with other genes than the *EML4* gene. We also compared the suitability of the method IHC as a screening method for testing *ALK* fusion protein in cases of NSCLC/AC. It turns out, however, that the IHC method does not fully correspond with the results of FISH method. It is questionable whether the set cut-off values for the presence of *ALK* gene rearrangement are fully consistent with the phenotype of cancer cells and whether patients with such values benefit from the selected targeted therapies. For the assessment of such conclusions, however, we have do not enough clinical data.

Supported by grant of Ministry of Health of the Slovak republic 2012/24-UKMA-1 „Detection of predictive relevant parameters in diagnostic algorithm of bioptic examination of colon and lung cancer“, and projects CEPV II (ITMS: 26220120036) and MBRKM (ITMS: 26220220113) co-financed by EU sources.

DO GLUCAGON-LIKE PEPTIDE - 1 ANALOGUES AFFECT EARLY PHASE OF LIVER REGENERATION AFTER PARTIAL HEPATECTOMY IN RATS?

Josef Fontana

E-mail: josef.fontana@lf3.cuni.cz

Centre for Research of Diabetes, Metabolism and Nutrition, Third Faculty of Medicine,
Charles University in Prague

Laboratory of experimental hepatology, Department of Physiology, Faculty of Medicine
in Hradec Králové, Charles University in Prague

Co-author: O. Kučera

Tutors: prof. MUDr. Michal Anděl, CSc., prof. MUDr. Zuzana Červinková, CSc.

Introduction

Liver failure leads quite often to the death. Its treatment is very difficult and for many patients is the only option liver transplantation. Therefore, there is an intensive search for new effective treatment. Glucagon-like peptide - 1 (GLP-1) is an incretin hormone known for its proliferative and antiapoptotic effects on pancreatic β -cells (1). These effects are currently widely discussed in diabetology. From literature data, it is evident that GLP-1 affects liver functions and liver metabolism (mainly metabolism of lipids and saccharides) (2, 3). Very little is known about its ability to modulate liver regeneration and proliferation of hepatocytes (4). GLP-1 has a short biological half-life, because it is effectively degraded by ubiquitous enzyme dipeptidyl peptidase IV (DPP IV) (5). Therefore, analogues of GLP-1 that are resistant to degradation action of DPP IV are used in clinical practice and also in research. Currently two analogues: Exenatide (Ex4) and Liraglutide (LIRA) are commonly available. 2/3 partial hepatectomy (PHx - removal of 65-70 % of liver tissue) is a model of liver regeneration that in contrast to methods using hepatotoxins is not accompanied by inflammation and we can clearly identify the beginning of the regeneration (6).

Aims

To determine the effect of GLP-1 analogues, exenatide and liraglutide, on early phase of liver regeneration and selected metabolic parameters in a model of 2/3 partial hepatectomy in male Wistar rats.

Methods

Experiments were performed on Male Wistar rats with initial weight 264 ± 17 g. They were divided into 6 groups (n = 6). On the first day, two doses of either GLP-1 analogues (Ex4 - 42 μ g/kg body weight, liraglutide - 0.75 mg/kg b.w.), or equivalent amount of saline (S) were injected intraperitoneally. On the second day, the animals were submitted to the 2/3 partial hepatectomy or sham operation - laparotomy (LAP). The third dose of analogues or saline was injected intraperitoneally immediately after the surgery. On the third day, 23 hrs after the surgery, bromodeoxyuridine (BrdU - 100 mg/kg b.w.) was administered. The animals were sacrificed one hour after the BrdU application by exsanguination from abdominal aorta. Liver and serum samples were taken. Samples for consequent evaluation were immediately frozen in liquid nitrogen and stored at -80 °C until analysis. We analysed these parameters: body weight, absolute and relative liver weight, liver BrdU incorporation, liver content of DNA, triacylglycerols (TAG) and cholesterol, serum concentrations of urea, creatinine, total bilirubin, glucose, total cholesterol and TAG, serum activities of alanine aminotransferase (ALT), aspartate aminotransferase (AST) and alkaline phosphatase (ALP) and mitochondrial respiration.

Results

In the rats after PHx, both analogues compared to saline controls decreased BrdU labeling ($p < 0.001$) - marker of S-phase activity. Liraglutide compared to Ex4 caused even lower BrdU labeling ($p < 0.001$) (Fig. 1). This effect was reflected in a decreased liver DNA content in the rats after PHx receiving liraglutide compared to both Ex4 ($p < 0.001$) and saline group ($p < 0.001$) (Fig. 2). Laparotomy groups did not exert significant differences in BrdU labeling and DNA content (Fig. 1, Fig. 2).

**Bromodeoxyuridine incorporation in liver
24 hrs after surgery**

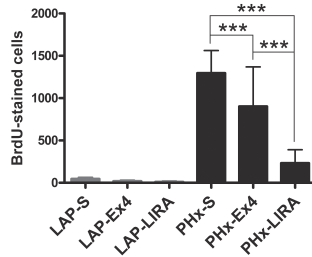


Fig. 1. Number of BrdU-stained cells in the liver 24 hrs after the surgery (***) $P < 0.001$.

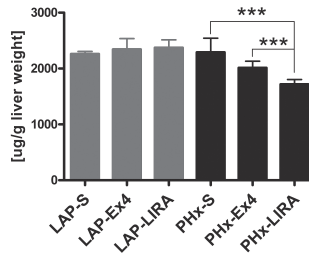


Fig. 2. DNA content in the liver 24 hrs after the surgery (***) $P < 0.001$.

Liraglutide treatment in contrast to both saline and Ex4 treatment led after any surgery (PHx, LAP) to an increase in serum urea level (LAP-LIRA vs LAP-S: $p < 0.001$; LAP-LIRA vs LAP-Ex4: $p < 0.001$; PHx-LIRA vs PHx-S: $p < 0.05$; PHx-LIRA vs PHx-Ex4: $p < 0.01$). Ex4 did not exert any effect on serum urea (Fig. 3). Both analogues had no significant effect on serum creatinine level (data not shown).

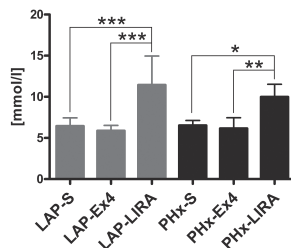


Fig. 3. Serum urea concentration 24 hrs after the surgery (* $P < 0.05$; ** $P < 0.01$; *** $P < 0.001$).

Liraglutide also reduced serum total bilirubin ($p < 0.05$), serum TAG ($p < 0.001$) and liver cholesterol content ($p < 0.05$) in the rats after PHx (data not shown). Analogues had no significant effect on body weight, liver weight, serum creatinine, serum total cholesterol, serum activities of AST, ALT and ALP, liver triacylglycerols content and mitochondrial respiration (data not shown).

Discussion

Our work described that GLP-1 analogues, exenatide and liraglutide, affect the early phase of liver regeneration after PHx. The only until now published work (4) has described a positive effect of exenatide on the proliferation of hepatocytes. Our work described the negative effect of both GLP-1 analogues marked by a decreased count of BrdU-stained cells in the liver and by decreased liver DNA content 24 hrs after partial hepatectomy. There are many methodological differences between our work and work of Aviv et al. (4). Their study was performed on human hepatocytes cultivated *in vitro* and stimulated by Epidermal growth factor simultaneously. Thus, the comparison of our and their results is very difficult.

Our original hypothesis that GLP-1 analogues would have a positive effect on liver regeneration was not confirmed. In the light of facts, that GLP-1 is sometimes accused of increasing the risk of some cancers (pancreas, thyroid) (7), our results could indicate that similar concerns would not apply in relation to liver cells.

Conclusion

Our results suggest that GLP-1 analogues, exenatide and liraglutide, significantly diminish early phase of liver regeneration after 2/3 partial hepatectomy. Liraglutide effect was even more pronounced. Interesting finding is an effect of liraglutide on a serum urea level, without a concomitant effect on serum creatinine concentration. Contrary to our expectations hepatocytes do not respond to incretins by the stimulation of proliferation, at least during the early phase of liver regeneration after PHx.

Summary

Glucagon-like peptide - 1 (GLP-1) is an incretin hormone known for its proliferative and antiapoptotic effects on pancreatic β -cells. These effects are currently widely discussed in diabetology. From literature data, it is evident that GLP-1 affects liver functions and liver metabolism. Very little is known about its ability to modulate liver regeneration and proliferation of hepatocytes. Our aim was to determine the effect of GLP-1 analogues, exenatide (Ex4) and liraglutide (LIRA) on early phase of liver regeneration and selected metabolic parameters in a model of 2/3 partial hepatectomy in male Wistar rats. Animals (264 ± 17 g) were divided into 6 groups ($n = 6$). On the first day, two doses of either GLP-1 analogues (Ex4 - 42 mg/kg, LIRA - 0.75 mg/kg), or equivalent amount of saline (S) were injected intraperitoneally. On the second day, the animals were submitted to the 2/3 partial hepatectomy (PHx) (1) or sham laparotomy (LAP). The third dose of analogues or saline was injected immediately after the surgery. The animals were sacrificed 24 hours after the surgery and the intensity of liver regeneration and selected metabolic parameters were evaluated. In the rats after PHx, both analogues compared to saline controls decreased bromodeoxyuridine (BrdU) labeling - marker of S-phase activity. Liraglutide compared to Ex4 caused even lower BrdU labeling. This effect was reflected in a decreased liver DNA content in the rats after PHx receiving liraglutide compared to both Ex4 and saline group. Laparotomy groups did not exert significant differences in BrdU labeling and DNA content. Liraglutide treatment in contrast to both saline and Ex4 treatment led after any surgery (PHx, LAP) to an increase in serum urea. Ex4 did not exert any effect on serum urea concentration. Liraglutide also reduced serum total bilirubin, serum triacylglycerols and liver cholesterol content in the rats after PHx. Our results suggest that GLP-1 analogues, exenatide and liraglutide, significantly diminish early phase of liver regeneration after 2/3 partial hepatectomy. Liraglutide effect was even more pronounced. Interesting finding is an effect of liraglutide on a serum urea level, without a concomitant effect on serum creatinine concentration.

Contrary to our expectations hepatocytes do not respond to incretins by the stimulation of proliferation, at least during the early phase of liver regeneration after PHx.

References

1. Xu G, Stoffers DA, Habener JF et al.: Exendin-4 stimulates both beta cell replication and neogenesis, resulting in increased beta-cell mass and improved glucose tolerance in diabetic rats. *Diabetes* 1999 Dec; 48(12): 2270-6.
2. Valverde I, Morales M, Clemente F et al.: Glucagon-like peptide 1: a potent glycogenic hormone. *FEBS Lett* 1994 Aug 1; 349(2): 313-6.
3. Ding X, Saxena NK, Lin S et al.: Exendin-4, a glucagon-like protein-1 receptor agonist, reverses hepatic steatosis in ob/ob mice. *Hepatology* 2006 Jan; 43(1): 173-81.
4. Aviv V, Meivar-Levy I, Rachmut IH et al.: Exendin-4 promotes liver cell proliferation and enhances the PDX-1-induced liver to pancreas transdifferentiation process. *J Biol Chem*. 2009 Nov 27; 284(48): 33509-20.
5. Vilsbøll T, Agersø H, Krarup T et al.: Similar elimination rates of glucagon-like peptide-1 in obese type 2 diabetic patients and healthy subjects. *J. Clin Endocrinol Metab* 2003 Jan;88(1): 220-4.
6. Higgins GM, Anderson RM: Experimental pathology of the liver I. Restoration of the liver of the white rat following partial surgical removal. *Arch Pathol* 1931, 12: 186-202.
7. Elashoff M, Matveyenko AV, Gier B et al.: Pancreatitis, pancreatic, and thyroid cancer with glucagon-like peptide-1-based therapies. *Gastroenterology* 2011 Jul; 141(1): 150-6.

A NOVEL INSIGHT INTO THE EFFECT OF L-ASPARAGINASE ON LEUKAEMIC CELLS

Ivana Heřmanová

E-mail: Ivana.hermanova@lfmotol.cuni.cz

Childhood Leukaemia Investigation Prague, Department of Pediatric Hematology/Oncology,
2nd Faculty of Medicine, Charles University Prague, Czech Republic

Co-authors: Hana Nůšková, Karel Vališ, Karel Fišer, Sonia Fernández,
Josef Houšťek, Arkaitz Carracedo, Jan Trka
Tutor: Mgr. Júlia Starková, Ph.D.

Introduction, Aims

Acute lymphoblastic leukaemia (ALL) is the most frequent type of childhood cancer (1). It is treated according to the international protocols that cause remission in 98 % of patients. Despite the impressive advances in therapy, relapses occur approximately in 15 - 20% of patients (2). The protocols used for ALL treatment require a combination of chemotherapeutics with the critical component L-asparaginase (L-asp). L-asp is an enzyme that hydrolyses non-essential aminoacids asparagine and glutamine (3). The traditional explanation of anti-leukaemic effect of L-asp is based on a lower activity of asparagine synthetase (ASNS) in leukaemic cells compared with healthy cells. Therefore, leukaemic cells are not able to compensate for the lack of aminoacids that consequently impairs proteosynthesis and causes cell death (4, 5). The exact mechanism of cytotoxic effect has not been elucidated so far. ALL patients have different sensitivity to L-asp and some of them suffer serious side effects.

Our aim is to describe the effect of L-asp in leukaemic cells in detail and to find a relevant marker of patients' resistance for the therapy.

Methods

We established cell lines resistant to L-asp derived from the B-cell precursor ALL REH (TEL/AML1[+]; very sensitive) and NALM6 (TEL/PDGFRB[+]; medium sensitive) cells by long-term incubation with L-asp. The sensitivity of these cell lines was proved by the [3-(4,5-dimethylthiazol-2-yl)-5-(3-carboxymethoxyphenyl)-2-(4-sulfophenyl)-2H-tetrazolium, inner salt (MTS) test. Gene expression profiles of parental and resistant cell lines (GEP) were determined by Microarray NimbleGene. We applied the pathway analysis (MetaCore software) of GEP data from the cell lines and patient samples sensitive/resistant to L-asp (6). GEP data were validated by qRT-PCR. Proteins were detected by western blot. Respiration was measured by oxygraph (Oroboros). Glucose up-take and fatty acid oxidation were quantitated by liquid scintillation counting. The amount of lactate was determined spectrophotometrically using lactate kit. The amount of ATP was measured by luminiscent ATP detection assay kit.

Results

There was 837 genes with significantly changed expression in resistant REH cell line and 392 in resistant NALM6 compared with the parental cell lines. 30 genes were identical for both cell lines. Among the highest scoring pathways found by pathway analysis were translation regulation and lipid and glucose metabolism. Next to glucose, glutamine is the other major cellular energy source also important for the activation of PI3K/Akt/mTOR pathway. Since L-asp has also glutaminase activity we focused on the effect of L-asp treatment on translation and bioenergetics in leukaemic cells.

mTORC1 activates cell translation via phosphorylation of P70S6K. The amount of p-P70S6K protein and its downstream target p-S6 were reduced in REH and NALM6 after treatment with L-asp. The phosphorylation of 4EBP1 was also decreased (Fig. 1). These results clearly indicate the inhibition

of translation in leukaemic cells after L-asp treatment. We measured the cytostatic effect of co-treatment: L-asp with mTORC1 inhibitor (rapamycin); with dual inhibitor of mTORC1 and PI3K (LY294002); and with specific inhibitor of PI3K (PX866). The MTS assay proved that the L-asp/rapamycin combination is the most effective.

Next, we determined the impact of L-asp on metabolism of leukaemic cells. The protein level of C-MYC, the activator of glucose and glutamine catabolism, and glucose transporter 1 (GLUT-1) was decreased in REH and NALM6 after L-asp treatment. The inhibition of glycolysis was confirmed by the decrease of glucose uptake (Fig. 2) and by the decrease of lactate production in cells treated with L-asp.

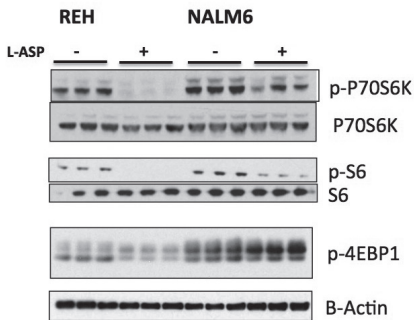


Fig. 1. Protein level of p-P70S6K, P70S6K, p-S6, S6 and p-4EBP1 in leukaemic cells treated with L-asp. Protein content was measured by Western blot analysis. REH and NALM6 cells displayed an decrease in p-P70S6K, p-S6 and p-4EBP1 protein after L-asp treatment.

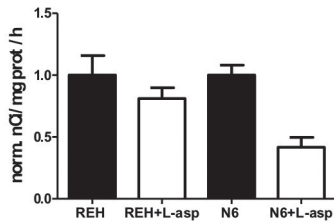


Fig. 2. Glucose up-take in leukaemic cells treated with L-asp. Glucose uptake was measured using radiolabeled 2-deoxyglucose. REH and NALM6 cells decreased glucose-uptake after L-asp treatment.

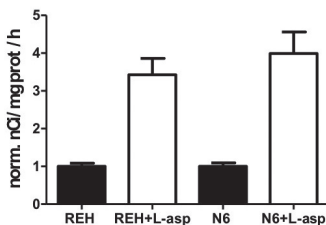


Fig. 3. Fatty acid oxidation in leukaemic cells treated with L-asp. Fatty acid oxidation was measured using radiolabeled palmitate. REH and NALM6 cells increased fatty acid oxidation after L-asp treatment.

Besides the glutamine and glucose metabolism, fatty acids are the next substrates for ATP production. Fatty acid oxidation (FAO) was significantly increased in both cell lines after L-asp (Fig. 3). The co-treatment of L-asp and etomoxir, the specific inhibitor of FAO, significantly decreased the cell survival in both cell lines. Since the product of FAO, acetylCoA, enters the Krebs cycle and the product of the Krebs cycle NADH activates respiratory chain, we measured the impact of L-asp on respiratory chain as well. The capacity of cell respiration was increased after L-asp administration, indicating increased oxidative phosphorylation in the cells. Decreased levels of ATP did not confirm this assumption.

Discussion

Our results indicate that L-asp inhibits translation in leukaemic cells. Moreover we show that leukaemic cells, which normally depend on glycolysis, are able to switch to fatty acid oxidation followed by activation of respiratory chain under amino acid deprivation stress. The remaining key question is what the objective of these changes is. The decrease of ATP levels after L-asp treatment shows that the metabolic switch does not serve to produce energy. We hypothesize that the main reason is to obtain intermediates from Krebs cycle to supply depleted amino acids. Although L-asp has an apoptotic effect, it probably also triggers the rescue mechanism. The activation of the rescue pathways could distinguish between sensitive and resistant patients.

Conclusion

L-asp has already been in use for decades. Its importance in the therapy of childhood ALL is unquestionable. Recently, it is also used in the therapy of adult ALL. The effect of L-asp is studied in the therapy of ovarian cancer as well. Nevertheless, the exact mechanism of action has been elucidated neither in leukaemic cells nor in the ovarian cancer cells. Our study describes for the first time the strong effect of L-asp on the metabolism of leukaemic cells. These results will help to explain the cytotoxic effect, the reason of resistance and side effects development.

Summary

Acute lymphoblastic leukaemia (ALL) is the most frequent type of childhood cancer. It is treated according to the international protocols that cause remission in 98 % of patients. Despite the impressive advances in therapy, relapses occur approximately in 15 - 20% of patients. L-asparaginase (L-asp) is the important component of the combined chemotherapy. L-asp depletes extracellular asparagine and glutamine. The antileukaemic effect of L-asp was traditionally attributed to the lower function of asparagine synthetase (ASNS) in leukaemic cells compared with healthy cells. We have previously shown that expression level of ASNS is not responsible for the differential sensitivity of various leukaemic cells to treatment with L-asp (Krejčí, Starková et al, *Leukemia* 2004; Heřmanová et al, *Exp Hematol* 2012).

In the current project, we study the mechanism of L-asp effect on the energy production and proteosynthesis of the leukaemic cells. Cancer cells are energetically mostly dependent on glycolysis. Under the treatment with L-asp, glycolysis is impaired, and the cells utilize fatty acid oxidation followed by activation of respiratory chain as an alternative bioenergetic pathway. Moreover, L-asp inhibits the mTOR signaling in leukaemic cells, thus decreasing the proteosynthesis. We believe that these changes are mainly caused by the effort of the cells to mobilize metabolism with the aim to supply depleted amino acids. Resistance of the particular leukaemia subtypes is likely caused by the better biochemical adaptability to these processes.

References

1. Pui CH, Evans WE. Acute lymphoblastic leukemia. *N Engl J Med.* 1998 Aug 27; 339(9): 605-15.
2. Pui CH, Evans WE. Treatment of acute lymphoblastic leukemia. *N Engl J Med.* 2006 Jan 12; 354(2): 166-78.
3. Cooney DA, Handschumacher RE. L-asparaginase and L-asparagine metabolism. *Annu Rev Pharmacol.* 1970; 10: 421-40.
4. Asselin BL, Ryan D, Frantz CN, Bernal SD, Leavitt P, Sallan SE, et al. In vitro and in vivo killing of acute lymphoblastic leukemia cells by L-asparaginase. *Cancer Res.* 1989 Aug 1; 49(15): 4363-8.
5. Haskell CM, Canellos GP. L-asparaginase resistance in human leukemia--asparagine synthetase. *Biochem Pharmacol.* 1969 Oct; 18(10): 2578-80.
6. Holleman A, Cheok MH, den Boer ML, Yang W, Veerman AJ, Kazemier KM, et al. Gene-expression patterns in drug-resistant acute lymphoblastic leukemia cells and response to treatment. *N Engl J Med.* 2004 Aug 5; 351(6): 533-42.

THE EFFECTS OF ENRICHED ENVIRONMENT ON THE NEUROBEHAVIORAL DEFICITS INDUCED BY GLUTAMATE TOXICITY IN RATS

Gábor Horváth

E-mail: figgol@freemail.hu

Department of Anatomy, PTE-MTA Lendület PACAP Research Team, University of Pecs,
Pecs, Hungary

Coauthor: Gyongyver Vadasz

Tutors: Dora Reglodi, MD, PhD, DSc., Dr. Habil, Peter Kiss, MD, PhD

Introduction

Environmental enrichment is a popular strategy to enhance motor and cognitive performance and to counteract the effects of various harmful stimuli. The protective effects of enriched environment have been shown in traumatic, ischemic and toxic nervous system lesions.

The first description of the positive effects of environmental enrichment comes from the neuroscientist, Donald P. Hebb. In his paper in 1947, he described that the animals kept as pets, *i.e.*, under enriched environment, showed better performance in memory and learning tasks [1]. Since then, hundreds of experimental data have accumulated regarding environmental factors and their importance. Among others, enriched environment has been shown to influence the development of the nervous system including that of the visual system [2-4]. It is proven that environmental factors have a major influence on the outcome of different neuronal lesions [5] and so environmental enrichment is a popular strategy to counteract central nervous system injuries. Recently we have shown, for the first time, that environmental enrichment has a protective effect in neonatal lesion of the retina [6,7]. Numerous studies have proven that enriched environment can reduce lesions induced by toxic [8-10], ischemic and traumatic injuries. The mechanism underlying this protective effect includes stimulating synaptic plasticity and neurogenesis, increase of dendritic spines and stimulating the expression of neurotrophic factors like brain-derived neurotrophic factor, insulin-like growth factor and nerve growth factor.

Discussion

Several neurotoxicants are known to induce neurodegeneration and have negative behavioral consequences in the developing or adult brain. Among toxic lesions, lead-induced injury has been proven to be counteracted by environmental enrichment [9]. In our model we used monosodium-glutamate (MSG). This agent is also known as umami or E621 additive food flavoring agent. MSG has toxic effects only if it reaches the central nervous system in high concentration, which happens only in the newborn rodent brain (with subcutaneously MSG treatment on postnatal days 1, 5 and 9), when MSG can pass through the blood-brain barrier. Glutamate toxicity occurs through overexcitation of the N-methyl-D-aspartate (NMDA) receptors. This then leads to increased calcium ion influx and finally cell death. MSG toxicity in rodents is known to cause degeneration of the retina, optic nerve, arcuate nucleus and various parts of the cortex.

The development of newborn rats during the first three postnatal weeks follows a general pattern of reflex appearance and maturation of motor skills. Previously we have shown how different perinatal insults delay neurobehavioral development: most severe retardation was observed in hypoxia and asphyxia, while perinatal stress only led to minor changes. We have demonstrated that treating newborn rats with MSG delays the development of neurological reflexes and motor coordination skills.

Aims

The aim of our study was to investigate whether environmental enrichment alters neurobehavioral development and whether it provides protection against the neurobehavioral consequences of neonatal MSG toxicity.

Methods

For environmental enrichment, we placed rats in larger cages, supplemented with different toys that were altered daily. Normal control and enriched control rats received saline treatment only. Physical parameters such as weight, day of eye opening, incisor eruption and ear unfolding were recorded. Animals were observed for appearance of reflexes such as negative geotaxis, righting reflexes, fore- and hindlimb grasp, fore- and hindlimb placing, sensory reflexes and gait. In cases of negative geotaxis, surface righting and gait, the time to perform the reflex was also recorded daily. For examining motor coordination, we performed grid walking, footfault, footfault, rope suspension, rota-rod, inclined board and walk initiation tests.

Results

We found that enriched environment alone did not lead to marked alterations in the course of development. On the other hand, MSG treatment caused a slight delay in reflex development and a pronounced delay in weight gain and motor coordination maturation. This delay in most signs and tests could be reversed by enriched environment: MSG-treated pups kept under enriched conditions showed no weight retardation, no reflex delay in some signs and performed better in most coordination tests. These results show that environmental enrichment is able to decrease the neurobehavioral delay caused by neonatal excitotoxicity.

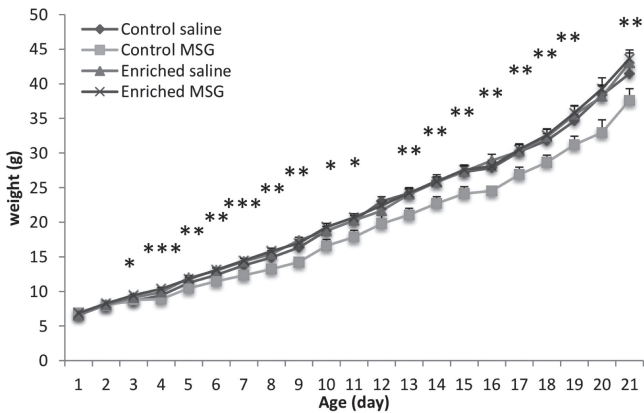


Figure 1. Daily changes in body weight (*: $p < 0.05$, **: $p < 0.01$, ***: $p < 0.001$ control monosodium glutamate (MSG) vs. all other groups).

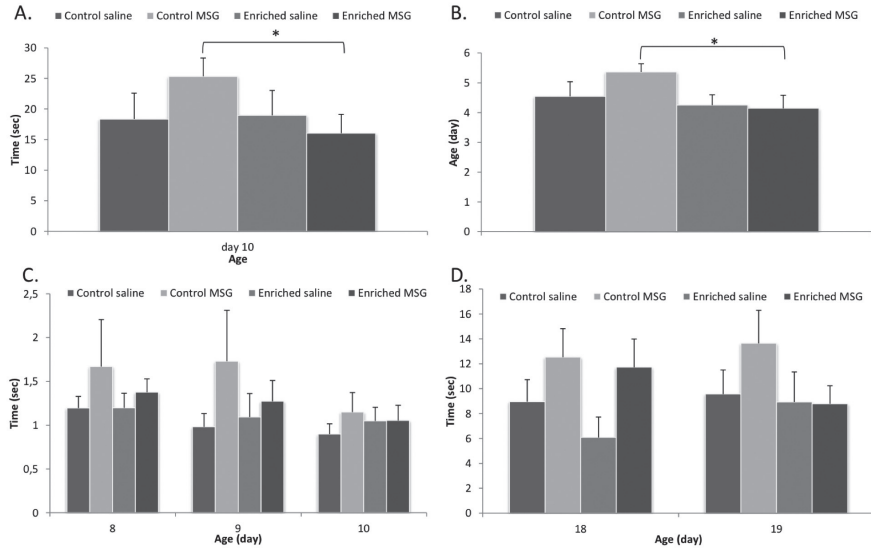


Figure 2. Development of reflex performance. (A) Gait performance; (B) Air righting reflex appearance; (C) Surface righting reflex performance; (D) Negative geotaxis performance (*: $p < 0.05$).

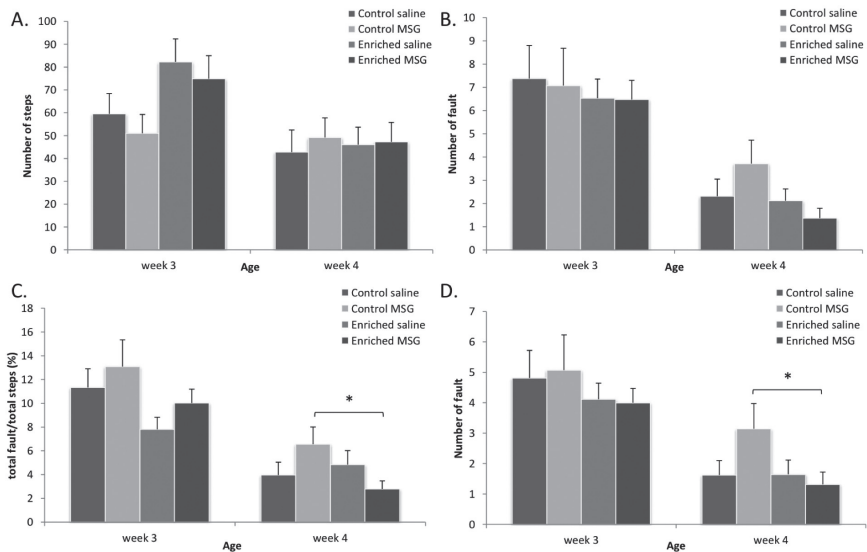


Figure 3. Motor coordination tests I: Grid walking and footfault test. (A) Number of total steps; (B) Number of total faults; (C) Total faults/total steps ratio; (D) Number of forelimb faults (*: $p < 0.05$).

Conclusions

Our results show that while raising pups in enriched environment does not considerably alter neurobehavioral development, it can decrease the delaying effects of the excitotoxic MSG treatment.

Summary:

In summary, our present results show that enriched housing conditions can reduce the delaying effects of the excitotoxic glutamate treatment on neurobehavioral development in newborn rat pups.

References

1. Hebb, D.O. The effects of early experience on problem solving at maturity. *Am. Psychol.* 1947, 2, 306-307.
2. Landi, S.; Ciucci, F.; Maffei, L.; Berardi, N.; Cenni, M.C. Setting the pace for retinal development: Environmental enrichment acts through insulin-like growth factor 1 and brain-derived neurotrophic factor. *J. Neurosci.* 2009, 29, 10809-10819.
3. Sale, A.; Cenni, M.C.; Ciucci, F.; Putignano, E.; Chierzi, S.; Maffei, L. Maternal enrichment during pregnancy accelerates retinal development of the fetus. *PLoS One* 2007, 2, e1160.
4. Ortuzar, N.; Argandoña, E.G.; Bengoetxea, H.; Lafuente, J.V. Combination of intracortically administered VEGF and environmental enrichment enhances brain protection in developing rats. *J. Neural Transm.* 2011, 118, 135-144.
5. Van Praag, H.; Kempermann, G.; Gage, F.H. Neural consequences of environmental enrichment. *Nat. Rev. Neurosci.* 2000, 1, 191-198.
6. Szabadfi, K.; Atlasz, T.; Horvath, G.; Kiss, P.; Hamza, L.; Farkas, J.; Tamas, A.; Lubics, A.; Gabriel, R.; Reglodi, D. Early postnatal enriched environment decreases retinal degeneration induced by monosodium glutamate treatment. *Brain Res.* 2009, 1259, 107-112.
7. Kiss, P.; Atlasz, T.; Szabadfi, K.; Horvath, G.; Griecs, M.; Farkas, J.; Matkovits, A.; Toth, G.; Lubics, A.; Tamas, A.; *et al.* Comparison between PACAP- and enriched environment-induced retinal protection in MSG-treated newborn rats. *Neurosci. Lett.* 2011, 487, 400-405.
8. Kazl, C.; Foote, L.T.; Kim, M.J.; Koh, S. Early-life experience alters response of developing brain to seizures. *Brain Res.* 2009, 1285, 174-181.
9. Schneider, T.; Lee, M.H.; Anderson, D.W.; Zuck, L.; Lidsky, T.I. Enriched environment during development is protective against lead-induced neurotoxicity. *Brain Res.* 2001, 896, 48-55.
10. Soeda, F.; Tanaka, A.; Shirasaki, T.; Takahama, K. An enriched environment mitigates the brain-disruptive effects of prenatal diethylstilbestrol exposure in mice. *Neuroscience* 2010, 169, 223-228.

A NOVEL METHOD FOR COMPUTER AIDED DIAGNOSTICS OF SCHIZOPHRENIA BASED ON MAGNETIC RESONANCE BRAIN IMAGES

Eva Janoušová

E-mail: janousova@iba.muni.cz

Institute of Biostatistics and Analyses at the Faculty of Medicine and the Faculty of Science of the Masaryk University, Brno, Czech Republic

Co-authors: D. Schwarz, G. Montana, T. Kašpárek

Tutor: Ing. Daniel Schwarz, Ph.D.

Introduction

Advances in medical imaging techniques have enabled identification of brain regions affected by schizophrenia (Shenton et al., 2001). There is also an effort to use medical images to help diagnostics of this disabling psychiatric disorder, as early and accurate diagnostics can significantly improve patient recovery rates and the overall prognosis (Perkins et al., 2005).

Algorithms proposed for diagnostics are based on classification of brain images of schizophrenia patients and healthy controls (HC). Due to large amount of imaging features, classification is often preceded by data reduction. So far, only few studies have presented complex pipelines for data reduction and classification, such as the COMPARE method (Fan et al., 2007), which showed promising results in discrimination of first-episode schizophrenia (FES) and chronic patients from HC (91.8% accuracy). However, only FES patients should be used in classification as medication affects brain structure in chronic patients and thus leads to over-optimistic results. Indeed, when the COMPARE algorithm was used for classification of FES patients and HC, the accuracy was only 73.4% (Zanetti et al., 2012).

The aim of this paper is to present a new data-driven complex pipeline for distinguishing FES patients from HC with high accuracy and thus aiding schizophrenia diagnostics.

Methods

The proposed data-driven complex pipeline is based on combining deformation-based morphometry (DBM) with penalised regression with resampling (PRWR). In DBM, high-resolution nonlinear registration of 3-D brain images with a digital brain atlas is performed (Schwarz et al., 2007). The resulting 3-D deformations clearly show how the brain anatomy of a subject differs from the normal template anatomy in terms of local volume contractions and expansions.

After logarithmic transformation, the 3-D deformations are transformed into 1-D vectors and arranged in $(n \times p)$ matrix \mathbf{X} , where n and p are numbers of individuals and imaging features, respectively. Class labels of each subject (1 stands for patients and 0 for controls) are arranged to $(n \times 1)$ vector \mathbf{y} . The \mathbf{X} and \mathbf{y} are used in PRWR for identification of brain regions most discriminating FES patients and HC. Specifically, both \mathbf{y} and \mathbf{X} are inputs into a regression model $\mathbf{y} = \mathbf{X}\boldsymbol{\beta} + \boldsymbol{\varepsilon}$. The aim is to estimate regression coefficients $\boldsymbol{\beta} = (\beta_1, \dots, \beta_p)$ such that the model would enable to select most discriminating imaging features, while correlated features would be selected in groups. Therefore, elastic net penalty (Zou and Hastie, 2005) is used here as it consists of l_1 (lasso) penalty which enables selection of the imaging features (Tibshirani, 1996), and l_2 (ridge) penalty which induces a grouping effect on correlated variables (Zou and Hastie, 2005). The $\hat{\boldsymbol{\beta}}$ estimates are found by following formula:

$$\operatorname{argmin}_{\boldsymbol{\beta}} \{ \|\mathbf{y} - \mathbf{X}\boldsymbol{\beta}\|_2^2 + \lambda \|\boldsymbol{\beta}\|_1 + \mu \|\boldsymbol{\beta}\|_2^2 \}, \quad (1)$$

where $\lambda > \mu$ and $\mu > 0$ are regularization parameters introduced for the l_1 and l_2 penalties, respectively, and $\kappa = (1 + \mu)^{-1}$ corrects for double shrinkage caused by applying both penalties. After re-writing the

Equation (1) and setting μ to infinity, whilst still maintaining the grouping effect (Zou and Hastie, 2005), the regression coefficients \mathbf{b} are estimated using:

$$\hat{\beta}_j = \text{sign}(\mathbf{x}'_j \mathbf{y}) \left(|\mathbf{x}'_j \mathbf{y}| - \lambda/2 \right)_+, \quad (2)$$

where $(\alpha)_+$ is defined as $\max(0, \alpha)$, $\mathbf{x}'_j, j = 1, \dots, p$ is a column vector in the matrix \mathbf{X} , and λ controls the amount of imaging features selected as most discriminative between patients and HC. Specifically, when λ is zero, all features are selected. As λ increases, fewer features are selected. To find optimal λ a resampling method proposed for sparse predictive modelling (Meinshausen and Bühlmann, 2010) was applied. This resampling procedure aims to calculate selection probabilities for features by repeatedly fitting the penalised regression model on random subsets of the dataset, while keeping track of the selected features. The final set of the most discriminative features consists of those with selection probability higher than 0.5. The selected features are then used for classification of individuals as patients or HC using linear discriminant analysis.

Results

The proposed classification pipeline was tested in an experiment with T1-weighted magnetic resonance brain images of 52 male FES patients and 52 sex- and age-matched healthy subjects. The median age of the patients and controls was 22.9 (range 17-40) and 23.0 (range 18-38) years, respectively. All subjects signed an informed consent before entering the study.

The classification efficiency of the proposed algorithm was evaluated with the leave-one-out cross-validation technique to avoid biased results. The performance measures, namely accuracy, sensitivity and specificity, obtained in classification of the 104 subjects are summarized in Table 1. Our results demonstrate that the accuracy is stable for various values of λ . The best cross-validated accuracy was 85.6% (sensitivity 84.6%, specificity 86.5%) while selecting about 30000 most discriminative imaging features, which are visualized in Figure 1. The selected features form connected regions in the left prefrontal cortex, the right anterior insula, the medial parts of the thalamus, and the cerebellar cortex.

λ	Number of features	Accuracy	Sensitivity	Specificity
0.3	315 123	82.7	84.6	80.8
0.4	107 967	84.6	86.5	82.7
0.5	30 461	85.6	84.6	86.5
0.6	5 113	83.7	78.8	88.5

Table 1. Number of selected imaging features and cross-validated classification performance measures in percentage for various λ values.

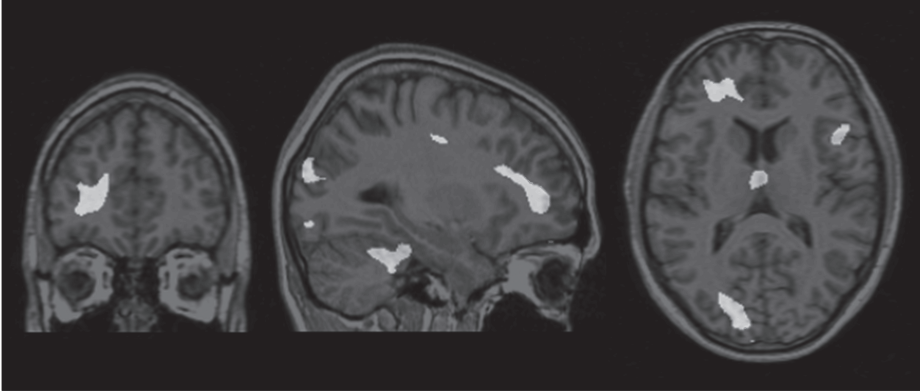


Figure 1. Coronal, transversal and sagittal slices showing the automatically detected highly discriminative imaging features between FES patients and HC (in white).

Discussion

A classification pipeline for discriminating FES patients from healthy individuals based on brain images has been presented here. The data-driven algorithm consisted of DBM and PRWR and enabled identification of most discriminating imaging features as well as subject discrimination. The features identified using magnetic resonance images of 52 FES patients and 52 HC were located in regions in the left prefrontal cortex, the right anterior insula, the medial parts of the thalamus, and the cerebellar cortex. It is known that these brain regions are involved in higher cognitive, integrative and regulatory functions that are impaired in schizophrenia (Shenton et al., 2001). High classification accuracy (85.6%), sensitivity (84.6%) and specificity (86.5%) have been achieved in the experiment with the 104 subjects. The efficiency of the algorithm is superior to results published by Zanetti et al. (2013).

Conclusion

In conclusion, the connections between discriminating morphology features and their significance for the neurobiology of schizophrenia and the high accuracy of classification of patients and healthy controls demonstrate the face validity of the approach combining DBM and PRWR for distinguishing FES patients from healthy subjects.

Summary

This paper presents a new data-driven classification pipeline for discriminating patients with first-episode schizophrenia from healthy subjects based on medical images of their brain. The proposed method comprising deformation-based morphometry and penalised regression with resampling identified brain-imaging biomarkers localised in the left prefrontal cortex, right anterior insula, medial parts of the thalamus, and cerebellar cortex, which are brain areas involved in higher cognitive, integrative and regulatory functions that are impaired in schizophrenia. Moreover, the method distinguished 52 first-episode schizophrenia patients from 52 healthy controls with accuracy of 85.6%, sensitivity of 84.6%, and specificity of 86.5%.

References

1. Fan Y, Dinggang S, Ruben CG et al.: COMPARE: Classification of morphological patterns using adaptive regional elements. *IEEE Trans Med Imaging* 2007; 26, 93-105.
2. Hoerl AE and Kennard RW: Ridge regression - applications to nonorthogonal problems. *Technometrics* 1970; 12, 69-82.
3. Meinshausen N and Bühlmann P: Stability Selection. *J R Stat Soc* 2010; 72, 417-473.
4. Perkins DO, Gu HB, Boteva K et al.: Relationship between duration of untreated psychosis and outcome in first-episode schizophrenia: A critical review and meta-analysis. *Am J Psych* 2005; 162, 1785-1804.
5. Shenton ME, Dickey CC, Frumin M et al.: A Review of MRI findings in schizophrenia. *Schizophr Res* 2001; 49, 1-52.
6. Schwarz D, Kasperek T, Provaznik I et al.: A deformable registration method for automated morphometry of MRI brain images in neuropsychiatric research. *IEEE Trans Med Imaging* 2007; 26, 452-461.
7. Tibshirani R: Regression shrinkage and selection via the lasso. *J R Stat Soc* 1996; 58, 267-288.
8. Zanetti MV, Schaufelberger MS, Doshi J et al.: Neuroanatomical pattern classification in a population-based sample of first-episode schizophrenia. *Prog Neuropsychopharmacol Biol Psychiatry* 2013; 43, 116-125.
9. Zou H, Hastie T: Regularization and variable selection via the elastic net. *J R Stat Soc* 2005; 67, 301-320.

CHARACTERISTICS OF PATIENTS WITH CARDIORENAL SYNDROME ADMITTED TO OUR DEPARTMENT

Lucia Jedličková

E-mail: lucia.jedlickova@gmail.com

1st Department of Internal Medicine, Faculty of Medicine,
Pavol Jozef Šafárik University in Košice,
Louis Pasteur University Hospital in Košice, Slovak Republic

Co-authors: L. Jacková, L. Merkovská, T. Lopuchovský, K. Brúsiková, J. Fedáčko
Tutor: prof. MUDr. Daniel Pella, Ph.D.

Introduction

Cardiorenal syndrome was firstly officially defined at a consensus conference of the Acute Dialysis Quality Initiative (ADQI) in 2008, as a disorder of the heart and kidneys whereby acute or chronic dysfunction in one organ may induce acute or chronic dysfunction of the other. It is classified into five subtypes: Acute cardio-renal syndrome (type 1): acute worsening of heart function leading to kidney injury and/or dysfunction. Chronic cardio-renal syndrome (type 2): chronic abnormalities in heart function leading to kidney injury or dysfunction. Acute reno-cardiac syndrome (type 3): acute worsening of kidney function leading to heart injury and/or dysfunction. Chronic reno-cardiac syndrome (type 4): chronic kidney disease leading to heart injury, disease and/or dysfunction. Secondary cardio-renal syndrome (type 5): systemic conditions leading to simultaneous injury and/or dysfunction of heart and kidney (1,2). Our goal was to identify the characteristics of patients with cardiorenal syndrome admitted to our department.

Methods

We analyzed retrospectively history, clinical, anthropometric, biochemical and treatment characteristics of patients admitted to our department (from January to December 2010) and diagnosed with cardiorenal syndrome according to ADQI definition (1). We calculated estimated glomerular filtration (eGFR) by Cockcroft-Gault formula and MDRD formula (Modification of Diet in Renal Disease, variation GFRMDRD186) (3,4).

Results

Out of all admitted patients, 124 (10,22%) were diagnosed with cardiorenal syndrome. 65 (52,4%) were males, mean age of the patients was $74,2 \pm 9,3$ years, mean length of their hospitalization was $7,9 \pm 2,9$ days. 119 had arterial hypertension, 121 had ischemic heart disease, 75 had diabetes mellitus. Mean left ventricular ejection fraction was $40,23 \pm 12,5\%$. Cardiorenal syndrome type 1 had only 3 patients, type 2 had 25 (20%) patients, type 4 had 11 patients and type 5 had 85 (68,5%) patients. There were no patients with cardiorenal syndrome type 3. The most prescribed medication were beta-blockers (76%) and furosemide (65,3%), 56 (45,1%) patients were treated with the inhibitors of renin angiotensin system. Only 2 patients were treated with hemodialysis and only in 5 cases dobutamine was used.

Conclusion

Cardiorenal syndrome was frequent among older patients admitted to our department. The mean age was $74,2 \pm 9,3$ years. The most common was type 5 (68,5%), and the most common reason for hospitalisation was chronic heart failure (48%). Coexistence of cardiac and renal diseases significantly increases morbidity and mortality (1). It is important to recognize cardiorenal syndrome early to optimize the management of patient with both conditions.

	Type 1 n= 3 (2,4%)	Type 2 n=25 (20%)	Type 4 n=11 (8,8%)	Type 5 n=85 (68,5%)	All n=124
Age (years)	78,3 ± 11,6	75,12 ± 11,7	70,3 ± 9,1	75,7 ± 9,0	74,2 ± 9,3
Sex (M/F)	2/1	13/12	5/6	45/40	65/59
Hemoglobine (g/dl)	12,8 ± 2,0	12,18 ± 1,8	10,7 ± 1,9	11,8 ± 2,2	11,87 ± 2,1
Total protein (g/l)	68,45 ± 2,4	63,8 ± 8,6	59,6 ± 2,9	65,2 ± 6,0	64,26 ± 6,5
Albumin (g/l)	42,1 ± 8,7	38,4 ± 5,3	37,4 ± 2,5	38,3 ± 5,0	39,05 ± 4,9
Systolic BP (mmHg)	141,6 ± 25,6	126,16 ± 24,7	124,5 ± 15,5	137,3 ± 25,6	132,39 ± 24,9
Diastolic BP (mmHg)	80,0 ± 10,0	77,72 ± 13,3	75,1 ± 9,5	81,7 ± 11,6	78,63 ± 11,8
LVEF (%)	45,0 ± 13,2	36,6 ± 10,7	47,5 ± 7,2	43,1 ± 13,1	40,23 ± 12,5
Duration of hospitalisation (days)	7,3 ± 1,5	8,2 ± 2,6	7,5 ± 3,3	7,8 ± 3,0	7,9 ± 2,9

Table 1. Basic data of patients with cardiorenal syndrome

	Type 1 n= 3 (2,4%)	Type 2 n=25 (20%)	Type 4 n=11 (8,8%)	Type 5 n=85 (68,5%)	All n=124
Creatinine (µmol/L)	164,5 ± 47,5	133,7 ± 39,7	210 ± 114,5	140,8 ± 76,9	162,25 ± 76,6
GFR-Cockcroft-Gault (ml/min)	22,18 ± 0	46,76 ± 20,7	40,5 ± 16,3	51,28 ± 23,6	40,18 ± 22,7
GFR-MDRD 186 (ml/min/1,73 m ²)	28,15 ± 9,9	43,7 ± 11,6	32,6 ± 15,4	48,8 ± 17,0	38,31 ± 16,2

Table 2. Glomerular filtration in cardiorenal syndrome (GFR)

%	Type 1 n= 3 (2,4%)	Type 2 n=25 (20%)	Type 4 n=11 (8,8%)	Type 5 n=85 (68,5%)	All n=124
Arterial hypertension	100	84	100	97	95
Smoking	0	12	27	0	10
Ischaemic heart disease	100	92	100	98	97
Peripheral arterial disease	0	12	0	12	12
Diabetes mellitus	33	32	63	69	60
Cerebrovascular disease	0	40	18	22	25

Table 3. Anamnesis of patients with cardiorenal syndrome

References

1. Ronco C, McCullough P, Anker SD et al.: Cardio-renal syndromes: report from the consensus conference of the Acute Dialysis Quality Initiative. *European Heart Journal* 2010; 31, 703–711.
2. Waldum B, Os I.: The Cardiorenal Syndrome: What the Cardiologist Needs to Know. *Cardiology* 2013;126, 175-186.
3. Cockcroft DW, Gault MH.: Prediction of creatinine clearance from serum creatinine. *Nephron* 1976; 16, 31-41.
4. Levey AS, Greene T, Kusek JW, Beck GJ.: A simplified equation to predict glomerular filtration rate from serum creatinine. *J Am Soc Nephrol* 2000; 11, 155A.

MITOCHONDRIAL MEMBRANE ASSEMBLY AND MULTIPLE FORMS OF TMEM70 PROTEIN

Hana Kratochvílová

E-mail: hana.kratochvilova@lf1.cuni.cz

Department of Pediatrics and Adolescent Medicine, Laboratory for Study Mitochondrial Disorders, First Faculty of Medicine, Charles University and General University Hospital in Prague, Czech Republic.

Co-authors: Kateřina Hejzlarová, Marek Vrbacký, Tomáš Mráček, Vendula Karbanová, Markéta Tesařová, Adriána Gombitová, Dušan Cmarko, Ilka Wittig, Jiří Zeman and Josef Houštěk

Tutor: Ing. Markéta Tesařová, PhD

Introduction

TMEM70 is protein functioning as specific, ancillary factor of mammalian ATPsynthase and is uniquely specific for higher eukaryotes. Its absence results in an isolated decrease of the content of fully assembled ATPsynthase and reduction of enzyme activity. Mutation in TMEM70 factor represents the frequent cause of fatal mitochondrial disease, autosomal recessive encephalo-cardiomyopathy (Cizkova et. al, 2008). TMEM70 is a 21 kDa mitochondrial protein of the inner mitochondrial membrane synthesized as a 29 kDa precursor. It contains two putative transmembrane regions in the central part of the structure (Hejzlarova et. al, 2011).

Aims

The aims of the present study were to determine topology of TMEM70 protein in the inner mitochondrial membrane, native forms and interaction with ATPsynthase using C-tagged forms of TMEM70 protein (TMEM70-GFP, TMEM70-FLAG, TMEM70-MYC-FLAG) expressed in HEK293 cells.

Methods

The membrane topology of protein TMEM70 was studied by two different approaches: digestion test with trypsin protease and test with dye Trypan Blue, quanching fluorescence signal. Blue native electrophoresis analysis in first dimension (BN-PAGE) and second dimension (BN-PAGE/SDS-PAGE) were used to explore native forms of TMEM70 protein in model cells. Two different immunoprecipitaion procedures (anti-FLAG immunoprecipitation, ATP-synthase immunocapture test) and immunogold analysis were used to investigated possible interaction of TMEM70 and ATPsynhtase.

Results

Based on accessibility to trypsin (Fig. 1) or membrane-impermeable dye Trypan Blue we demonstrated that TMEM70 protein has a hairpin structure with N- and C- termini oriented towards mitochondrial matrix. These findings is in accordance with the previously bioinformatic predictions (Jonckheere et. al, 2011). When solubilized with mild detergents and resolved by BN-PAGE, TMEM70 is detected in multiple homooligomeric forms, dimers and higher oligomers. Variable portion of tagged TMEM70 is found in high molecular weight region, partly overlapping with assembled ATP synthase. Extensive immunoprecipitation studies as well as immunogold electron microscopy analysis confirmed interactions between TMEM70 molecules but no direct interactions with ATP synthase subunits.

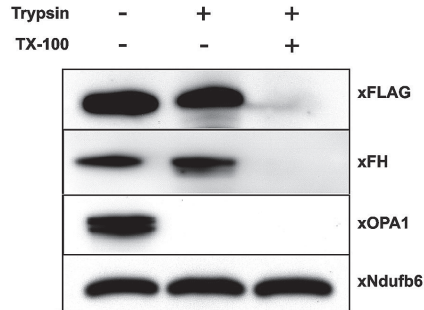


Fig. 1. Freshly isolated mitochondria from HEK293 cells expressing *TMEM70_FLAG* were swollen using hypotonic medium to disrupt outer mitochondrial membrane but keeping the inner mitochondrial membrane intact. The swollen mitochondria were incubated with/without trypsin and with/without TRITON X-100. Samples were separated by 12% SDS-PAGE and immunoblotted with antibodies. *OPA1* (located in the inner mitochondrial membrane facing the intermembrane space) was completely digested when trypsin was added, whereas *TMEM70_FLAG* and *FH* (located in matrix) was completely protected from trypsin digestion. *NDUFB6* was used as loading control (protein protected before trypsin digestion by structure of complex I).

Discussion and conclusion

In conclusion *TMEM70* protein is with its both terminus facing to the mitochondrial matrix. In cells is present in several higher oligomeric forms and there is no evidence of interaction *TMEM70* and ATPsynthase subunits, indicating that the biological function of *TMEM70* in ATPsynthase biogenesis may be mediated through interaction with some other protein.

Acknowledgment

This work was supported by the grants UNCE 204011, IGA MZ ČR NT13114-4 and RVO-VFN64165/2012.

References

1. Cízková A, Stránecký V, Mayr JA, Tesarová M, Havlíčková V, Paul J, Ivánek R, Kuss AW, Hansíková H, Kaplanová V, Vrbacký M, Hartmannová H, Nosková L, Honzík T, Drahotka Z, Magner M, Hejzlarová K, Sperl W, Zeman J, Houstek J, Kmoch S.: *TMEM70* mutations cause isolated ATP synthase deficiency and neonatal mitochondrial encephalomyopathy. *Nature Genet.* 2008; 40, 1288-90.
2. Hejzlarová K, Tesařová M, Vrbacká-Čížková A, Vrbacký M, Hartmannová H, Kaplanová V, Nosková L, Kratochvílová H, Buzková J, Havlíčková V, Zeman J, Kmoch S, Houštěk J.: Expression and processing of the *TMEM70* protein., *Biochim Biophys Acta.* 2011; 1807, 144-9.
3. Jonckheere AI, Huijsloot M, Lammens M, Jansen J, van den Heuvel LP, Spiekerkoetter U, Kleist-Retzow JC, Forkink M, Koopman WJ, Szklarczyk R, Huynen MA, Fransen JA, Smeitink JA, Rodenburg RJ.: Restoration of complex V deficiency caused by a novel deletion in the human *TMEM70* gene normalizes mitochondrial morphology. *Mitochondrion.* 2011; 11: 954-63.

DIFFERENTIATION OF NEURAL CREST CELLS FROM HUMAN EMBRYONIC STEM CELLS AND THEIR ODONTOGENIC INDUCTION

Jan Křivánek

E-mail: kriv.jan@gmail.com

Department of Histology and Embryology, Masaryk University,
Faculty of Medicine in Brno, Czech Republic

Co-authors: K. Souček, R. Fedr, E. Švandová, E. Matalová

Tutor: doc. MVDr. Aleš Hampl, CSc.

Introduction

Neural Crest (NC) cells are transient, multipotent cell population with migratory ability and originate from neural plate borders fusion, which occurs during neural tube invagination. NC cells give rise to many different cell types such as Schwann cells, melanocytes, connective tissue cells or odontoblasts. From this point of view NC cells can be an interesting aim in stem cell therapy.

Aims

- Differentiation of NC cells from human Embryonic Stem (hES) cells and optimization of cultivating conditions
- Molecular and functional characterisation of the obtained cells
- Quantification of expression of early odontogenesis characteristic markers after FGF8 application

Methods

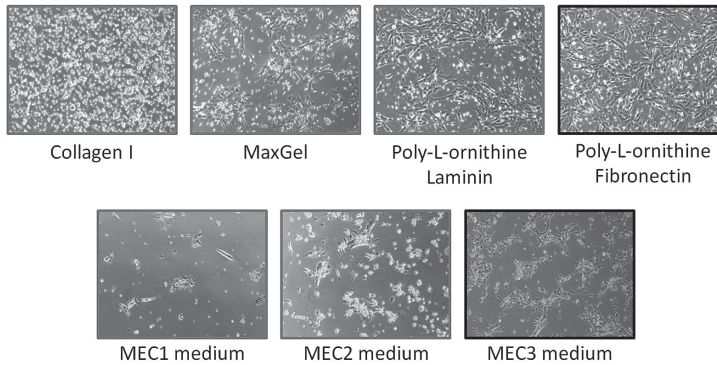
hES cells were differentiated according to a protocol published by Lee *et al.* 2007 (later innovated by Kim *et al.* 2012). Heterogeneous cell population was obtained. From this population NC cells were sorted by FACS (Fluorescence-Activated Cell Sorting) based on immunological CD271 (LNGFR, Low-Affinity Nerve Growth Factor Receptor; marker of NC cells) staining. Subsequently expression of other proteins characteristic for NC cells was determined at these sorted cells by immunocytochemistry and flow cytometry. Besides molecular characterisation, functional characterisation of connective tissues differentiation was carried out. Finally, expression of early odontogenesis markers was quantified after specific differentiation inductors treatment at mRNA level by qRT-PCR (Quantitative Real-Time Polymerase Chain Reaction) method.

hES cells lineage CCTL14 (Centre of Cell Therapy Line 14) was used for NC cells differentiation. A method of direct differentiation through dual SMAD inhibition (Lee *et al.* 2007, Kim *et al.* 2012) was used. Undifferentiated hES cells were propagated on extracellular matrix (Matrigel™, BD 354234) until cell confluence reached 60 % of culture dish. In this phase SMAD inhibitors (10µM SB431542, 500 ng/ml NOGGIN) were added into cultivating media and the differentiation itself started. KSR (Knockout Serum Replacement) medium, in which the cells were cultivated at the beginning of differentiation, was gradually replaced with MEC media – media for long-term NC cell propagation. Three different MEC media (MEC1-3) were used for cultivation. The composition of MEC1 and MEC2 was described in previous works (Lee *et al.* 2007, Kim *et al.* 2012) and MEC3 medium was designed by our group. The main difference in MEC3 media is addition of non-essential amino acids, β-mercaptoethanol, higher concentration of growth factors FGF2 and EGF.

After 12 days of differentiation NC cells were sorted according to CD271 (antibody: FITC conjugated, anti-human CD271, Biolegend #345104) expression on BD FACSAria II instrument and subsequently a CD271 positive population was cultivated.

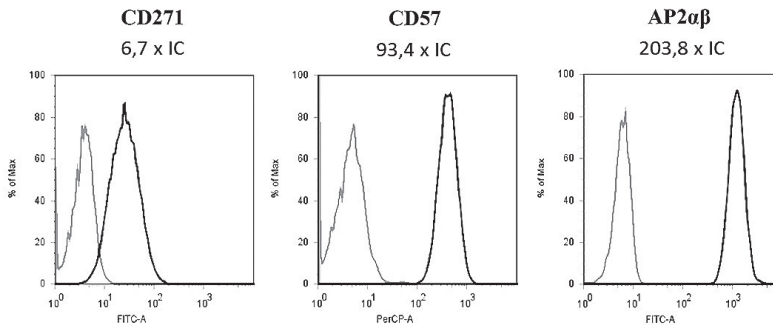
Results

After 12 days of differentiation the cells were seeded on MaxGel (MaxGel™ ECM, Sigma E0282) coated dishes. However, these cells were not phenotypically stable and a lot of them (20-30 %) died of anoikis. That is why alternative surface coating was tested. Cells cultivated on Poly-L-ornithine/Fibronectin coating grow fast and maintain homogeneity during time. Poly-L-ornithine/Laminine coating also provides good grow, but with no homogeneity. Collagen I is absolutely unsuitable for cultivating these cell, the cells do not attach to this surface. MEC3 was the best one of the cultivating media tested, because of low amount of dying cells, fast growth and homogeneity of cell population. Influence of different coating and cultivating media can be seen in picture 1.



Picture 1. Influence of different dishes coating and media

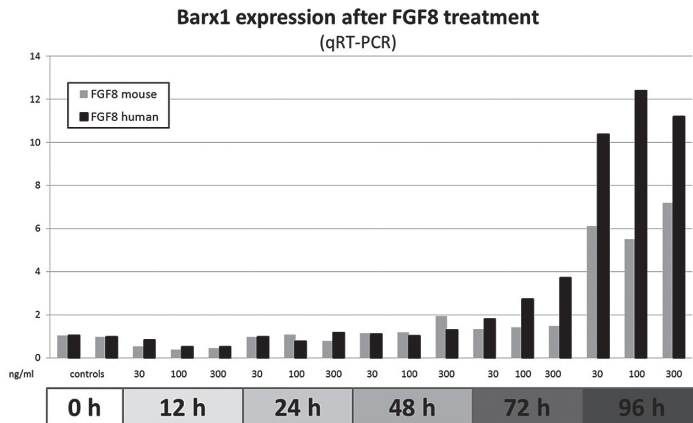
Expression of some characteristic molecular markers of NC cells was elucidated. SOX9 (transcription factor, skeletal development) and SOX10 (transcription factor, neural crest and peripheral nervous system development) expression was detected by immunocytochemistry and CD271, CD57 (HNK1, modulate cell adhesion in neural cells) and AP2 (transcription factor, expressed during eye, face or neural tube development) by flow cytometry. Expression of CD271, CD57 and AP2 α is depicted in flow cytometry graph in picture 2.



Picture 2. Expression of CD271, CD57 and AP2 α in differentiated cells measured by flow cytometry method. Grey (on the left side) line represents the intensity of fluorescence of isotype control and dark (on the right side) the intensity of fluorescence of specific antibody stained cells. Results are in folds of isotype control. Axis x is logarithmic scale.

These cells can be differentiated into adipogenic lineage. After 3 weeks in adipogenic differentiation medium and oil red O staining red coloured lipid granules can be seen in the cells.

BARX1 is homeobox gene expressed during early odontogenesis. It plays role in the development of teeth and craniofacial mesenchyme of neural crest. Increased expression at mRNA level was found out after treatment with FGF8 (Fibroblast Growth Factor 8, key molecule initiating signalling from dental epithelia to neural crest). Increased BARX1 expression was detected after 72 and more significantly after 96 hours after the beginning of the treatment, as can be seen in picture 3.



Picture 3. BARX1 expression after FGF8 treatment

Discussion

Although increased expression of BARX1 gene was observed, expression of other homeobox genes participating in odontogenic induction, such as DLX2, MSX1, PAX9, was not detected. Currently, the stimulation of differentiated cells with other signalling molecules is being studied. Increased BARX1 expression was also detected during mouse FGF8 treatment, which is important especially for the process of co-cultivation of these cells with mouse embryonic dental epithelia in order to prove ability of forming functional odontoblast.

Conclusion

In this study differentiation of hES cells toward cells possessing molecular (expression of characteristic proteins) and functional (adipogenic differentiation) signs of neural crest cells was introduced. Cultivating conditions were optimised for these cells – combination of new MEC3 medium, Poly-L-ornithine and Fibronectin coating. Under these conditions the cells can be cultivated long-term. Expression of BARX1 homeobox gene was upregulated after FGF8 treatment.

Summary

The presence of neural crest is a crucial step in (vertebrate) evolution. NC cells participate in development of many organs, wrong function of these cells is connected with congenital diseases such as Waardenburg or DiGeorge syndrome. Proper understanding of neural crest function in developing organism can provide a powerful tool for regenerative medicine. This is the first study dedicated to differentiation of hES cells into odontogenic lineage and suggests the way of next investigations and future clinical application.

References

1. Lee G, Kim H, Elkabetz Y, Al Shamy G, Panagiotakos G, Barberi T, Tabar V and Studer L.: Isolation and directed differentiation of neural crest stem cells derived from human embryonic stem cells. *Nat Biotechnol* 2007; 25(12), 1468-1475.
2. Kim H, Lee G, Chambers S, Tomishima M. a Studer L. Derivation of neural crest cells from human pluripotent stem cells. 2012. *Nature Protocol*.

EVALUATION OF SERUM LEVELS OF MULTIPLE CYTOKINES AND ADHESION MOLECULES IN PATIENTS TREATED FOR ACUTE MYELOID LEUKEMIA

Tomáš Kupsa

E-mail: Tomas.Kupsa@seznam.cz

Department of Field Internal Medicine, University of Defence, Faculty of Military Health Sciences in Hradec Králové, Czech Republic

4th Department of Internal Medicine – Hematology, Charles University in Prague, Faculty of Medicine in Hradec Králové, Czech Republic

Tutor: doc. MUDr. Jan M. Horáček, Ph.D.

Introduction

Acute myeloid leukemia (AML) shows a high degree of heterogeneity owing to a variety of mutations and mechanisms involved in leukemogenesis. Standard prognostic indicators as cytogenetics and molecular genetics^{1,2} often do not fully reflect the course of the disease and patient outcome. Cytokines and adhesion molecules also play a role in leukemogenesis, AML cell persistence, extramedullary infiltration and treatment outcome. The role of cytokines in AML has been reviewed recently³. Modulation of the cytokine network and adhesive interactions can disrupt signalling pathway activation and overcome the high resistance to treatment and improve outcomes of AML treatment. Further knowledge gained from multiple cytokine and adhesion molecule analysis should allow more precise risk stratification and better disease management. This research activity follows the recently published pivotal trial performed by our group⁴.

Aims

The aim of our study was to evaluate baseline serum levels of multiple cytokines and adhesion molecules in a context of respected prognostic indicators in patients treated for AML.

Methods

A total of 47 newly diagnosed AML patients, 17 males and 30 females, mean age 52.4 ± 13.4 , median 54.9 years, 10 low risk, 8 intermediate-1 risk, 12 intermediate-2 risk and 17 high risk, treated with “3+7” induction chemotherapy, followed by “HiDAC” consolidation alone or escalated with high-dose chemotherapy “FLAG-Ida” and allogeneic hematopoietic stem cell transplantation in 28 cases (preparative regimen Bu/Flu/ \pm ATG), were studied. We evaluated serum levels of the following 17 cytokines and 5 adhesion molecules: interleukins (IL-1 α , IL-1 β , IL-2, IL-3, IL-4, IL-6, IL-7, IL-8, IL-10, IL-12, IL-13, IL-23), vascular endothelial growth factor (VEGF), tumor necrosis factor- α (TNF- α), interferon- γ (IFN- γ), epidermal growth factor (EGF), monocyte chemoattractant protein-1 (MCP-1), E-selectin, L-selectin, P-selectin, intercellular adhesion molecule-1 (ICAM-1), vascular cell adhesion molecule-1 (VCAM-1). All biomarkers were measured by biochip array technology on Evidence Investigator analyzer (Randox) in sera collected at the diagnosis of AML. Biochip array technology enables simultaneous detection of multiple cytokines and adhesion molecules in a single sample and provides valuable information relating to each tested analyte and possible associations between analytes in each sample. The levels of cytokines and adhesion molecules were compared with defined prognostic indicators and course of the disease. Probability values (p) < 0.05 were considered statistically significant.

Results

All the patients' samples were collected after exclusion of clinically manifest infection, the differences in CRP levels were not significant in any analysis performed.

Comparing the whole group of newly diagnosed AML patients with a control group of healthy individuals (blood donors), significant increase in IL-6 (14.05 ± 13.23 ng/L vs. 0.52 ± 0.25 ng/L, $p < 0.05$), VCAM-1 (730 ± 293 ug/L vs. 328 ± 62 ug/L, $p < 0.005$), ICAM-1 (352 ± 137 ug/L vs. 197 ± 30 ug/L, $p < 0.005$) and L-selectin (2572 ± 978 ug/L vs. 1104 ± 210 ug/L, $p < 0.000005$) and decrease in IL-1 β (0.99 ± 0.64 ng/L vs. 2.23 ± 2.21 ng/L, $p < 0.05$), IL-2 (3.14 ± 2.59 ng/L vs. 6.28 ± 3.24 ng/L, $p < 0.01$) and IL-4 (1.51 ± 1.04 ng/L vs. 3.27 ± 1.47 ng/L, $p < 0.0005$) levels was found. Very similar results were obtained from analysing any of defined prognostic subgroups itself when compared to control group.

The de novo AML patients ($n=34$) differed from secondary AML patients ($n=13$) in higher IL-2 (3.88 ± 2.65 ng/L vs. 1.19 ± 1.19 ng/L, $p < 0.05$), lower IL-7 (4.16 ± 2.42 ng/L vs. 9.03 ± 8.42 ng/L, $p < 0.05$) levels and age (49.3 ± 14.2 vs. 60.6 ± 7.6 years).

Patients with initial hyperleukocytosis ($n=8$) had higher levels of IL-1 β (2.22 ± 1.12 ng/L vs. 0.74 ± 0.45 ng/L, $p=0.00001$), IL-10 (10.35 ± 8.93 ng/L vs. 3.05 ± 2.85 ng/L, $p < 0.05$), TNF- α (5.84 ± 4.31 ng/L vs. 2.18 ± 1.05 ng/L, $p < 0.0005$), VCAM-1 (1260 ± 638 ug/L vs. 622 ± 174 ug/L, $p=0.0001$), E-selectin (38.4 ± 13.5 ug/L vs. 20.7 ± 14.9 ug/L, $p < 0.05$) and L-selectin (3309 ± 265 ug/L vs. 2421 ± 1016 ug/L, $p < 0.05$), and lower levels of MCP-1 (117 ± 61 ng/L vs. 225 ± 114 ng/L, $p < 0.05$) and INF- γ (0.39 ± 0.35 ng/L vs. 2.20 ± 1.67 ng/L, $p < 0.05$).

In elderly patients (age over 65 years, $n=15$) an increase in IL-6 (23.34 ± 23.33 ng/L vs. 9.70 ± 8.86 ng/L, $p < 0.05$) and decrease in IL-12 (0.85 ± 1.13 pg/L vs. 4.36 ± 3.99 pg/L, $p < 0.05$) and IL-13 (2.03 ± 3.24 ng/L vs. 5.27 ± 4.21 ng/L, $p < 0.05$) levels was found. These patients were excluded from further analyses.

Finally, we analyzed a group of 22 patients who either survive without disease progression for at least 6 months after completion of chemotherapy or allogeneic hematopoietic stem cell transplantation, or relapsed. Those patients who are doing well ($n=12$) had higher IL-1 β (1.12 ± 0.65 ng/L vs. 0.34 ± 0.43 ng/L, $p < 0.05$) and lower VCAM-1 (569 ± 158 ug/L vs. 823 ± 226 ug/L, $p < 0.05$) and ICAM-1 (263 ± 46 ug/L vs. 422 ± 168 ug/L, $p < 0.05$) levels at the time of diagnosis. Furthermore, we found moderate correlation between IL-1 β ($r = 0.42$) and inverse correlations between VCAM-1 ($r = -0.49$) and E-selectin ($r = -0.41$) and progression free survival. Out of these 12 well doing patients, 7 belong to low + intermediate-1 and 5 to intermediate-2 + high risk subgroup.

Comparing cytokine and adhesion molecule profile among subgroups of patients organized according to standard risk stratification has not revealed any statistically significant differences.

Discussion

Analysing this group as a whole, same as analysing defined prognostic subgroups, reveals changes associated with the activity of the disease⁴. To assess the possible cytokine-mediated changes, exact subgroups of patients, comprising patients from various prognostic subgroups according to standard indicators, need to be analysed. The prognostic stratification of AML according to cytogenetics and molecular genetics was validated in large cohorts of patients, where individual changes disappear in the majority. We subdivide patients according to clinical course of the disease and try to identify appropriate changes in cytokine and adhesion molecule profile. We realize that the analysed group is small and at the moment we can not evaluate the impact of cytokine and adhesion molecule profile on overall survival.

Conclusion

Standard prognostic indicators are important in AML patient management, but can not identify patients with an aggressive disease marked as low or intermediate-1 risk, same as patients marked as

intermediate-2 or high risk and less aggressive disease. The cytokine and adhesion molecule profile is capable to uncover more profound differences in a specifically defined patient subgroups and seems to be more personalized. To validate our data, further investigation in a larger number of patients is necessary.

Summary

Cytokines and adhesion molecules have been studied as markers of immune system activation in various diseases including AML. A total of 47 newly diagnosed AML patients, who were treated with intensive chemotherapy and in indicated cases allotransplanted in the period from 2010 to 2013, were evaluated for baseline cytokine and adhesion molecule profile. The findings were compared with standard risk stratification according to cytogenetics and molecular genetics, and in subsequent analyses cytokine and adhesion molecule patterns in defined subgroups of patients were estimated. We provide evidence about differences in cytokine and adhesion molecule profile linked to hyperleukocytosis, age and secondary AML origin. Finally, we identified a cytokine pattern associated with improved progression free survival, which seems to be caused by lower aggressiveness of the disease. Due to relatively short follow-up we are not able to identify cytokine and adhesion molecule pattern associated with improved overall survival yet. Our analyses are limited by low patient count. Analyses in a larger cohort of patients would be probably even more exciting.

Acknowledgement

The work was supported by Specific research project “Analysis of defined prognostic factors in acute myeloid leukemia” (Faculty of Military Health Sciences in Hradec Kralove) and by a long-term organisation development plan 1011 (Faculty of Military Health Sciences in Hradec Kralove).

References

1. Döhner H, Estey EH, Appelbaum FR et al.: Diagnosis and management of acute myeloid leukemia in adults: recommendation from an international expert panel, on behalf of the European leukemia Net. *Blood* 2010; 115, 453-473.
2. Damm F, Heuser M, Morgan M et al.: Integrative prognostic risk score in acute myeloid leukemia with normal karyotype. *Blood* 2011; 117, 4561-4568.
3. Kupsa T, Horacek JM, Jebavy L.: The role of cytokines in acute myeloid leukemia: a systematic review. *Biomed Pap Med Fac Univ Palacky Olomouc Czech Repub* 2012; 156, 291-301.
4. Horacek JM, Vasatova M, Kupsa T et al.: Multi-analytical evaluation of serum levels of cytokines and adhesion molecules in patients treated for acute myeloid leukemia using biochip array technology. *Biomed Pap Med Fac Univ Palacky Olomouc Czech Repub* 2013, doi: 10.5507/bp.2013.073. [Epub ahead of print]

NOVEL INSIGHTS INTO THE MOLECULAR MECHANISMS OF ACQUIRED AND CONGENITAL POLYCYTHEMIAS

Lucie Láníková

E-mail: l.lanikova@upol.cz

Department of Biology, Faculty of Medicine and Dentistry,
Palacky University Olomouc, Czech Republic

Co-Authors: N. Ljubas, Ch. Huff, Z. Ye, L. Cheng

Tutors: doc. RNDr. Vladimír Divoký, Ph.D., prof. MUDr. Josef T. Prchal

Introduction

Polycythemia vera (PV) and primary familial and congenital polycythemia (PFCP) are primary polycythemic disorders with erythroid progenitors hypersensitive to erythropoietin (EPO). They are caused by somatic (PV) or germ-line (PFCP) mutations that are intrinsic to erythroid progenitors and result in an augmented response to EPO [1]. PV is an acquired clonal hematopoietic stem cell (HSC) disease characterized by increased production of erythrocytes, granulocytes, platelets and largely polyclonal T lymphocytes. Over 95% of PV patients carry a somatic *JAK2*^{V617F} gain-of-function mutation [2]. Evidence suggests that *JAK2*^{V617F} is not the disease-initiating mutation and constitutes only part of the clone [3]. One of the major challenges in order to identify genetic lesion preceding *JAK2*^{V617F} is to isolate and expand the disease-initiating HSC clones *in vitro*.

Secondary polycythemias may be subdivided into appropriate and inappropriate, when the former responding normally to tissue hypoxia (i.e. high-altitude polycythemia and hemoglobins with increased affinity for oxygen) and the latter is stimulated by aberrant production of EPO. So called Chuvash polycythemia shares features of both primary and secondary polycythemias. The underlying genetic defect is the homozygosity with respect to a C→T missense mutation in *VHL* gene, causing an arginine-to-tryptophan change at amino-acid residue 200 (Arg200Trp) [4]. Germline *von Hippel-Lindau (VHL)* gene mutations underlie dominantly inherited familial VHL tumor syndrome. It was proposed that different positions of loss-of-function *VHL* mutations are associated with *VHL* syndrome cancer predisposition and only C-terminal domain encoding *VHL* mutations would cause polycythemia.

Methods

Peripheral blood samples were collected in EDTA and/or ACD tubes. Written inform consent was obtained from all participants. The virus-free, integration-free induced pluripotent stem cells (iPSCs) from female PV patient were derived according to protocol described previously [5]. Human iPSCs were differentiated into hematopoietic cells following a spin-EB protocol [6]. Functional analysis of *VHL* mutations are described in details elsewhere [7,8]. Briefly, genomic DNA was isolated from granulocytes using Gentra-Puregene Kit (Qiagen, Germantown, MD), and *VHL* gene's exons were amplified using Hot Star Master Mix (Qiagen). 786-0 cell line (renal cell adenocarcinoma origin) was purchased from ATCC (CRL-1932™, Manassas, VA). VHL Human cDNA ORF Clone was obtained from OriGene (RC216151, Rockville, MD). Site-directed mutagenesis was performed using the QuickChange II Site-Directed Mutagenesis Kit (Agilent Technologies, Santa Clara, CA) and allele-specific oligonucleotides.

Results

Derivation of PV-specific iPSCs clones and their analysis. Using blood and bone marrow progenitors from female patient with typical PV (with high allele burden (99%) of *JAK2*^{V617F}, and ~1% of wild-type *JAK2*) dozens of iPSC clones were generated by episomal vectors with several distinct *JAK2* genotypes.

The erythroid differentiation of 5 representative PV-iPSC lines and normal control were examined. The hematopoietic progenitor cells (HPCs) derived from *JAK2*^{V617F} iPSCs had enhanced erythropoiesis compared to wild-type *JAK2* iPSCs, as expected. iPSCs were sequentially differentiated to specific blood lineages and sensitivity to given drugs (JAK2 inhibitors) at various developmental stages were tested. Our results show the ineffectiveness of the JAK2 inhibitors to eliminate the disease-initiating clones in PV patient.

Comparison of Croatian and Chuvash polycythemia. We report a second polycythemic Croatian *VHL*^{H191D} homozygote distantly related to the first propositus [9]. Three generations of both families were genotyped for analysis of shared ancestry. The *VHL*^{H191D} mutation did not segregate in the families defined by the known common ancestors of the two subjects, suggesting a high prevalence in Croats, but haplotype analysis indicated an undocumented common ancestor ~six generations ago as the founder of this mutation. We show that EPO levels in homozygous *VHL*^{H191D} individuals are higher than in *VHL*^{R200W} patients of similar age, and their native erythroid progenitors, unlike Chuvash R200W, are not hypersensitive to EPO.

Novel homozygous *VHL* mutation associated with polycythemia but not with the cancer. We report a novel homozygous variant of the *VHL* gene located in the middle of coding region in exon-2; 413C>T:P138L. The propositus' parents are *VHL*^{P138L} heterozygotes and no VHL tumors are reported in the extended family, in contrast to the other *VHL*^{P138} residue (P138R, P138T) mutations that have been reported in VHL syndrome and renal cancer. We show that *VHL*^{P138L} has perturbed interaction with hypoxia-inducible transcription factor (HIF)-1 α . Further, *VHL*^{P138L} protein has decreased stability *in vitro*. Similarly to what was reported in Chuvash polycythemia and some other instances of HIFs upregulation, *VHL*^{P138L} erythroid progenitors are hypersensitive to EPO.

Discussion and Conclusions

The nature of the pre-*JAK2*^{V617F} somatic and germline mutations has not yet been identified, and the search for these predisposing genetic lesions using marrow and blood cells is hampered by their genetic heterogeneity. In order to overcome this obstacle, we generated several iPSC cell lines from the same PV female with different *JAK2* genomic configuration. iPSC clones are currently analyzed to reveal potential genetic defects involved in the early pathogenesis of PV.

Mutations of *VHL* (a negative regulator of hypoxia-inducible factor) have position-dependent distinct cancer phenotypes. Only two known inherited homozygous *VHL* mutations exist and they cause polycythemia: Chuvash R200W and Croatian H191D. We described and characterized a novel homozygous *VHL* mutation, in exon-2, which is associated in the affected homozygote with congenital polycythemia but not in her, or her heterozygous relatives, with cancer. We also reported a second polycythemic Croatian *VHL*^{H191D} homozygote and performed several biochemical and molecular tests to better define the phenotype.

Summary

These studies will lead to better understanding of the genetic lesions in PV-initiating clones. We further define the hematologic phenotype of *VHL*^{H191D} and *VHL*^{P138L} mutations and provide additional evidence for phenotypic heterogeneity associated with the positional effects of *VHL* mutations.

References

1. Prchal JF, Prchal JT. Molecular basis for polycythemia. *Curr Opin Hematol.* 1999; 6(2): 100-109.
2. Kralovics R, Passamonti F, Buser A, et al. A gain-of-function mutation of *JAK2* in myeloproliferative disorders. *N Engl J Med.* 2005; 352(17): 1779-1790.
3. Nussenzveig RH, Swierczek SI, Jelinek J, Gaikwad A, Liu E, Verstovsek S, Prchal JF, Prchal JT. Polycythemia vera is not initiated by *JAK2*^{V617F} mutation. *Exp Hematol.* 2007; 35(1): 32-8.

4. Ang SO, Chen H, Hirota K, et al. Disruption of oxygen homeostasis underlies congenital Chuvash polycythemia. *Nat Genet.* 2002; 32(4): 614-621.
5. Doney SN, Huang X, Chou BK, Ye Z, Cheng L. Generation of integration-free human induced pluripotent stem cells from postnatal blood mononuclear cells by plasmid vector expression. *Nat Protoc.* 2012; 7(11): 2013-2021.
6. Ye Z, Zhan H, Mali P, et al. Human-induced pluripotent stem cells from blood cells of healthy donors and patients with acquired blood disorders. *Blood.* 2009; 114(27): 5473-5480.
7. Lanikova L, Lorenzo F, Yang CH, Vankayalapati H, Drachtman R, Divoky V, Prchal JT. Novel homozygous *VHL* mutation in exon 2 is associated with congenital polycythemia but not with cancer. *Blood.* 2013; 121(19): 3918-24.
8. Piterkova L*, Tomasic Ljubas N*, Huff Ch, et al. Polycythemia due to Croatian homozygous *VHL* (571C>G:H191D) mutation has a different phenotype than Chuvash polycythemia (*VHL* 598C>T:R200W). *Haematologica.* 2013; 98(4): 560-7.
9. Pastore Y, Jedlickova K, Guan Y, et al. Mutations of von Hippel-Lindau tumor-suppressor gene and congenital polycythemia. *Am J Hum Genet.* 2003; 73(2): 412-9.

EFFECT OF INCB018424, A JAK1 AND JAK2 INHIBITOR, ON SENESENCE PHENOTYPE IN OLD MICE

Vojtěch Mezera

E-mail: mezev5ar@lfhk.cuni.cz

Department of Physiology, Faculty of Medicine in Hradec Králové,
Charles University in Prague, Czech Republic

Co-authors: T. Tchkonina, T. Pirtskhalava, T. White, J. L. Kirkland, Robert and Arlene Kogod
Tutor: Prof. Zuzana Červinková, MD, PhD

Introduction & Aims

Aging is a major risk factor for many chronic diseases, particularly atherosclerosis, cancer, diabetes mellitus, dementia, and more. These are then responsible for the majority of morbidity in developed countries.

Senescence, i.e. aging at the cellular level, was originally defined as a result of shortening of the telomeres at the end of chromosomes due to repeated cell division. Other factors independent on cell replication, e.g. oxidative stress, may also cause senescence. Senescence is associated with inflammation and with senescence-associated secretory phenotype (SASP), when senescent cells produce various cytokines in order to attract immune cells and in order to get removed^{2,3}.

The aim of our study was to determine if INCB018424, a selective inhibitor of Janus kinases JAK1 and JAK2⁴, has an effect on senescent cell accumulation and/or SASP in adipose tissue of chronologically old mice.

Methods

26-month-old BL75/6 male mice were treated with INCB018424 or vehicle for two months. Mice were treated daily with a single dose (60 mg/kg/ body weight) of INCB018424 mixed with food. Epididymal, inguinal, mesenterial, perirenal, and subscapular adipose tissues were collected after treatment. The fat tissues were fixed and stained for senescence-associated beta-galactosidase (SA-beta-gal), a marker of cellular senescence, and counterstained with DAPI, a nuclear stain. Images of histological samples were taken and the percentage of SA-beta-gal positive cells estimated using computer-aided image analysis. RNA was isolated from fat depots. SASP components and senescence markers were assayed using qRT-PCR.

Results

No difference was observed in SA-beta-gal positivity in epididymal depots. In all other depots, there was a non-significant trend to lower SA-beta-gal positivity in INCB018424 treated animals when compared to controls. However, expression of following senescence markers and SASP components were downregulated in the fat tissue of treated mice compared to controls: p16, p21, IL6, Emr1, MMP3, MMP9, MMP12, CEBP α , ZFN423, Hmgb1. Expression of other genes (PAI, TNF- α , FABP4, PPAR- γ , MCP1) was not different.

Discussion & Conclusions

In previous study, health span was increased by removing senescent cells in progeroid mice¹. INCB018424 ameliorated some symptoms of geriatric frailty in patients with myelofibrosis⁴ and seems to be a promising agent in preventing tissue dysfunction associated with inflammation.

In the present study, we observed that INCB018424 did not change senescent cells abundance, but significantly reduced senescence-associated inflammation in adipose tissue in chronologically old mice. Thus, INCB018424 might prevent age-associated adipose tissue dysfunction.

Based on results above, targeting the JAK1 and JAK2 with INCB018424 seems to be promising way of ameliorating SASP. More studies are necessary to determine if inhibiting the JAK1 and JAK2 kinases can promote health span.

References

1. Baker DJ, Wijshake T, Tchkonja T, et al. Clearance of p16Ink4a-positive senescent cells delays ageing-associated disorders. *Nature*. 2011 Nov 2; 479(7372): 232-6.
2. Minamino T, Orimo M, Shimizu I, et al. A crucial role for adipose tissue p53 in the regulation of insulin resistance. *Nat Med*. 2009 Sep;15(9): 1082-7.
3. Tchkonja T, Zhu Y, van Deursen J, Campisi J, Kirkland JL. Cellular senescence and the senescent secretory phenotype: therapeutic opportunities. *J Clin Invest*. 2013 Mar 1; 123(3): 966-72.
4. Verstovsek S, Kantarjian H, Mesa RA, et al. Safety and efficacy of INCB018424, a JAK1 and JAK2 inhibitor, in myelofibrosis. *N Engl J Med*. 2010 Sep 16; 363(12):1117-27.

RESISTANCE TO CLOPIDOGREL – ETIOLOGY, MEASUREMENT AND IMPACT ON THE PROGNOSIS OF PATIENTS WITH CORONARY ARTERY DISEASE

Petra Paulů

E-mail: paulu.p@centrum.cz

Cardiocenter University Hospital Kralovske Vinohrady and Third Faculty of Medicine,
Charles University in Prague, Czech Republic

Co-authors: P. Toušek, P. Widimský

Tutor: doc. MUDr. Pavel Osmančík, Ph.D.

Introduction

Dual antiplatelet therapy with aspirin and clopidogrel is the gold standard of modern pharmacotherapy in cardiovascular atherothrombotic diseases. Many studies in the past 20 years have confirmed, that the combination of aspirin and clopidogrel dramatically reduces the rate of major adverse cardiac events in patients with acute coronary syndromes and following percutaneous coronary intervention (PCI) [1,2]. However, significant numbers of patients treated with clopidogrel do not have an adequate response to the treatment and are considered to be clopidogrel non-responders. This is called clopidogrel resistance, which can be divided into clinical resistance (recurrence of ischaemic events despite adequate therapy) or laboratory resistance (higher platelet reactivity during antiplatelet therapy). The incidence of laboratory resistance varies from 4.8 to 40% depending on the study [3]. The etiology is multifactorial, there are both clinical and cellular and genetic causes. There are many studies that have confirmed poor prognosis of patients with acute coronary syndrome with worse response to clopidogrel compared with the patients with sufficient clopidogrel action. The clopidogrel effectiveness can be routinely measured by different point-of-care assays. One of them is Verify Now. Early studies involving the measurement of clopidogrel efficacy had shown the prognostic promise [4-6]. However, results from some recent trials have failed to confirm the prognostic value [7,8].

Aim

The aim of our study was to determine the incidence of clopidogrel resistance in the real practise, detect the factors associated with poor response to clopidogrel and evaluate if the clopidogrel resistance measured by VerifyNow is connected with worse prognosis of patients with coronary artery disease.

Methods

Three hundred and forty five consecutive patients, who underwent PCI due to stable angina pectoris or acute coronary syndrome and were indicated to dual antiplatelet therapy, were enrolled to our study. Exclusion criteria were as follows: planned cardiac surgery, noncompliance, coagulopathy with higher risk of bleeding, life expectancy less than one year, administration of GP IIb/IIIa inhibitors (other than bolus of eptifibatide). Each patient received a 600 mg loading dose of clopidogrel during PCI or less than 2 hours before PCI, then followed by a daily maintenance dose of 75 mg. Venous blood samples were taken from each patient within 24 hours of the clopidogrel loading dose not before 2 hours after PCI. At the same time, genetics samples and standard laboratory measurements (biochemistry, hematology) were drawn. Two samples (2 ml venous blood anticoagulated with sodium citrate 0.109 mol/L ratio 9:1) from each patient for measuring platelet reactivity using the VerifyNow assay (Accumetrics) were also taken. The results were reported as PRU (platelet reaction units) and as a percentage of the baseline (pre-treatment) PRU. All 378 of patients were contacted 6 months after randomization to assess the predefined endpoints - MI (STEMI, NSTEMI), stroke and death.

Non responders were defined as patients with PRU > 240. DNA was isolated using the standard spin-column protocol. After isolation the target DNA segments were amplified using polymerase chain reaction (PCR). Denaturing capillary electrophoresis (DCE) was used to find gene polymorphisms of CYP2C19, CYP2C9, GP1IIa, GPVI, and MDR in obtained fragments. A 96 capillary sequencer (MegaBACE 1000, Amersham Biosciences, NJ) was used for the separation.

Results

From April 2009 to October 2010, 410 patients were enrolled. The mean age was 67.2 ± 12.8 years, weight 82.4 ± 16.4 kg, height 171.0 ± 10.1 cm, BMI 28.9 ± 17.7 . There were 262 (69.3%) men and 116 (30.7%) women. 116 patients had diabetes (30.7%), 223 patients had hypertension (58.9%), and there were 224 (59.3%) current or former smokers. 243 (64.3%) were classified as clopidogrel responders and 135 (35.7%) as clopidogrel non-responders. Variables, which were independently associated with clopidogrel non-responsiveness were age (OR 1,03 [1,01-1,05], $p < 0,05$), higher weight (OR 1,02 [1,01-1,03], $p < 0,05$), diabetes (OR 2,2, [1,7-5,5], $p < 0,05$), female gender (OR 1,9 [1,1-3,1], $p < 0,05$), mechanical ventilation (OR 8,2 [1,9-74,8], $p < 0,05$), higher leukocyte count (OR 1,1 [1,05-1,7], $p < 0,05$), higher concentration of interleukin-10 (OR 1,29 [1,03-1,60], $p < 0,05$) and the presence of AA allele of CYP 2C19*2 (OR 1,8 [1,2-3,2], $p < 0,05$). During the 6-months follow-up, 30 patients (7.94%) had at least one of the pre-defined end-points. Twelve patients (3.17 %) had a MI, 5 patients (1.32 %) had a stroke and 15 patients (3.97 %) died. The remaining 348 patients (92.06 %) were end-point free. In multivariate analysis factors associated independently with poor prognosis were: the leukocyte count (OR 1.7 [1.2-2.4], $p < 0.01$), the concentration of serum creatinine (OR 1.4 [1.1-2.5], $p < 0.05$) and with borderline significance the presence of the AA allele of gene CYP2C19*2 (OR 2.5 [0.99-4.1], $p = 0.052$). There was no difference in PRU or PRU% values between the groups.

Discussion and conclusion

The influence of clopidogrel effectiveness on the prognosis of patients has been described in many presented studies (4,5). Our result show that more than 30 % of patients treated with clopidogrel have higher on treatment platelet reactivity (OTPR). These are patients older, females, with diabetes, more often treated by mechanical ventilation, with higher leukocyte count, concentration of interleukin-10 and with more frequent presence of the AA allele of gene CYP2C19*2. These results are consistent with many published studies, moreover in our study OTPR was connected also with mechanical ventilation. Nevertheless the biggest surprise of our study was the absence of prognostic impact of PRU value. The groups with and without endpoints differed only leukocyte count, serum creatinine and borderline the AA allele of gene CYP2C19*2. Our results are in one line with some studies (8,9,10), on the other hand differ from the others (4,5,6). The reason why the results of similarly designed studies are so different is not clear. In our opinion, the main argument is that platelet reactivity is complex process affected by many factors, and not only single laboratory value. Also the presentation of PRU as the marker of platelet reactivity is just one of many possible. In the future we will need complex algorithm containing both laboratory and clinical values to individualized antiplatelet treatment.

Summary

Three hundred and seventy-eight patients were enrolled into the study. The incidence of clopidogrel resistance was 35,7%. Variables, which were associated with clopidogrel non-responsiveness were higher age, higher weight, diabetes, female gender, mechanical ventilation, higher leukocyte count, higher concentration of interleukin-10 and the presence of AA alele of CYP 2C19*2. Thirty patients underwent MI, stroke or died during following 6 months. Variables associated with poor prognosis were higher concentration of creatinine and higher leukocyte count, on borderline level the presence of AA alele of CYP2C19*2.

Literature

1. Baigent C, Collins R, Appleby P, Parish S, Sleight P, Peto R (1998) ISIS-2: 10 year survival among patients with suspected acute myocardial infarction in randomised comparison of intravenous streptokinase, oral aspirin, both, or neither. *BMJ* 316(7141): 1337-43.
2. Antiplatelet Trialists' Collaboration (2002) Collaborative meta-analysis of randomised trials of antiplatelet therapy for prevention of death, myocardial infarction and stroke in high risk patients. *Br Med J* 324: 71-86.
3. Wang TH, Bhatt DL, Topol E (2006) Aspirin and clopidogrel resistance: an emerging clinical entity. *Eur Heart J* 27: 647-54.
4. Marcucci R, Gori AM, Paniccia R, Giusti B, Valente S, Giglioli C, Buonamici P, Antoniucci D, Abbate R, Gensini GF (2009) Cardiovascular death and nonfatal myocardial infarction in acute coronary syndrome patients receiving coronary stenting are predicted by residual platelet reactivity to ADP detected by a point-of-care assay: a 12-month follow up. *Circulation* 119: 237-42.
5. Price MJ, Endemann S, Gollapudi R, Valencia R, Stinis CT, Levisay JP, Ernst A, Sawhney NS, Schatz RA, Teirstein PS (2008) Prognostic significance of post-clopidogrel platelet reactivity assessed by a point-of-care assay on thrombotic events after drug-eluting stent implantation. *Eur Heart J* 29: 992-1000.
6. Patti G, Nusca A, Mangiacapra F, Gatto L, D'Ambrosio A, Di Sciascio G (2008) Point-of-care measurement of clopidogrel responsiveness predicts clinical outcome in patients undergoing percutaneous coronary intervention results of the ARMYDA-PRO (Antiplatelet therapy for Reduction of MYocardial Damage during Angioplasty-Platelet Reactivity Predicts Outcome) study. *J Am Coll Cardiol* 52: 1128-33.
7. Trenk D, Stone GW, Gawaz M, Kastrati A, Angiolillo DJ, Müller U, Richardt G, Jakubowski JA, Neumann FJA (2012) Randomized Trial of Prasugrel Versus Clopidogrel in Patients With High Platelet Reactivity on Clopidogrel After Elective Percutaneous Coronary Intervention With Implantation of Drug-Eluting Stents : Results of the TRIGGER-PCI (Testing Platelet Reactivity In Patients Undergoing Elective Stent Placement on Clopidogrel to Guide Alternative Therapy With Prasugrel) Study. *J Am Coll Cardiol* 59(24): 2159-64.
8. Price MJ, Berger PB, Teirstein PS, Tanguay JF, Angiolillo DJ, Spriggs D, Puri S, Robbins M, Garratt KN, Bertrand OF, Stillabower ME, Aragon JR, Kandzari DE, Stinis CT, Lee MS, Manoukian SV, Cannon CP, Schork NJ, Topol EJ (2011) Standard- vs high dose clopidogrel based on platelet function testing after percutaneous coronary intervention: the GRAVITAS randomized trial. *JAMA* 305: 1097-105.
9. Trenk D, Stone GW, Gawaz M, Kastrati A, Angiolillo DJ, Müller U, Richardt G, Jakubowski JA, Neumann FJA (2012) Randomized Trial of Prasugrel Versus Clopidogrel in Patients With High Platelet Reactivity on Clopidogrel After Elective Percutaneous Coronary Intervention With Implantation of Drug-Eluting Stents : Results of the TRIGGER-PCI (Testing Platelet Reactivity In Patients Undergoing Elective Stent Placement on Clopidogrel to Guide Alternative Therapy With Prasugrel) Study. *J Am Coll Cardiol* 59(24): 2159-64.
10. Price MJ, Berger PB, Teirstein PS, Tanguay JF, Angiolillo DJ, Spriggs D, Puri S, Robbins M, Garratt KN, Bertrand OF, Stillabower ME, Aragon JR, Kandzari DE, Stinis CT, Lee MS, Manoukian SV, Cannon CP, Schork NJ, Topol EJ (2011) Standard- vs high dose clopidogrel based on platelet function testing after percutaneous coronary intervention: the GRAVITAS randomized trial. *JAMA* 305: 1097-105.

THE USE OF THE PLASMA LEUCOCYTE ELASTASE, CALPROTECTIN, LACTOFERIN, INTESTINAL FATTY ACID BINDING PROTEIN (I-FABP) AND NEOPTERIN CONCENTRATION IN THE DIAGNOSIS AND ASSESSMENT THE CLINICAL ACTIVITY OF CROHN'S DISEASE AND ULCERATIVE COLITIS

Dorota Pawlica-Gosiewska

Department of Diagnostics, Chair of Clinical Biochemistry
Jagiellonian University Medical College Krakow, Poland

Department of Gastroenterology,
Hepatology and Infectious DiseasesThe Krakow University Hospital

Co-authors: Dr. Katarzyna Gawlik, Dr. Danuta Fedak, Dr. Beata Kusnierz-Cabala,
Dr. Danuta Owczarek, Dr. Dorota Cibor, Prof. Tomasz Mach
Tutor: Prof. Bogdan Solnica

Introduction

Diagnosis of inflammatory bowel diseases (IBD) is based on histopathology, endoscopy or radiography, which makes the diagnostics time consuming, expensive, and sometimes invasive[3]. For this reason new laboratory parameters that can be an objective tool for assessing disease activity, prediction of severity and treatment monitoring are needed[3]. Both in Crohn's disease (CD) and in ulcerative colitis (UC), the prognosis is unfavorable. In many patients only a periodic remission can be achieved. Both diseases are considered incurable and the only possibility is the symptomatic treatment. These diseases significantly reduce the quality of patient's life limiting the performance of many activities of day-to-day life and professional activity, often leading to chronic disability, not only physical but also psychosocial [4]. Therefore, in addition to improvement of treatment methods new diagnostic tools are developed to improve early diagnosis, risk stratification and treatment monitoring of these diseases[3].

The aim of this study is to evaluate the diagnostic usefulness of selected proteins released from neutrophils and intestinal epithelial cells:

- in differential diagnostics of CD and UC
- in assessment of both diseases' severity

Methods

The study population was a group of 60 patients with inflammatory bowel disease (33 – ulcerative colitis and 27 – crohn's disease) and 20 healthy subjects in the control group. The UC patients were divided into active phase of disease (23 patients) and inactive phase of disease (10 patients) subgroups according to the Mayo index (assessing amount of defecation per day and systemic disorders). The CD patients were divided into active phase of disease (20 patients) and inactive phase of disease (7 patients) subgroups according to the Crohn's disease activity index (assessing amount of defecation per day and systemic disorders).

C-reactive protein CRP was measured using immunonephelometry on the Nephelometer II Analyzer (Siemens Healthcare Diagnostics). Leukocyte Elastase (HLE) were determined using ELISA (PMN Elastase ELISA BioVendor). Calprotectine, Lactoferrin and free fatty acids binding protein (I-FABP) were determined using ELISA and Human Caprotectin (Hycult (Biotechnology Company, USA), (Human Lactoferrin (Hycult Biotechnology Company, USA) and Human Intestinal Fatty Acid Binding Protein (Biotechnology company Hycult, USA) reagents, respectively. Plasma neopterin was measured using ELISA (IBL International, Germany).

Normality of distribution of the results will be tested using the Kormogolow-Smirnov test. If the analyzed results showed a normal distribution, means were compared using test t. When analyzed the results did not show a normal distribution, medians were compared using U-Mann Witney test. That significance level for analysed parameters is $p < 0.05$. The result which were normally distributed and are presented as means and standard deviations. The result which were not normally distributed and are presented as medians and quartiles. The logistic regression results were shown as IR and OD with 95% CI.

This study was funded by a National Science Center Grant (number: DEC-2011/01/N/NZ5/000054).

Results

CRP, Lactoferrin, Calprotectin, Leukocytes elastase were significantly higher in the group of patients with CD than in controls (Tab 1).

	Control Group	Crohn's disease	P
Hs CRP	1,06 (0,51-2,14)	5,55 (0,71-18,83)	0,025248
Neopterin	6,81 (5,67-8,16)	6,87 (5,75-8,49)	0,777703
I-FABP	572,2 (468,6-760,9)	447,5 (368,0-648,6)	0,138987
Lactoferrin	565,9 (440,5-754,5)	235,2 (181,2-269,9)	0,000011
Calprotectin	69,94±22,10	135,12±62,57	0,000054
Leukocytes Elastase	30,12±7,73	56,76±22,57	0,000007

Tab. 1. Comparison of plasma concentrations of chosen parameters in patients with Crohn's disease with a control group

CRP, Lactoferrin, Calprotectin, Leukocytes elastase were significantly higher in the group of patients with CU than controls (Tab 2).

	Control Group	Crohn's disease	P
Hs CRP	1,06 (0,51-2,14)	2,26 (1,11-19,59)	0,011635
Neopterin	6,81 (5,67-8,16)	7,94 (5,83-10,23)	0,144627
I-FABP	572,2 (468,6-760,9)	429,2 (329,1-938,3)	0,392481
Lactoferrin	565,9 (440,5-754,5)	217,1 (176,6-303,9)	0,000008
Calprotectin	69,94±22,10	161,41±97,61	0,000143
Leukocytes Elastase	30,12±7,73	67,21±45,64	0,000743

Tab. 2. Comparison of plasma concentrations of chosen parameters in patients with Ulcerative Colitis with a control group

Comparison of the studied parameters in patients with Crohn's disease and patients with Ulcerative Colitis were not statistically significant.

The relationship between the analysed parameters and the occurrence of Crohn's disease in this study was assessed using logistic regression (statistical significance was observed for: hs CRP 1,282 (1,007-1,633), Lactoferrin 0,990 (0,985-0,996), Calprotectin 1,037 (1,014-1,061) and Leukocytes Elastase 1,175 (1,074-1,287)). The relationship between the studied parameters and the occurrence of Ulcerative Colitis in this study was also assessed using logistic regression (statistical significance was observed for: hs CRP 1,252 (1,003-1,562), Lactoferrin 0,990 (0,985-0,995), Calprotectin 1,034 (1,012-1,057) and Leukocytes Elastase 1,166 (1,058-1,285)).

It has been shown that the comparison of the studied parameters useful for differentiation of patients with CD from the control group (the highest area under the ROC curve) were: Lactoferrin = 0,866, Leukocytes Elastase = 0,926 and Calprotectin = 0,892) and in group of patients with CU from control group (the highest area under the curve were: Lactoferrin= 0,853, Leukocytes Elastase = 0,897 and Calprotectin = 0,833) Fig. 1.

CRP was significantly higher in patients with the active phase of Crohn's disease (10,52 (2,0-23,6)) than in patients with remission (0,54 (0,13-6,41), $p = 0,026889$). Similarly, neopterin was significantly higher in patients with the active phase of Crohn's disease (7,42 (6,05-8,96)) than in patients with remission (5,90 (4,81-6,96), $p = 0,04212$). CRP was significantly higher in patients with active phase of ulcerative colitis (11,67(1,27-27,24)) than in patients with remission (0,87 (0,49-1,87), $p = 0,029297$). Other parameters were not statistically significant in clinical activity in both diseases.

Conclusion

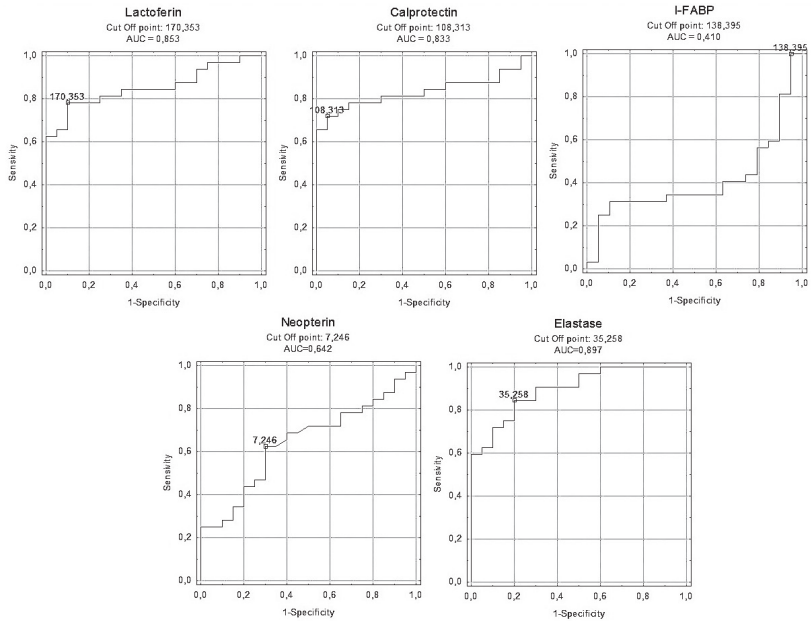
Determination of leukocyte elastase, lactoferrin and calprotectin in faeces in patients with IBD are postulated noninvasive indicators of the inflammatory process located in intestines in the course of CD and UC [1]. It was found that CRP, Lactoferrin, Calprotectin and Leukocytes elastase levels in patients suffering from CD and CU were higher than in the control group. Thus, these parameters may be considered useful biomarkers in the diagnosis of CD and CU. Leucocytes elastase had the highest AUC_{ROC} may be helpful in differential diagnosis in both of this diseases. Plasma leukocyte elastase may be an useful independent marker of IBD activity, particularly effective in identifying patients in remission and it has been shown to be a better parameter than the ESR and CRP [2]. It has been shown that only CRP and neopterin can be useful in the assessment of clinical activity of the respective disease, but because of the small number of patients in remission, this requires further study.

Summary

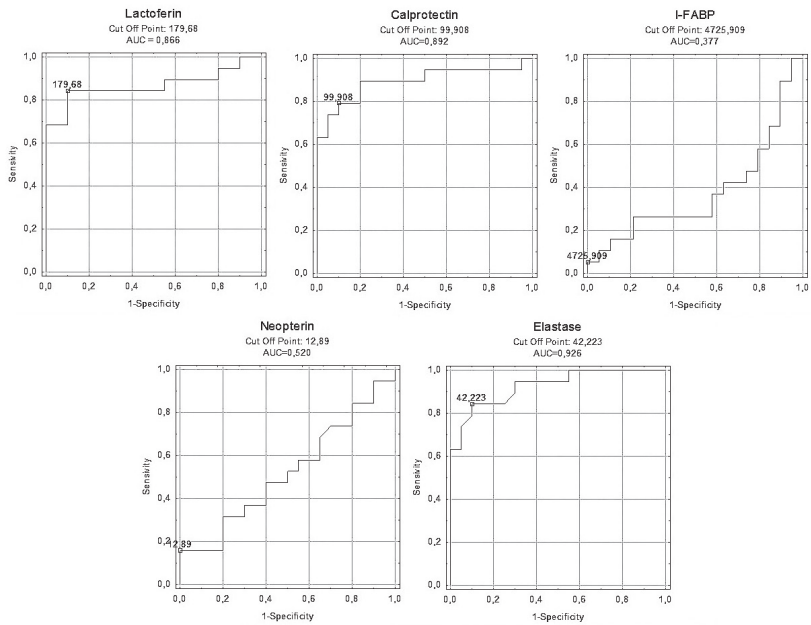
Diagnosis of inflammatory bowel diseases (IBD) is time consuming, expensive, and sometimes invasive. For this reason new laboratory parameters that can be an objective tool for assessing disease activity, prediction of severity and treatment monitoring are needed. The aim of this study is to evaluate the diagnostic usefulness of selected proteins: lactoferrin, calprotectin, I-FABP, Leucocytes elastase and neopterin. The study population was a group of 60 patients with inflammatory bowel disease (33 – ulcerative colitis and 27 – crohn's disease) and 20 healthy subjects in the control group. Determination of chosen parameters were determined using ELISA method. It was found that CRP, Lactoferrin, Calprotectin and Leukocytes elastase levels in patients suffering from CD and CU were higher than in the control group. Thus, these parameters may be considered useful biomarkers in the diagnosis of CD and CU. Leucocytes elastase had the highest AUC_{ROC} may be helpful in differential diagnosis in both of this diseases. It has been shown that only CRP and neopterin can be useful in the assessment of clinical activity of the respective disease, but because of the small number of patients in remission, this requires further study.

References:

1. Burns S., Bisset W., Golden B.: Faecal calprotectin: an objective measure of bowel inflammation in childhood inflammatory bowel disease. *J of Paediat Gastroenterol* 2001, 32, 171–177
2. Gouni-Berthold I., Baumeister B., Wegel E., Berthold H.K., i wsp.: Neutrophil-elastase in a chronic inflammatory bowel disease: a marker of activity? *Hepato gastroenterol* 1999, 46, 2315-2320
3. Mendoza JL, Abreu MT. Biological markers in inflammatory bowel disease: practical consideration for clinicians. *Gastroenterol Clin Biol.* 2009 Jun; 33 Suppl 3: S158-73.
4. Casellas F, Arenas JJ, Baudet JS, Fábregas S, García N, Gelabert J, Medina C, Ochotorena I, Papo M, Rodrigo L, Malagelada JR: Impairment of health-related quality of life in patients with inflammatory bowel disease: a Spanish multicenter study. *Inflamm Bowel Dis.* 2005 May;11(5): 488-96.



ULCERATIVE COLITIS



CROHN'S DISEASE

Fig. 1. ROC curve for chosen parameters group of patients with Crohn's disease and Ulcerative colitis

NON-SPECIFIC CHANGES AFTER SOMAN POISONING

Jaroslav Pejchal

E-mail: jaroslav.pejchal@seznam.cz

Centre of Advanced Studies and Department of Toxicology, Faculty of Military Health Sciences in Hradec Králové, Czech Republic

Co-authors: F. Caisberger

Tutor: prof. MUDr. Jiří Kassa, CSc.

Introduction

Soman is a highly toxic nerve agent exerting its toxicity via irreversible binding to and inactivation of acetylcholinesterase. This is associated with accumulation of acetylcholine at the synapses and overstimulation of cholinergic nervous system. By contrast, less is known about soman-induced non-specific effects, especially in extracranial tissues.

Herein, we present the results of biochemical (blood), histopathological (heart, lung, liver, kidney, small and large intestine) and molecular changes (large intestine) following soman poisoning.

Methods

Male Wistar rats were *i.m.* administered with saline (control) or soman [2-(fluoromethylfosforyl)oxy-3,3-dimethylbutan] at the dose of 60 µg/kg (70% LD₅₀). Heparinized blood, heart, lung, liver, kidney, small and large intestine were collected 1, 3 and 7 days after the administration. In blood, glucose, urea, creatinine, bilirubin, conjugated bilirubin, cholesterol, TAG, total protein, ALT, AST, ALP, GMT, CK, and LDH were measured in the Department of Clinical Biochemistry and Diagnostics (Faculty hospital, Hradec Kralove). Heart, lung, liver, kidney, small and large intestine samples were fixed with formalin, embedded into paraffin and 5 µm tissue sections were cut. Samples were stained with hematoxylin-eosin (HE). In heart, Mallory's PTAH staining was used to detect myolysis. In lung, liver and kidney, apoptosis was evaluated using TUNEL technique and immunohistochemical detection of activated/cleaved-caspase-3 (standard peroxidase technique), while in small and large intestine, only HE and detection of cleaved-caspase-3 were utilized. In large intestine (1 and 3 day intervals), immunohistochemical detection of phospho-p53^{Ser15}, p21, phospho-JNK^{Thr183/Tyr185}, phospho-p38^{Thr180/Tyr182}, phospho-Elk-1^{Ser-383}, phospho-c-Myc^{Thr-58/Ser-62}, phospho-ATF-2^{Thr-69/71}, and phospho-CREB^{Ser-133} was performed (standard peroxidase technique). Samples were evaluated using the BX-51 microscope and computer image analysis ImagePro5.1. Ten microscopic fields at a 400-fold magnification were randomly selected from each sample. Image analysis was performed separately in apical and cryptal enterocytes in the area of 2250 µm² (30 – 40 cells per field and compartment). Integral optical density of the immunoreactive structures was measured in the inverted RGB scale. The Mann-Whitney test was used for the statistical analysis giving mean ± 2 × SEM. The differences were considered significant when p ≤ 0.05.

Results

Five of 24 animals died. Symptoms of soman poisoning appeared 5 min and disappeared withing 24 h after the poisoning. Biochemical and histopathological changes are summarized in Tab 1. Amount of apoptotic (all tissues) and mitotic cells (intestine only) is summarized in Tab 2. Activation of p53, JNK, p38, Elk-1, c-Myc, ATF-2, and CREB and expression of p21 in large intestine are summarized in Tab. 3.

Discussion and conclusions

According to our results, soman intoxication induces mild biochemical changes in blood and histopathological changes in heart, lung and intestine. In blood, increased CK and AST were found

3 days after the poisoning. In regards to unaffected ALT and CK/AST ratio being less than 10, the probable source of both enzymes was damaged heart muscle. This correlated with findings in heart, in which multifocal acute myolysis (eosinophilic sarcoplasm, contraction bands, picnotic nuclei) was found in 7 of 19 (37%) animals. In 5 animals, individual cells were damaged, whereas in 2 animals larger foci with inflammatory infiltration were found. The 7 animals were also the only ones that suffered from seizures. This implies hypoxia to be a very significant factor resulting in soman-induced cardiomyopathy. In lungs, decreased air/tissue ratio due to hyperaemia and multifocal intraseptal oedema was found 1 day after the poisoning. These findings could be explained by the ability of acetylcholine to regulate vascular permeability (1), nevertheless, heart and/or pulmonary circulation dysfunction may contribute. Contrariwise, structural heart damage does not seem related to the morphological changes in lungs, since multifocal acute myolysis was found in 1 of 5 animals 1 day after the soman intoxication, while the soman-induced changes in lungs were observed in the whole group. After the initial phase, lungs recovered and only intraalveolar erythrocytes as a sign of previous intraalveolar bleeding were recorded 3 days after the poisoning. In the 7 day interval, multifocal intraseptal oedema and hyperaemia reappeared again accompanied with inflammatory infiltration and increased amount of apoptotic cells. This course suggests a presence of a residual damage that persists in lungs after the soman intoxication and activates delayed inflammatory process. Findings observed in small and large intestine had a very similar character. One day after the poisoning, a significantly decreased mitotic activity was measured in crypts correlating with decreased activity of Elk-1 and c-Myc. Both participate in cell cycle regulation via cyclin expression (2). In the apical compartment, we found decreased amount of apoptotic cells, which is probably a compensatory reaction to low cellular output from crypts regulated by decreased activity of JNK and its substrate c-Myc (3, 4). No other changes were observed except for lymphangiectasia in small intestine of 2 animals. Lymphangiectasia might be related to impaired lymph drainage due to circulatory stagnation. In the 3 day interval, the mitotic activity in crypts was restored with phospho-Elk-1 being at the control level and c-Myc being overactivated. In the apical compartment, the amount of apoptotic cells was increased, which corresponded to increased proapoptotic JNK/c-Myc signalling and decreased p38 activity [p38 protects enterocytes against apoptosis (3, 5)]. Accelerated cell loss correlating with 3 – 5 day cycle of complete cellular exchange may indicate an effort of intestinal tissue to dispose of cells damaged in crypts early after the poisoning. JNK also regulates intestinal permeability (6), therefore, subepithelial oedema could be found. Significance and mechanism decreasing mitotic activity in crypts in the 7 day interval is uncertain. Theoretically, it might indicate a persisting damage (as discussed before) that was not successfully repaired and expresses again after several cell cycles. The character of the damage remains unknown. Nevertheless, soman is capable of forming DNA adducts and interferes with DNA metabolism *in vitro* (7, 8). Thus, we may argue that it forms DNA adducts *in vivo*. Such damage does not seem so deleterious to activate p53/p21 signalling but it appears significant enough to downregulate proliferation, and possibly activates DNA repair mechanism, in which CREB may participate via regulation of genes involved in base and nucleotide excision repair systems (9, 10).

Summary

Purpose: The aim of our study is to explore biochemical (blood), histopathological (heart, lung, liver, kidney, small and large intestine) and molecular changes (large intestine - p53 and MAPK signalling) following soman poisoning.

Methods: Male Wistar rats were *i.m.* administered with saline or soman (70% LD₅₀). Blood, heart, lung, liver, kidney, small and large intestine were collected 1, 3 and 7 days after the administration. In blood, glucose, urea, creatinine, bilirubin, conjugated bilirubin, cholesterol, TAG, total protein, ALT, AST, ALP, GMT, CK, and LDH were measured. Organs were stained with hematoxylin-eosin, Mallory's PTAH (heart) and TUNEL (lung, liver, kidney) and immunohistochemical detection of activated-caspase-3 (lung, liver, kidney, intestine) and phospho-p53^{Ser15}, p21, phospho-JNK^{Thr183/Tyr185}, phospho-p38^{Thr180/Tyr182},

phospho-Elk-1^{Ser-383}, phospho-c-Myc^{Thr-58/Ser-62}, phospho-ATF-2^{Thr-69/71}, and phospho-CREB^{Ser-133} (large intestine) was performed.

Results

In blood, increased CK and AST were measured 3 days after the soman poisoning. In heart, we found multifocal acute myolysis in 7 of 19 intoxicated animals. In lungs, decreased air/tissue ratio, hypereamia and multifocal intraseptal oedema were found 1 day after the poisoning. In the 3 day interval, only intraalveolar erythrocytes were recorded, while in the 7 day interval multifocal intraseptal oedema and hyperaemia reappeared accompanied with inflammatory infiltration and increased apoptosis. In intestine, we observed decreased mitotic activity in crypts 1 day, increased apoptotic activity in apical cells 3 days and decreased mitotic activity in crypts 7 days after the poisoning. We also found lymphangiectasia in small intestine of 2 animals in the 1 day interval and subepithelial oedema in large intestine of an animal from the 3 day group. In the apical compartment of large intestine, we measured decreased JNK/c-Myc signalling 1 day after the poisoning, while it increased together with increased activity of CREB and decreased activity of p38 in the 3 day interval. In crypts, we observed decreased Elk-1 and c-Myc and increased CREB activity 1 day after the poisoning. In the 3 day interval, we found increased activities of JNK, c-Myc and CREB.

Conclusion

Soman poisoning causes biochemical changes in blood and morphological changes in heart, lungs, small and large intestine. In large intestine, dysregulation of MAPK signalling pathways can be observed.

References

1. Delaunois A, Gustin P, Garbarg M, Ansay M. Modulation of acetylcholine, capsaicin and substance P effects by histamine H3 receptors in isolated perfused rabbit lungs. *Eur J Pharmacol.* 1995; 277, 243-250.
2. Pejchal J, Osterreicher J, Kassa J, Tichy A, Sinkorova Z, Zarybnicka L, Kubelkova K, Kuca K. Soman and VX: different effect on cellular signalling. *J Appl Biomed.* 2012; 10, 51-61.
3. Seisenbacher G, Hafen E, Stocker H. MK2-dependent p38b signalling protects *Drosophila* hindgut enterocytes against JNK-induced apoptosis under chronic stress. *PLoS Genet.* 2011; 7, 1-14.
4. Ciclitira, PJ, Stewart J, Evan G, Wight DG, Sikora K. Expression of c-myc oncogene in coeliac disease. *J Clin Pathol.* 1987; 40, 307-311.
5. Beutheu Youmba S, Belmonte L, Galas L, Boukhattala N, Bôle-Feysot C, Déchelotte P, Coëffier M. Methotrexate modulates tight junctions through NF- κ B, MEK, and JNK pathways. *J Pediatr Gastroenterol Nutr.* 2012; 54, 463-470.
6. Pejchal J, Novotný J, Mařák V, Osterreicher J, Tichý A, Vávrová J, Sinkorová Z, Zarybnická L, Novotná E, Chládek J, Babicová A, Kubelková K, Kuča K. Activation of p38 MAPK and expression of TGF- β 1 in rat colon enterocytes after whole body γ -irradiation. *Int J Radiat Biol.* 2012; 88, 348-358.
7. Ivanović V, Rapić V, Bosković B. Pinacolyl methylphosphonochloridate: in vitro covalent binding to DNA and mutagenicity in the Ames test. *Mutat Res.* 1985; 142, 9-12.
8. Klein AK, Nasr ML, Goldman M. The effects of in vitro exposure to the neurotoxins sarin (GB) and soman (GD) on unscheduled DNA synthesis by rat hepatocytes. *Toxicol Lett.* 1987; 38, 239-249.
9. Grösch S, Kaina B. Transcriptional activation of apurinic/aprimidinic endonuclease (Ape, Ref-1) by oxidative stress requires CREB. *Biochem Biophys Res Commun.* 1999; 261, 859-863.
10. Lemée F, Bavoux C, Pillaire MJ, Bieth A, Machado CR, Pena SD, Guimbaud R, Selves J, Hoffmann JS, Cazaux C. Characterization of promoter regulatory elements involved in downexpression of the DNA polymerase kappa in colorectal cancer. *Oncogene.* 2007; 26, 3387-3394.

groups	control			soman		
	1 d	3 d	7 d	1 d	3 d	7 d
No. of animals in group	6	6	6	8	8	8
dead before time of examination	0	0	0	3	1	1
<i>BLOOD</i>						
AST	1.2 ± 0.2	1.4 ± 0.3	1.1 ± 0.1	1.4 ± 0.3	2.1 ± 0.2	1.3 ± 0.4
creatin kinase (CK)	5.4 ± 1.0	8.6 ± 4.5	5.7 ± 0.9	4.5 ± 1.5	17.3 ± 4.6	5.9 ± 2.3
<i>HEART</i>						
acute myolysis	0	0	0	+ (1)	+ /++ (4)	+ (2)
inflammatory infiltration	0	0	0	0	+ (2)	+ (1)
<i>LUNG</i>						
intraalveolar oedema	0	0	0	++ /+++ (5)	0	+ /++ (4)
hyperaemia	0	0	0	++ /+++ (5)	0	+ /++ (4)
intraalveolar bleeding	0	0	0	+ (3)	+ (3)	+ (4)
inflammatory infiltration	0	0	0	0	0	+ (4)
bronchial subepithelial oedema	0	0	0	+ (1)	0	0
air in microscopic field (%)	72 ± 2	68 ± 3	69 ± 3	59 ± 4	70 ± 3	65 ± 4
<i>SMALL INTESTINE</i>						
lymphangiectasia	0	0	0	++ (2)	0	0
<i>LARGE INTESTINE</i>						
subepithelial oedema	0	0	0	0	++ (1)	0

Tab 1. Biochemical and histopathological changes found in rats after soman poisoning.

+ - rare, ++ - mild, +++ - middle, ++++ - strong change

Significant differences between control and intoxicated animals: $p \leq 0.05$ – **bold**

		control			soman		
groups		1 d	3 d	Groups	1 d	3 d	Groups
<i>HEART (myolytic cells per microscopic field at 400-fold magnification)</i>							
PTAH ⁺	subendocard	0 ± 0	0 ± 0	0 ± 0	0.2 ± 0.4	4.1 ± 2.7	1.0 ± 3.0
	myocard	0 ± 0	0 ± 0	0 ± 0	0.1 ± 0.1	1.0 ± 1.0	0.3 ± 0.5
<i>LUNG (apoptotic cells per microscopic field at 400-fold magnification)</i>							
activated-caspase-3 ⁺		0.2 ± 0.2	0.2 ± 0.1	0.1 ± 0.1	0.3 ± 0.2	0.4 ± 0.2	0.7 ± 0.2
TUNEL ⁺		0.1 ± 0.1	0.1 ± 0.1	0.1 ± 0.1	0.1 ± 0.0	0.3 ± 0.1	0.3 ± 0.1
<i>LIVER (apoptotic cells per microscopic field at 400-fold magnification)</i>							
activated-caspase-3 ⁺		0.4 ± 0.1	0.5 ± 0.2	0.3 ± 0.1	0.5 ± 0.2	0.6 ± 0.2	0.4 ± 0.1
TUNEL ⁺		0.5 ± 0.1	0.4 ± 0.2	0.4 ± 0.2	0.7 ± 0.2	0.7 ± 0.2	0.3 ± 0.1
<i>KIDNEY (apoptotic cells per microscopic field at 400-fold magnification)</i>							
cortex	activated-caspase-3 ⁺	0.4 ± 0.3	0.3 ± 0.2	0.3 ± 0.2	0.3 ± 0.1	0.3 ± 0.2	0.5 ± 0.4
	TUNEL ⁺	0.1 ± 0.1	0.1 ± 0.1	0.2 ± 0.1	0.2 ± 0.3	0.1 ± 0.1	0.1 ± 0.1
medulla	activated-caspase-3 ⁺	0.4 ± 0.2	0.2 ± 0.2	0.3 ± 0.2	0.2 ± 0.1	0.3 ± 0.2	0.3 ± 0.3
	TUNEL ⁺	0.2 ± 0.1	0.1 ± 0.1	0.2 ± 0.1	0.3 ± 0.2	0.2 ± 0.1	0.3 ± 0.2
<i>SMALL INTESTINE (apoptotic index, %)</i>							
apical cells	HE	1.1 ± 0.1	1.0 ± 0.1	1.0 ± 0.1	0.7 ± 0.2	1.0 ± 0.1	0.9 ± 0.2
	activated-caspase-3 ⁺	1.3 ± 0.1	1.1 ± 0.2	1.3 ± 0.2	0.9 ± 0.2	1.6 ± 0.2	0.9 ± 0.2
cypts	HE	0.6 ± 0.2	0.7 ± 0.2	0.7 ± 0.3	0.6 ± 0.3	0.8 ± 0.5	0.5 ± 0.2
	activated-caspase-3 ⁺	0.5 ± 0.1	0.6 ± 0.1	0.6 ± 0.1	0.4 ± 0.3	0.4 ± 0.2	0.5 ± 0.2
mitotic index, %		3.4 ± 0.5	3.3 ± 0.5	3.2 ± 0.6	2.5 ± 0.4	4.1 ± 0.6	2.3 ± 0.3
<i>LARGE INTESTINE (apoptotic index, %)</i>							
apical cells	HE	2.0 ± 0.3	2.1 ± 0.3	2.0 ± 0.3	1.3 ± 0.3	2.8 ± 0.4	1.6 ± 0.1
	activated-caspase-3 ⁺	1.9 ± 0.2	2.1 ± 0.3	2.0 ± 0.3	1.5 ± 0.3	3.0 ± 0.5	2.0 ± 0.4
cypts	HE	1.3 ± 0.1	1.3 ± 0.3	1.5 ± 0.2	1.3 ± 0.3	1.1 ± 0.3	1.5 ± 0.3
	activated-caspase-3 ⁺	1.1 ± 0.3	1.1 ± 0.3	1.1 ± 0.3	1.0 ± 0.4	1.2 ± 0.3	1.4 ± 0.3
mitotic index, %		1.1 ± 0.2	1.3 ± 0.2	1.0 ± 0.3	0.5 ± 0.2	1.2 ± 0.3	0.6 ± 0.1

Tab 2. Amount of apoptotic cells in heart, lung, liver, kidney, small and large intestine and amount of mitotic cells in small and large intestine in rats after soman poisoning.

Significant differences between control and intoxicated animals: $p \leq 0.05$ – **bold**.

HE – hematoxylin-eosin.

In intestine, apoptotic index was assessed within 1000 cells at the luminal surface and both apoptotic and mitotic indexes were evaluated in 50 crypts within the cells from the 1st to the 14th position starting at the midpoint at the base of the crypt.

groups	control		soman	
	1 d	3 d	1 d	3 d
<i>apical enterocytes</i>				
p-p53 ^{Ser15}	400 ± 100	400 ± 100	700 ± 300	500 ± 100
p21	2000 ± 600	1700 ± 1200	2500 ± 1300	1500 ± 900
p-JNK ^{Thr183/Tyr185}	2200 ± 700	1700 ± 800	900 ± 300	5600 ± 3200
p-p38 ^{Thr180/Tyr182}	2400 ± 1200	3300 ± 1200	1600 ± 400	1100 ± 300
p-Elk-1 ^{Ser-383}	32400 ± 6500	28600 ± 3700	31300 ± 7200	36800 ± 6300
p-c-Myc ^{Thr-58/Ser-62}	12100 ± 3600	8100 ± 2200	6500 ± 3700	17400 ± 4000
p-ATF-2 ^{Thr-69/71}	500 ± 100	400 ± 200	700 ± 200	500 ± 100
p-CREB ^{Ser-133}	1200 ± 300	1400 ± 700	2000 ± 900	4300 ± 2300
<i>crypts</i>				
p-p53 ^{Ser15}	100 ± 100	0 ± 0	100 ± 0	0 ± 0
p21	100 ± 0	100 ± 100	200 ± 100	0 ± 0
p-JNK ^{Thr183/Tyr185}	200 ± 100	300 ± 100	200 ± 200	2600 ± 2000
p-p38 ^{Thr180/Tyr182}	500 ± 200	200 ± 100	300 ± 100	400 ± 200
p-Elk-1 ^{Ser-383}	28800 ± 6100	30000 ± 3700	17500 ± 5500	22700 ± 4200
p-c-Myc ^{Thr-58/Ser-62}	3500 ± 700	4600 ± 800	2200 ± 600	6300 ± 1200
p-ATF-2 ^{Thr-69/71}	300 ± 100	600 ± 200	300 ± 100	700 ± 200
p-CREB ^{Ser-133}	500 ± 100	1300 ± 600	1600 ± 400	2200 ± 700

Tab 3. IOD values of p53, JNK, p38, Elk-1, c-Myc, ATF-2, and CREB activation and p21 expression in rat large intestine following soman poisoning.

Significant differences between control and intoxicated animals: $p \leq 0.05$ – **bold**

REGULATION OF CDX2 AND INTESTINAL DIFFERENTIATION IN HOMEOSTASIS AND CARCINOGENESIS: UNVEILING THE ROLE OF THE RNA-BINDING PROTEIN MEX3A

Bruno Miguel Correia Pereira

E-mail: bpereira@ipatimup.pt

Differentiation and Cancer group, Institute of Molecular Pathology and Immunology of the University of Porto (IPATIMUP), Portugal and Faculty of Medicine of the University of Porto (FMUP), Portugal

Co-authors: S. Sousa, R. Barros, L. Carreto, P. Oliveira, C. Oliveira, N. T. Chartier, M. Plateroti, JP. Rouault, JN. Freund, M. Billaud, R. Almeida

Supervisor: Raquel Almeida, PhD

Co-supervisor: Prof. Leonor David, MD, PhD

Introduction

Gastrointestinal (GI) malignancies are a leading cause of morbidity worldwide, affecting over two million individuals per year (Ferlay *et al.* 2010). This health burden has been intensively tackled during the last decades in the search for new approaches of prevention and management. Deregulated expression of the homeobox transcription factor CDX2, a master regulator of intestinal differentiation, is associated with GI carcinogenesis (Barros *et al.* 2012). In the stomach, *de novo* CDX2 expression drives a preneoplastic lesion known as intestinal metaplasia that confers increased risk of gastric cancer development (Almeida *et al.* 2003), whereas it has been classically considered a tumour-suppressor in intestinal epithelial cells (Bonhomme *et al.* 2003). Since structural alterations in the *CDX2* locus are rarely detected (Woodford-Richens *et al.* 2001), efforts have been concentrated in thoroughly defining the regulatory mechanisms underlying its expression. In the long-run, the acquired knowledge could be integrated into alternative and more target-oriented therapeutic strategies. In the present work, we have established 3D gastric cell culture models that better mimic the *in vivo* setting, hypothesizing that this exploratory approach would allow uncovering new molecular mechanisms of CDX2 regulation.

Methods

Through genome-wide microarray screening of a 3D cell culture system comprising the gastric carcinoma AGS cell line and an extracellular matrix (matrigel), we disclosed the RNA-binding protein MEX3A as a putative CDX2 regulator. This regulation was validated by modulating MEX3A levels through overexpression of a myc-tagged MEX3A form and transient silencing of the endogenous transcripts using siRNAs. To assess interaction between MEX3A protein and *CDX2* mRNA, RNA-immunoprecipitation and luciferase reporter experiments were performed. Functional effects of MEX3A overexpression were addressed *in vitro* by assessing the expression profile of specific intestinal markers and employing 3D cell cyst formation assays in matrigel (Gao and Kaestner 2010). The MEX3A expression pattern was studied in murine intestine by immunofluorescence.

Results

We observed that CDX2 protein expression was abrogated in 3D culture, lacking correlation with its mRNA levels, suggesting a post-transcriptional regulation (Figure 1). Transcriptomic analysis revealed increased expression of the RNA-binding protein MEX3A in the 3D culture. MEX3A is one of the human orthologues of MEX-3, a translational repressor known to target the *CDX* orthologue *pal-1* in *Caenorhabditis elegans* and involved in specifying blastomere identity during early embryogenesis and totipotency in the adult germline (Ciosk *et al.* 2006; Pereira *et al.* 2013). A novel interaction

between human MEX3A and *CDX2* mRNA in a GI context could constitute a plausible explanation for the reduction of CDX2 protein levels observed in the 3D culture. MEX3A repressive function was determined by observing an inverse correlation with CDX2 protein levels, both in gastric and colorectal cell lines. Furthermore, we proved interaction of MEX3A with CDX2 mRNA 3' untranslated region (3'UTR) and defined the specific binding sequence (Figure 2). Phenotypic characterization of *in vitro* models demonstrated that MEX3A overexpression leads to loss of intestinal differentiation, as assessed by reduced levels of the enterocyte-specific marker Villin and the goblet cell-specific marker MUC2. Furthermore, MEX3A overexpressing cells have an altered cell cycle profile and increased expression of intestinal stem cell markers, namely *LGR5*, *BMI1* and *MSI1*. These cells also fail to elaborate 3D cysts with a well-defined central lumen, indicating that apical-basal polarity is affected (Figure 3). Finally, we show that MEX3A is expressed in the mouse small intestine and colon in a pattern that putatively correlates with CDX2 modulation and stem cell properties.

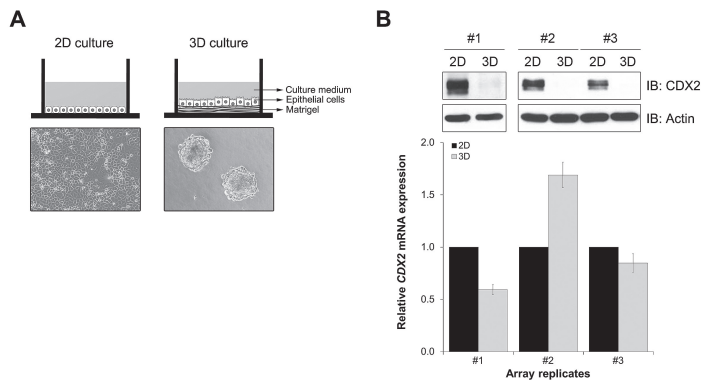


Figure 1. Establishment of AGS 3D cell cultures and characterization of CDX2 expression. (A) Schematic representation of the culture systems and cellular morphology at culture day 4 in bright field microscopy (original magnification, x100). (B) Western blot and real-time PCR of CDX2 expression in 2D and 3D after 2 weeks culture. Cardinal numbers represent biological replicates. Values for CDX2 mRNA expression in 2D culture were referred to as 1.

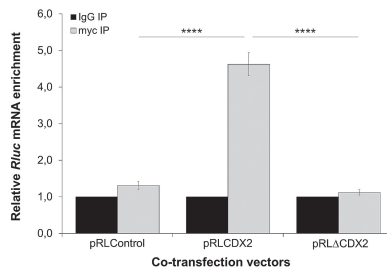


Figure 2. Mechanistic of MEX3A interaction with CDX2 mRNA in AGS cells. Real-time PCR showing the relative enrichment obtained after immunoprecipitation with a myc-tag antibody (directed against myc-tagged MEX3A) or control IgG for Renilla luciferase (*Rluc*) mRNA alone (pRLControl), for a fusion transcript between *Rluc* coding sequence and the CDX2 mRNA 3'UTR (pRLCDX2), and for a fusion transcript containing the CDX2 3'UTR with a mutated MEX-3 recognition element (pRLΔCDX2). Values for *Rluc* expression in IgG samples were referred to as 1 (**** $P < 0.0001$).

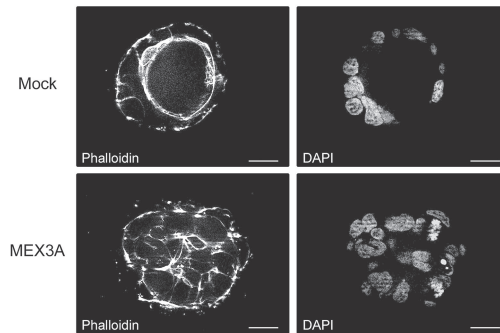


Figure 3. Polarity alterations induced by MEX3A in Caco-2 cells. Phalloidin and DAPI staining in Caco-2 cysts (original magnification, x630; scale bars 20 μ m).

Discussion

Our results bring forward a possible role for MEX3A in intestinal homeostasis and colorectal carcinogenesis, not only through CDX2 regulation, but also through its association with loss of polarity and gain of stemness properties. MEX3A might directly contribute to the decreased CDX2 expression observed in a subset of colorectal carcinomas, particularly those with minimal differentiation. The recent identification of *MEX3A* mRNA as being part of the transcriptomic signature of *LGR5*⁺ intestinal stem cells (Muñoz *et al.* 2012), and the fact that 74 to 85% of colorectal cancers display a *LGR5*⁺ associated transcriptional profile (Ziskin *et al.* 2013) favour a link between MEX3A and colorectal malignancy that we will explore in the near future.

Conclusions

This study describes a novel post-transcriptional process by which CDX2 expression is impaired in the GI setting and intestinal-like homeostasis compromised. Another layer of control is thus added to the complex CDX2 regulatory network, involving mRNA control by the RNA-binding protein MEX3A, which might have significant implications to GI carcinogenesis.

Summary

The homeodomain transcription factor CDX2 is a key player in intestinal differentiation. Therefore, it is not surprising to find its expression significantly altered in carcinogenic processes of the gastrointestinal tract. Several transcriptional, post-transcriptional and post-translational mechanisms have been described to control CDX2, making this a highly complex and tightly organized regulatory system. Through genome-wide screening of a 3D culture system, the RNA-binding protein MEX3A was identified as putatively involved in CDX2 regulation; therefore, its biological relevance was addressed by setting up cell-based assays together with expression studies in murine intestine. We demonstrate that MEX3A has a repressive function by controlling CDX2 levels in gastric and colorectal cellular models. This is dependent on the interaction with a specific binding determinant present in *CDX2* mRNA 3' untranslated region. We have further determined that MEX3A impairs intestinal differentiation and cellular polarization, affects cell cycle progression and promotes increased expression of intestinal stem cell markers. Finally, we show that MEX3A is expressed in mouse intestine, supporting a biological background for the regulation of CDX2. In this study, we provide the first demonstration that MEX3A represses CDX2 expression in the gastrointestinal context, putatively as a translational repressor, with direct implications in key mechanisms for tissue homeostasis that are also inextricably linked with cancer.

References

1. Almeida R, Silva E, Santos-Silva F, Silberg D, Wang J, De Bolós C, David L. 2003. Expression of intestine-specific transcription factors, CDX1 and CDX2, in intestinal metaplasia and gastric carcinomas. *J Pathol* 199: 36-40.
2. Barros R, Freund JN, David L, Almeida R. 2012. Gastric intestinal metaplasia revisited: function and regulation of CDX2. *Trends Mol Med* 18: 555-563.
3. Bonhomme C, Duluc I, Martin E, Chawengsaksophak K, Chenard MP, Kedinger M, Beck F, Freund JN, Domon-Dell C. 2003. The Cdx2 homeobox gene has a tumour suppressor function in the distal colon in addition to a homeotic role during gut development. *Gut* 52: 1465-1471.
4. Ciosk R, DePalma M, Priess JR. 2006. Translational regulators maintain totipotency in the *Caenorhabditis elegans* germline. *Science* 311: 851-853.
5. Ferlay J, Shin H, Bray F, Forman D, Mathers C, Parkin D. 2010. GLOBOCAN 2008 v2.0, Cancer Incidence and Mortality Worldwide: IARC CancerBase No. 10 [Online]. Lyon, France: International Agency for Research on Cancer. Available from: <http://globocan.iarc.fr>
6. Gao N, Kaestner KH. 2010. Cdx2 regulates endo-lysosomal function and epithelial cell polarity. *Genes Dev* 24: 1295-1305.
7. Muñoz J, Stange D, Schepers A, van de Wetering M, Koo BK, Itzkovitz S, Volckmann R, Kung K, Koster J, Radulescu S, *et al.* 2012. The *Lgr5* intestinal stem cell signature: robust expression of proposed quiescent '+4' cell markers. *EMBO J* 31: 3079-3091.
8. Pereira B, Le Borgne M, Chartier NT, Billaud M, Almeida R. 2013. MEX-3 proteins: recent insights on novel post-transcriptional regulators. *Trends Biochem Sci* 38: 477-479.
9. Woodford-Richens KL, Halford S, Rowan A, Bevan S, Aaltonen LA, Wasan H, Bicknell D, Bodmer WF, Houlston RS, Tomlinson IP. 2001. CDX2 mutations do not account for juvenile polyposis or Peutz-Jeghers syndrome and occur infrequently in sporadic colorectal cancers. *Br J Cancer* 84: 1314-1316.
10. Ziskin J, Dunlap D, Yaylaoglu M, Fodor I, Forrest W, Patel R, Ge N, Hutchins G, Pine J, Quirke P, *et al.* 2013. In situ validation of an intestinal stem cell signature in colorectal cancer. *Gut* 62: 1012-1023.

LOW GDP PERITONEAL DIALYSIS REGIMEN HAS A BENEFICIAL EFFECT ON PLASMA LEVELS OF PROINFLAMMATORY LIGANDS OF RECEPTOR FOR ADVANCED GLYCATION END PRODUCTS

Anna Pöpperlová

E-mail: popperlovaa@fnplzen.cz

Dept. of Medicine I, Charles University Medical School and Teaching Hospital Pilsen,
Czech Republic

Co-authors: S. Opatrná, M. Kalousová, T. Zima

Tutor: prof. MUDr. Sylvie Opatrná, Ph.D.

Introduction

The receptor for advanced glycation end products (RAGE) has originally been described as a receptor for AGEs and mediates many but not all of the effects of AGEs. Some of AGEs effects are direct, without any receptor, and some other effects are mediated via different receptors. AGEs accumulate in chronic kidney disease (CKD) patients. AGEs are a heterogeneous group of structures occurring as a consequence of nonenzymatic glycoxidation of proteins or lipids in presence of glucose and / or glucose degradation products (GDP). In peritoneal dialysis (PD) patients, AGEs may contribute to anatomical and functional changes of peritoneum which inevitably occur with long-term PD. Expression of RAGE is enhanced in CKD. RAGE is a multi-ligand receptor biology of which is driven by the diversity of its ligands, e.g. AGEs, S100A1- also known as EN-RAGE (extracellularly newly identified receptor for advanced glycation end products) (10,6kDa) (1), High mobility group box-1 (HMGB-1) (30kDa) (2) and others. Soluble RAGE (s-RAGE) (50kDa) (3) is one of the variants of RAGE (lacking the C-terminal (transmembrane) domain) acting as a naturally occurring inhibitor of pathological effects mediated via RAGE. S-RAGE levels are elevated in CKD patients and correlate inversely with glomerular filtration rate and atherosclerosis and inflammation in this patients' population (4). Engagement of RAGE by EN-RAGE has proinflammatory effect (5). HMGB-1 is present in the nucleus of almost all eukaryotic cells. If released extracellularly, it acts as an inflammatory mediator (6). PD patients, especially those treated with glucose-lactate PD solutions, are exposed to very high intraperitoneal load of GDP and glucose. Implementation of a PD regimen containing icodextrin or glucose-bicarbonate based dialysis solution in two-compartment PD bags enables to decrease the intraperitoneal GDP and / or glucose exposure and AGEs generation. With this in mind we designed a study to compare the plasma levels of s-RAGE, EN-RAGE and HMGB-1 between three patients' groups treated with a PD regimen which differ in GDP content and to compare s-RAGE and its above mentioned ligands between PD patients, CKD patients stage 3-5 and healthy volunteers (HV).

Methods

PD regimen with high GDP load (glucose-lactate PD fluid, D; n = 8) was compared with a low GDP load (glucose-bicarbonate/lactate with icodextrin exchange for overnight dwell, E; n = 9) and a very low GDP load (glucose-bicarbonate/lactate, P; n = 16).

Results

D group demonstrated higher plasma EN-RAGE levels, 77.8 ng/mL, vs. both E, 11.2, $p < 0.001$ and P, 27.0, $p < 0.001$ as well as higher plasma HMGB1 levels, 2.2 ng/mL vs. both E, 1.1, $p < 0.01$ and P, 1.5, $p < 0.01$. Plasma s-RAGE did not differ between the three PD regimen used. Peritoneal clearance of s-RAGE and EN-RAGE was higher with E compared to both D and P ($p < 0.001$ resp. $p < 0.01$). In the whole PD patients' group, those with dialysate-to-plasma creatinine ratio (D/Pcr) > 0.65 tended to

have higher s-RAGE plasma levels ($p = 0.056$); and those with CRP level above median demonstrated higher HMGB-1 and EN-RAGE ($p < 0.05$ for both).

Discussion

Patients treated with a PD regimen with decreased GDP content (with glucose–bicarbonate/lactate or icodextrin PD solutions), group P and E, demonstrated significantly lower plasma levels of proinflammatory EN-RAGE and HMGB-1 ligands compared to patients treated with conventional, high GDP PD solution (group D) (7). This finding suggests that prescription of low GDP PD solution might be associated with lower generation of AGEs in the systemic circulation as well as lower inflammatory response. Intraperitoneal GDP load seems to be an important factor of increased plasma levels of proinflammatory RAGE ligands. GDP content in PD solutions seems to be more important for AGEs generation than glucose concentration per se. GDPs disappear from the peritoneal cavity during the dwell but – due to their high reactivity – not all of them can be detected in plasma (8). We assume that higher plasma levels of proinflammatory RAGE ligands described in our study in PD patients treated with conventional PD solutions might reflect an accelerated AGEs production as a consequence of the high intraperitoneal GDP load. Our findings are consistent with the fact that EN-RAGE increases during inflammation (9) as we have shown a correlation between EN-RAGE and CRP in PD patients. Moreover, PD patients with CRP above median demonstrated also significantly higher EN-RAGE. HMGB-1 which is released extracellularly with profound cell damage or after proinflammatory stimulation (6) has not been extensively studied in PD patients as yet. Its higher plasma levels found with high GDP PD regimen might document the higher cytotoxicity of these conventional PD solutions. The fact that HMGB-1 concentration in PD effluent was higher than in plasma and lack of correlation between plasma and effluent HMGB-1 levels might suggest that HMGB-1 is generated intraperitoneally in significant quantities probably due to the cytotoxicity of instilled PD fluid. Mutual correlation between HMGB-1 and EN-RAGE demonstrated in our PD, CKD and HV subject supports the idea that the biological activity of these two proinflammatory ligands is closely interrelated. In PD and CKD patients – individuals with decreased renal function, a condition universally associated with microinflammation, HMGB-1 and EN-RAGE correlated with CRP. Intraperitoneal GDP load does not seem to directly effects plasma s-RAGE levels, because they did not differ between the three PD regimen studied. Plasma s-RAGE levels were higher than its effluent levels in all three PD regimen and significant positive mutual correlation between plasma and effluent levels was demonstrated. Interestingly, but not surprisingly, PD regimen using icodextrin (which is known to increases peritoneal clearance of middle molecular weight substances) (10) increased peritoneal clearance of both EN-RAGE (MW 10.6kDa) (1) and s-RAGE (MW 50 kDa) (3) compared to glucose-based PD regimen. However the design of our study does not enable us to quantify the relative contribution of this mechanism to the plasma levels.

Conclusions

A lower intraperitoneal GDP load is associated with decreased plasma levels of EN-RAGE and HMGB1 thus possibly reflecting reduced systemic AGEs generation. Peritoneal transport characteristics, microinflammation as well as the capability of icodextrin to increase removal of middle molecular weight substances might also exert an effect on plasma RAGE ligands levels.

Summary

Our study which demonstrated lower plasma proinflammatory RAGE ligands (EN-RAGE and HMGB-1) level when low GDP PD solutions are used support the findings that GDP load directly influences systemic AGEs levels.

References

1. Mirmohammadsadegh A, Tschakarjan E, Ljoljic A et al.: Calgranulin C is overexpressed in lesional psoriasis. *J Invest Dermatol.* 2000; 114(6): 1207-8.
2. Wang H, Yang H, Tracey KJ: Extracellular role of HMGB1 in inflammation and sepsis. *J Intern Med.* 2004; 255(3): 320-31.
3. Forbes JM, Thorpe SR, Thallas-Bonke V et al.: Modulation of soluble receptor for advanced glycation end products by angiotensin-converting enzyme-1 inhibition in diabetic nephropathy. *J Am Soc Nephrol.* 2005; 16(8): 2363-72.
4. Basta G, Leonardis D, Mallamaci F et al.: Circulating soluble receptor of advanced glycation end product inversely correlates with atherosclerosis in patients with chronic kidney disease. *Kidney Int.* 2010; 77(3): 225- 31.
5. Yang Z, Tao T, Raftery MJ, Youssef P, Di Girolamo N, Geczy CL: Proinflammatory properties of the human S100 protein S100A12. *J Leukoc Biol.* 2001; 69(6): 986-94.
6. Scaffidi P, Misteli T, Bianchi ME: Release of chromatin protein HMGB1 by necrotic cells triggers inflammation. *Nature.* 2002; 418(6894): 191-5.
7. Erixon M, Wieslander A, Lindén T et al.: How to avoid glucose degradation products in peritoneal dialysis fluids. *Perit Dial Int.* 2006; 26(4): 490-7.
8. Erixon M, Wieslander A, Lindén T et al.: 3,4-dideoxyglucosone-3-ene in peritoneal dialysis fluids infused into the peritoneal cavity cannot be found in plasma. *Perit Dial Int.* 2009; 29 Suppl 2:S28-31.
9. Foell D, Ichida F, Vogl T et al.: S100A12 (EN-RAGE) in monitoring Kawasaki disease. *Lancet.* 2003; 361(9365): 1270-2.
10. Opatrná S, Opatrný K Jr, Racek J, Sefrna F: Effect of icodextrin-based dialysis solution on peritoneal leptin clearance. *Perit Dial Int.* 2003; 23(1): 89-91

RESVERATROL, CURCUMIN AND METABOLITES CAN MODULATE CYTOKINE RELEASE BY JURKAT T-LYMPHOCYTES

Siân Helen Rose Richardson

E-mail: sian21@liv.ac.uk

Department of Musculoskeletal Biology II, Institute of Ageing and Chronic Disease,
University of Liverpool, Liverpool, UK

Co-authors: Christopher Ford, Silvina Lotito, Alan Crozier,
Anne McArdle, and Malcolm Jackson
Primary Supervisor: Prof. Malcolm Jackson PhD, DSc, FRCPath.

Introduction

As we age, multiple dysregulations occur in the immune system, resulting in a chronic, systemic pro-inflammatory state¹, known as inflamm-ageing. Chronic inflammation plays a major role in age-related cell and tissue dysfunction and the ability to modulate inflammation in older people may improve quality of life for these individuals. Characteristics of inflamm-ageing include increased expression of inflammatory genes such as tumour necrosis factor (TNF α)², elevated circulating inflammatory cytokines, and aberrant NF- κ B activation³.

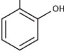
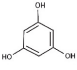
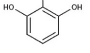
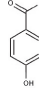
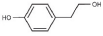
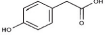
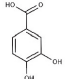
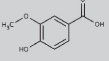
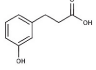
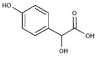
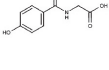
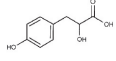
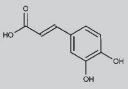
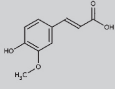
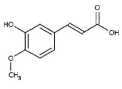
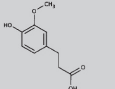
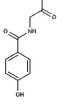
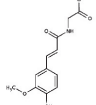
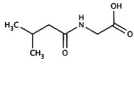
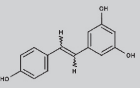
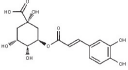
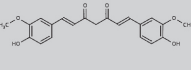
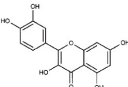
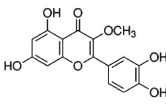
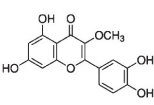
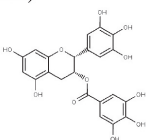
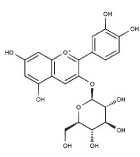
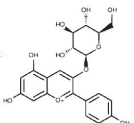
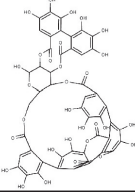
T-lymphocytes are the main component of the immune system; their number and function have been observed to decline with age⁴. Therefore the focus of this project was to reduce cytokine release in Jurkat T-lymphocytes with dietary phenolic compounds. These compounds are known to have antioxidant and anti-inflammatory properties⁵. An increased intake of dietary polyphenols has a number of health benefits including for cardiovascular disease⁶ and cancer⁷. Thousands of natural polyphenols have been identified, with different biological properties depending on their structure⁸, which affects their antioxidant capability and bioavailability. This study screened 29 phenolic compounds, from complex parent polyphenols to smaller phenolic acid metabolites, at the physiologically relevant concentration of 1 μ M. We determined changes in interleukin 2 (IL2), an important cytokine for T-cell activation and function, and also interleukin 8 (IL8) and TNF α , inflammatory mediators that increase as we age.

Aims

To identify phenolic compounds able to reduce release of IL2, IL8 and TNF α cytokines in Jurkat T lymphocytes.

Methods

Jurkat cells (an immortalized T-lymphocyte cell line) were seeded at 2×10^6 / ml in 48 well plates and treated with DMSO or 1 μ M phenolic compound for 48 h. At the 24 h time point cells were either left unstimulated or treated with 25 ng/ml phorbol myristate acetate (PMA) and 5 μ g/ml phytohaemagglutinin (PHA) to activate cells to induce cytokine release. Following incubation cell number was determined using 3-(4,5-dimethylthiazol-2-yl)-5-(3-carboxymethoxyphenyl)-2-(4-sulfophenyl)-2H-tetrazolium (MTS) assay and release of IL2, IL8, and TNF α was determined using multiplex assay, following the manufacturer's instructions (Bio-Rad, USA).

Phenolic acids			
Catechol 	Phloroglucinol 	Pyrogallol 	4-hydroxybenzoic acid 
Tyrosol 	4-hydroxyphenyllactic acid 	Protocatechuic acid 	Vanillic acid 
3-(3'-hydroxyphenyl)propionic acid 	4'-hydroxymandelic acid 	Hippuric acid 	3-(4'-hydroxyphenyl)lactic acid 
Caffeic acid 	Ferulic acid 	Isoferulic acid 	Dihydroferulic acid 
4'-hydroxyhippuric acid 	Feruloylglycine 	Isoferuloylglycine 	
Polyphenols			
Resveratrol[†] 	Chlorogenic acid 	Curcumin[†] 	Quercetin[†] 
3-O-methylquercetin[†] 	Isorhamnetin[†] 	Epigallocatechin gallate (EGCG)[†] 	Kuromanin[†] 
Callistephin chloride[†] 	Punicalagin[†] 	<i>Compounds provided by Professor Alan Crozier (University of Glasgow) unless otherwise stated with [†] (Sigma Aldrich, Dorset, UK). These compounds were chosen to represent complex native polyphenol obtained directly from foods, along with phenolic acids the metabolites of these polyphenols.</i>	

Tab. 1. Phenolic compounds dissolved in dimethyl sulfoxide (DMSO) at a stock concentration 5 mM.

Results & Discussion

From the screening process, the most anti-inflammatory polyphenols screened were curcumin, resveratrol, quercetin, and isorhamnetin. Fig. 1. Shows curcumin, the active principle of the dietary spice turmeric, lowered cytokine release of IL2 by $-43\% \pm 14\%$, IL8 by $-30\% \pm 7\%$ and $\text{TNF}\alpha$ $-21\% \pm 4\%$ in stimulated cells. The curcumin metabolites ferulic acid and dihydroferulic acid retained the anti-inflammatory effects observed with curcumin. Curcumin had less of an effect in unstimulated cells, whereas ferulic acid lowered IL8 by $-63\% \pm 3\%$. Curcumin blocks Ca^{2+} mobilization in T cells, preventing activation of nuclear factor of activated T cells (NFAT) and also nuclear factor kappaB (NF- κ B) via T cell receptor⁹ This may explain the decreases in both IL2 (expression regulated by NFAT) and IL-8 release (expression regulated by NF- κ B)¹⁰

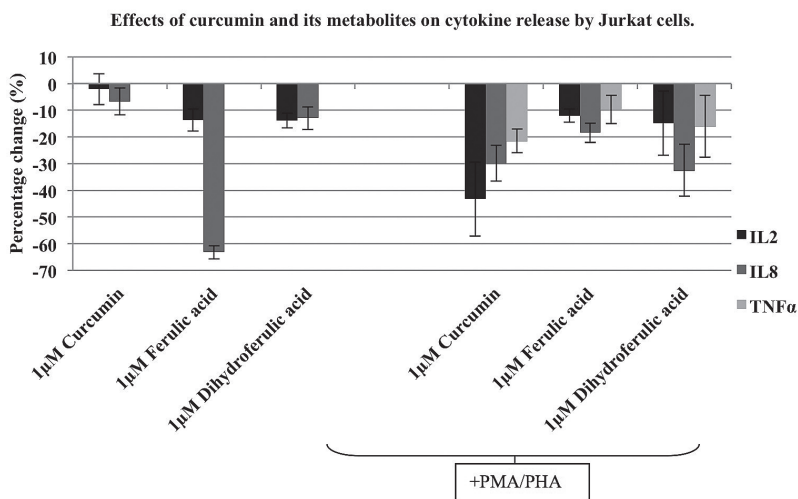


Figure 1. Effect of polyphenols on cytokine release from Jurkat cells (expressed as percentage change from DMSO carrier cells). Cells were treated with 1 μ M parent compound curcumin or metabolites, for 48h with and without PMA/PHA added at the 24h time point.

Resveratrol is found in red wine resulted in a decrease in IL2 by $-42 \pm 7\%$ and IL8 by $31\% \pm 3\%$ in unstimulated cells (fig. 2). The smaller phenolic acids vanillic acid and caffeic had similar effects especially in stimulated cells. Other studies have shown resveratrol to lower inflammation, with 5 μ M resveratrol suppress NF- κ B activation induced by $\text{TNF}\alpha$ in Jurkat cells¹¹

Effects of resveratrol and its metabolites on cytokine release by Jurkat cells.

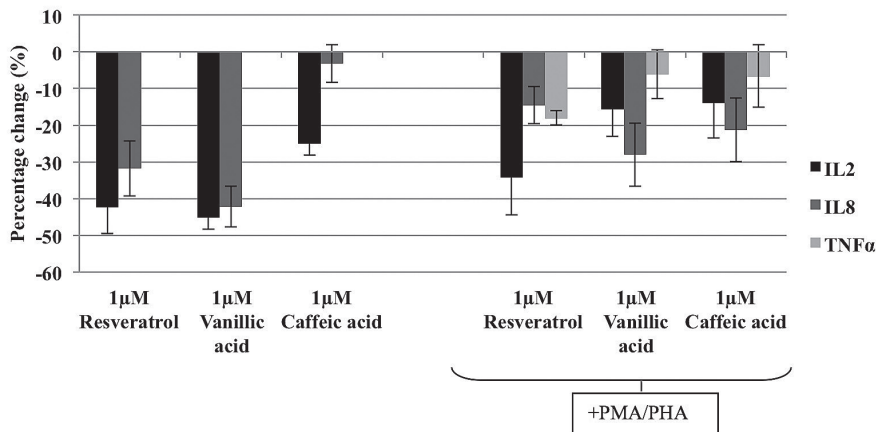


Figure 2. Effect of polyphenols on cytokine release from Jurkat cells (expressed as percentage change from DMSO carrier cells). Cells were treated with 1 μM parent compound resveratrol or metabolites and wine phenolic, for 48h with and without PMA/PHA added at the 24h time point.

The anti-inflammatory effects observed by polyphenols are thought to act through a number of different mechanisms from scavenging reactive oxygen species, to inhibiting transcription factors and kinases. Polyphenols inhibits the release and synthesis of pro-inflammatory mediators through NF-κB and activator protein-1 (AP-1). Compared with other polyphenol research, we have shown anti-inflammatory effects of these phenolic compounds at physiologically relevant concentrations with both polyphenols and their metabolites. These metabolites retained their anti-inflammatory effect or, in the case of ferulic acid, were more active than the native polyphenol found in food. These smaller phenolic acids have a greater bioavailability that polyphenols and can be generated from a number of food sources; therefore their effects *in vivo* maybe much greater than the native polyphenol and potentially more effective in reducing inflammation in the elderly.

Conclusion

Though this screening process a number of phenolic compounds showed potential for lowering cytokine release by T-lymphocytes both in un-stimulated cells as well as those that were stimulated (although only a few were highlighted here). Data also showed that metabolites could retain some of the anti-inflammatory properties observed with the parent compound. Thus, data suggests that curcumin, resveratrol and their metabolites provide promising nutritional interventions to modulate chronic inflammation in older people.

Summary

Ageing has been shown to be associated with low level chronic inflammation with particular increases in TNFα contributing to age-related pathogenesis like atherosclerosis¹² Lowering serum cytokine content is likely to be beneficial in age-related disease such as type 2 diabetes and Alzheimer's disease. Increased levels of TNFα are associated with the pathogenesis of these diseases. Dietary antioxidants such as polyphenols can reduce oxidation and potentially slow the progression of age-related diseases.

The structure of these polyphenols can be linked to their antioxidant capabilities and also their bioavailability. Therefore metabolites of these polyphenols are important to consider when analysing their effects over cellular processes such as inflammation. It is thought that the bioavailability is greater with the phenolic acids; therefore their effects *in vivo* would be greater than the parent compounds. The aim of this work was to determine potential phenolic compounds that will reduce the pro-inflammatory and oxidative state observed with ageing. A number of polyphenols have been identified as promising candidates for reducing inflammation. In particular, curcumin and resveratrol considerably lower the cytokine release of IL2, IL8 and TNF α by stimulated cells. In addition, metabolites and other smaller phenolic acids retained the anti-inflammatory effects observed with the more complex polyphenols.

References

1. Chung, H.Y., Casari, M., Anton, S., Marzetti, E., Giovannini, S., Seo, A.Y., Carter, C., Yu, B.P., and Leeuwenburgh, C. (2009). Molecular inflammation: underpinnings of ageing and age-related diseases. *Ageing Research Reviews*. 9: 18-30.
2. Bruunsgaard, H., Pedersen, M., and Pedersen, B.K. (2001). Aging and proinflammatory cytokines. *Curr Opin Hematol*. 8(3): 131-136.
3. Franceschi, C., Bonafè, M., Valensin, S., Olivieri, F., De Luca, M., Ottaviani, E., and De Benedictis, G. (2000). Inflamm-aging. An evolutionary perspective on immunosenescence. *Ann N Y Acad Sci*. 908: 244-54.
4. Larbi, A., Dupuis, G., Douziche, N., Khalil, A., and Fülöp Jr, T. (2006). Low-grade inflammation with aging has consequences for T-lymphocyte signalling. *Annals of the New York Academy of Sciences*. 1030(1).
5. Quideau, S., Deffieux, D., Douat-Casassus, C., and Pouysegu, L. (2011). Plant polyphenols: Chemical Properties, Biological Activities, and Synthesis. *Angewandte Chemie International Edition*. 50 (3), 586-621.
6. Hertog, M.G., Fesken, E.J., Hollman, P.C., Katan, M.B., and Kromhout, D. (1993). Dietary antioxidant flavonoids and risk of coronary heart disease: the Zutphen Elderly Study. *Lancet*. 342: 1007-1011.
7. Hertog, M.G., Fesken, E.J., Hollman, P.C., Katan, M.B., and Kromhout, D. (1994). Dietary flavonoids and cancer risk in the Zutphen Elderly Study. *Nutr Cancer*. 22: 175-184.
8. Scalbert, A., and Williamson, G. (2000). Dietary intake and bioavailability of polyphenols. *J. Nutr*. 130: 2073S-2085S.
9. Kliem, C., Merling, A., Giaisi, M., Köhler, R., Krammer, P.H., and Li-Weber, M. (2012). Curcumin suppresses T cell activation by blocking Ca²⁺ mobilization and nuclear factor of activated T cells (NFAT) activation. *The journal of biological chemistry*. 287(13): 10200-10209.
10. Fisher, W.G., Yang, P., Medikonduri, R.K., and Jafri, M.S. (2006). NFAT and NF κ B activation in T lymphocytes: A model of differential activation of gene expression. *Ann Biomed Eng*. 34(11): 1712-1728.
11. Manna, S.K., Mukhopadhyay, A., and Aggarwal, B.B. (2000). Resveratrol suppresses TNF-induced activation of nuclear transcription factor NF- κ B, activator protein-1, and apoptosis: potential role of reactive oxygen intermediates and lipid peroxidation. *Journal of immunology*. 164 (12): 6509-6519.
12. Bruunsgaard, H., and Pedersen, B.K. 2003. Age-related inflammatory cytokines and disease. *Immunol Allergy Clin North Am*. 23(1): 15-39

RADIO-SENSITIZATION OF HUMAN LEUKEMIC CELLS HL-60 BY ATR-KINASE INHIBITOR (VE-821): PHOSPHOPROTEOMIC ANALYSIS

Barbora Šalovská

salob5aa@lfhk.cuni.cz

Institute of Medical Biochemistry, Faculty of Medicine in Hradec Králové,
Charles University in Prague, Czech Republic

Co-authors: A. Tichý, I. Fabrik, M. Řezáčová, J. Vávrová, J. Stulík

Tutor: doc. MUDr. Martina Řezáčová, Ph.D.

Tutor-specialist: PharmDr. Aleš Tichý, Ph.D.

Introduction

One of the treatment modalities in oncology is radio-therapy. It often combines chemical agents increasing sensitivity towards ionising radiation (IR). IR induces the most deleterious lesions of DNA, double strand breaks (DSB), and their repair is regulated by ataxia telangiectasia-mutated kinase (ATM), DNA-dependent protein kinase (DNA-PK), and ATM and Rad3-related kinase (ATR), whose inhibition has been reported to increase radio-sensitivity (Tichy et al. 2010).

In 2011, a specific inhibitor of ATR kinase, VE-821, was developed (ChARRIER et al., 2011). There are a few publications that reported an excellent selectivity of this inhibitor in sensitizing of cancer cells towards various types of DNA damaging agents, whereas the normal tissue remained unaffected (Reaper et al., 2011, Pires et al., 2012, Prevo et al., 2012, Huntoon et al., 2013).

We have previously compared the effect of inhibitor of ATM (KU55933) and ATR kinases (VE-821) on the radio-sensitization of human promyelocyte leukaemia cells (HL-60), lacking functional protein p53. The inhibition of ATR by VE-821 resulted in a more pronounced radio-sensitizing effect in HL-60 cells compared to the inhibition of ATM. In contrast to KU55933, VE-821-treatment prevented HL-60 cells from undergoing G2 cell-cycle arrest (Vávrová et al. 2013).

Aims

Our goal was to describe the changes of phosphoproteome in radio-sensitized tumour cells, since in the DNA damage response (as well as in the other molecular processes) it is phosphorylation that frequently initiates and propagates signal transduction pathways. We aimed to characterise the effect of specific inhibition of ATR by VE-821 and to report the mechanisms and signalling pathways involved in the processes triggered by IR in a leukemic cell line that served as a model of p53-negative cells.

An inevitable part of a mass spectrometric analysis of phosphorylation is the enrichment of phosphorylated peptides from the mixture with their non-phosphorylated counterparts. It compensates their low abundance, insufficient ionization, and suppression effects of non-phosphorylated peptides (Tichy et al. 2011). Hence, we initially optimized the metal oxide affinity chromatography (MOAC) enrichment using titanium dioxide and applied it in our experiments (Salovska et al. 2013).

Methods

HL-60 cells were cultured either in SILAC light (Arg0/Lys0) or SILAC heavy (Arg6/Lys6) supplemented IMDM medium for at least 6 doublings. Thirty minutes prior irradiation by the dose of 6 Gy, VE-821 was added to the heavy labeled cells in concentration of 10 μ M (control cells were treated with DMSO at the same time-point). The cells were harvested 1 hour after irradiation and the proteins were extracted. After digestion with trypsin, peptides were separated into 22 fractions using HILIC chromatography. Each fraction was enriched for phosphopeptides using TiO₂ chromatography. The MS analysis was performed on nanoRPLC-ESI-MS/MS system using Thermo Fisher Q Exactive mass

spectrometer. Raw files were processed using MaxQuant software with Andromeda search engine. Gene ontology and Reactome pathways over-representation analysis was done using ConsensusPathDB's web tool. Sequence logos were created in IceLogo. 1D enrichment of consensus kinase motifs was performed using Perseus and kinases were predicted using Networkin 2.0 database (supported by PhosphositeAnalyzer software). Regulated subnetworks were extracted using Subextractor algorithm.

Results and Discussion

TiO₂ chromatography with HILIC pre-fractionation and nanoRPLC-ESI-MS/MS analysis revealed 6927 class I phosphorylation sites on 2430 proteins; among them 893 were differentially up- or down-regulated by phosphorylation (FDR 5%). Most of the regulated proteins were localized in the nuclear compartments. Nevertheless, a considerable fraction of regulated proteins was localized outside the nucleus, implying that ATR inhibition also affects various non-nuclear functions.

The proteins regulated by ATR inhibition were mostly involved in biological processes like metabolism of nucleic acids, cell-cycle phase transition, mitosis or DNA damage response.

ATR inhibition resulted in the increase of activity of cyclin-dependent kinases (indicating abrogation of cell-cycle checkpoints through the ATR inhibition-mediated decrease of CHK1 activity) and decreased activity of ATM/ATR group, which confirmed biological relevance of our data.

In addition, the increased activity of PLK1 kinase - an essential component of G2/M transition processes - was also proved in our study. The key role of ATR in regulation of PLK1 after UV-irradiation has been described recently (Qin et al., 2013) However, it is now for the first time that ATR regulation of PLK1 after IR-induced DNA damage has been reported. Interestingly, the activity of NEK family of protein kinases was also shown to be decreased in our study. While some kinases of the NEKs group are only checkpoint targets that are inhibited by DNA damage, e.g. NEK2 which is known to be PLK1-dependent, others have an important role in DNA damage response (DDR) DDR signalling (NEK1, NEK10, and NEK11). Among them, NEK11 is known to be activated in response to IR-induced DNA damage in an ATM/ATR dependent manner, whereas NEK1 activity seems to be independent on ATM/ATR kinases activities (reviewed in Fry et al., 2012).

The network analysis using Subextractor algorithm revealed regulated phosphoproteins involved in multiple types of DNA repair (single/double strand break repair and base excision repair) emphasizing the importance of ATR kinase in these molecular mechanisms.

Conclusion

Our phosphoproteomic study provided for the first time a complex insight into the mechanisms of inhibition of DNA repair enzyme, ATR kinase. We described phosphorylation processes triggered by radiation-induced DNA damage in radio-sensitized cancer cells and we proved that the novel potent and selective inhibitor VE-821 could be developed into a future drug for eradication of p53-negative tumour cells.

Summary

DNA damaging agents such as ionizing radiation or chemotherapy are frequently used in anti-cancer treatment. DNA damage response (DDR), which is triggered by the presence of gamma-radiation induced double strand breaks, is orchestrated mainly by three protein kinases belonging to the phosphatidylinositol-3 kinase family: ATM, DNA-PK and ATR. The activation of such kinases in radioresistant cells promotes cell-cycle arrest and thus provides sufficient time for DNA damage repair, which results into a failed therapy. A specific ATR inhibitor, VE-821, that was developed recently, has been shown to have a great potential in support of radio- and chemo-therapy. Its sensitizing effect has been reported to be delimited to cancer cells (mostly p53-negative) without affecting normal cells. In this study, we employed SILAC-based high resolution quantitative phosphoproteomics in order to better describe the mechanism of the radio-sensitizing effect of VE-821 in human promyelocytic

leukemic cells HL-60 (p53-negative) and the role of ATR kinase in DDR (1 hour after irradiation by 6 Gy). Titanium dioxide chromatography with HILIC prefractionation and LC-MS/MS analysis revealed 6927 class I phosphorylation sites. Proteins with up- or down- regulated phosphorylation on at least one phosphorylation site were mostly localized in nucleus and were involved in the cellular processes like cell-cycle progression, cell division and metabolism of nucleic acids. An overview of regulated pathways and kinases involved in signalling of radio-sensitized HL-60 cells will be given. Taken together, VE-821 proved as a potent radio-sensitizing agent for p53-negative cells.

References

1. Charrier J-D, Durrant SJ, Golec JMC, Kay DP, Knegtel RMA, MacCormick S, et al. Discovery of potent and selective inhibitors of ataxia telangiectasia mutated and Rad3 related (ATR) protein kinase as potential anticancer agents. *J. Med. Chem.* 2011; 54, 2320–30.
2. Fry AM, O'Regan L, Sabir SR, Bayliss R. Cell cycle regulation by the NEK family of protein kinases. *J Cell Sci.* 2012; 125, 4423–33.
3. Huntoon CJ, Flatten KS, Wahner Hendrickson AE, Huehls AM, Sutor SL, Kaufmann SH, et al. ATR Inhibition Broadly Sensitizes Ovarian Cancer Cells to Chemotherapy Independent of BRCA Status. *Cancer Res.* 2013; 73, 3683–91.
4. Qin B, Gao B, Yu J, Yuan J, Lou Z. Ataxia telangiectasia-mutated- and Rad3-related protein regulates the DNA damage-induced G2/M checkpoint through the Aurora A cofactor Bora protein. *J Biol Chem.* 2013; 288, 16139–44.
5. Pires IM, Olcina MM, Anbalagan S, Pollard JR, Reaper PM, Charlton PA, et al. Targeting radiation-resistant hypoxic tumour cells through ATR inhibition. *Br. J. Cancer.* 2012; 107, 291–9.
6. Prevo R, Fokas E, Reaper PM, Charlton PA, Pollard JR, McKenna WG, et al. The novel ATR inhibitor VE-821 increases sensitivity of pancreatic cancer cells to radiation and chemotherapy. *Cancer Biol. Ther.* 2012; 13, 1072–81.
7. Reaper PM, Griffiths MR, Long JM, Charrier J-D, MacCormick S, Charlton PA, et al. Selective killing of ATM- or p53-deficient cancer cells through inhibition of ATR. *Nat. Chem. Biol.* 2011; 7, 428–30.
8. Salovska B, Tichy A, Fabrik I, Rezacova M, Vavrova J. Comparison of Resins for Metal Oxide Affinity Chromatography with Mass Spectrometry Detection for the Determination of Phosphopeptides. *Analytical Letters* 2013; 46, 1505-1524.
9. Tichy A, Salovska B, Rehulka P, Klimentova J, Vavrova J, Stulik J, Hernychova L. Phosphoproteomics: searching for a needle in a haystack. *J Proteomics* 2013; 74, 2786-2797.
10. Tichy A, Vavrova J, Pejchal J, Rezacova M. Ataxia-telangiectasia mutated kinase (ATM) as a central regulator of radiation-induced DNA damage response. *Acta Medica (Hradec Kralove)* 2010; 53, 13-17.
11. Vávrová J, Zárybnická L, Lukášová E, Rezáčová M, Novotná E, Sinkorová Z, et al. Inhibition of ATR kinase with the selective inhibitor VE-821 results in radiosensitization of cells of promyelocytic leukaemia (HL-60). *Radiat Environ Biophys.* 2013; DOI: 10.1007/s00411-013-0486-5.

SHORT-TERM OUTCOME OF CONVULSIVE STATUS EPILEPTICUS (CSE) IN CHILDREN: HOSPITAL BASED PROSPECTIVE STUDY

Teona Shatirishvili

E-mail: tshatirishvili@yahoo.com

David Tvildiani Medical University; Department of Neuroscience,
M. Iashvili Children Central Hospital in Tbilisi, Georgia

Co-authors: T. Kipiani, N. Dixaminjia

Tutor: Prof. Dr. Nana Tatishvili

Introduction

Convulsive Status Epilepticus (CSE) is defined as a continuous generalized tonic-clonic seizure activity lasting longer than 30 minutes or two or more seizures without full recovery of consciousness during the interictal period.¹ CSE is the most common medical neurological emergency during childhood with the overall estimated incidence 18/100 000 cases per year.⁶ It is widely accepted that CSE has associated with morbidity and mortality. There is still no consensus about the relative predictive value of different factors such as: age, sex, etiology, seizure duration, time of the beginning of treatment etc. and their influence on outcome.^{2,3,4,5.}

The objectives of our study were to determine the predictive value of different risk factors and to evaluate influences of pre-hospital and hospital treatment strategies on the outcome of CSE.

Patient and methods

Our prospective hospital-based study was performed in Tbilisi (the capital of Georgia) and included 48 Patients with CSE, admitted to the emergency department of M. Iashvili Children's Central, from March 2007 to March 2012.

The study was approved by the M. Iashvili Children Central Hospital Research Ethics Committee.

Inclusion criteria for study were: (1) patients with CSE aged after neonatal period till 18 years; (2) patients with convulsive seizures or intermittent seizures without full recovery of consciousness between seizures, lasting ≥ 30 min.

Exclusion criteria : 1) seizures with duration < 30 min 2) unreliable data about duration of CSE, 3) patients with nonconvulsive status epilepticus (NCSE) 4) Age less than one month.³

The cases were reviewed according to history, underlying etiology, seizure type, seizure duration, recurrent CSE, existence abnormal neurological status before CSE, pre-hospital and hospital treatment strategies and outcome. All the information was recorded on a specially prepared form designed for this study.

Treatment protocol was based on "North Central London Epilepsy Network for Children & Young People" Guideline-"The Management of Convulsive Status Epilepticus" Published an April 2005, Review Date April 2007, Autumn 2010.¹³ This guideline was adapted for the Georgian reality. According to the above mentioned guideline an "appropriate treatment" was defined as treatment using one dose of BZD in pre-hospital setting and one dose of BZD in the hospital setting. In the case, where the pre-hospital dose of BZD was missing "appropriate" treatment was evaluated as using two dose of BZD in hospital setting . An "inappropriately high treatment" was defined as using more than one dose pre-hospital and more than one dose in hospital. "Timely" treatment was defined as a treatment started within 10 minutes from seizure onset and "late" treatment started after 10 minutes in the pre-hospital setting.

The etiology of CSE was summarized into five categories according to Shinar's classification: idiopathic/cryptogenic SE, remote symptomatic SE, febrile SE, acute symptomatic SE, and progressive encephalopathy.⁷

Seizures were classified by type as: primary generalized convulsive, secondary generalized convulsive. Children with no history of CSE before enrolment into the study were defined as first episode of CSE and children with medical history of CSE defined as having recurrent CSE.

The short-term outcome of CSE was evaluated after 30 days from admission and it was classified into three categories: unchanged neurologic status, neurological consequences (new neurologic deficit compared to the condition before SE), and fatal outcome. Evaluation was performed with the help of Age and Stage Questionnaire (ASQ) and “The functional independence measure for children (WeeFIM)”^{8,9}

Statistical analysis was performed with SPSS, version 16.0. Canonical Discriminant Functions analysis was used for testing the influence of different .Discriminant Functions Coefficient was 0.721 (more than 0.7 is high index coefficient). GLM-univariate full factorial model was used to determine influence of treatment on the CSE outcome. The predictive factors for the poor outcome were calculated with multivariable analysis of variance and Odds ratio (OR). Statistical significance for coefficient p was accepted as significant if $p < 0.001$.

Result

Among 870 hospital admissions with seizures during the specified five year period, there were 48(5.3%) cases of CSE. The average age of patients with CSE was 5.4 year. 54% were male and 45% female. According to seizure type secondary generalized seizures were the most frequent seizure type manifested in 62.5% patients. Recurrent form of CSE manifested in 9 (19%) patients. Most of patients had a favorable outcome: an unchanged neurologic status was described in 36 (75%) cases and new neurological deficit in eight (16.7%), four (8.3%) had a fatal outcome. The following neurological sequelae were recorded: diffuse persistent hypotonia, focal neurological deficit - hemiparesis, cranial nerve palsy, cognitive impairment and loss of previously reached milestones.

A high correlation was found between recurrence of CSE and increased incidence of new neurological deficit after CSE. (Canonical Discriminant Function Coefficients 0.795). The risk of development of new neurological deficit is 11.67 times higher after the recurrent CSE (RR=11, 67; CI (2.81; 48.40); $P < 0.001$). There is a statistically significant correlation between the existence of neurological abnormalities before CSE and the incidence of new neurological deficit (Canonical Discriminant Function Coefficients 0.428). Risk of development of new neurological deficit is 5.8 times higher in patients having abnormal neurological status before CSE. (RR=5.8; CI (1.33; 25.32); $P < 0.001$). There was no statistically significant correlation between sex, age and seizure type with the outcome of CSE (Canonical Discriminant Function Coefficient - 0.152).

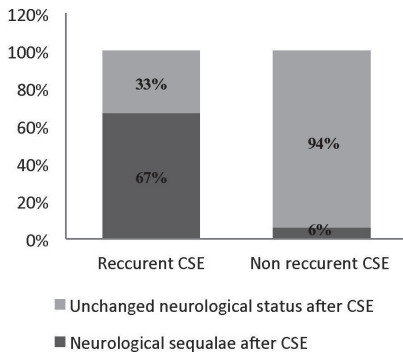


Figure 1. Recurrent CSE as a predictor of morbidity

In our study acute symptomatic, remote symptomatic and progressive encephalopathy were associated with higher morbidity and mortality. Progressive encephalopathy is the most frequent etiology group which led to development of new neurological sequelae in three patients. Oslo long duration of CSE mostly were associated with etiology of acute symptomatic and with progressive encephalopathies group (Canonical Discriminant Function Coefficient 0.462).

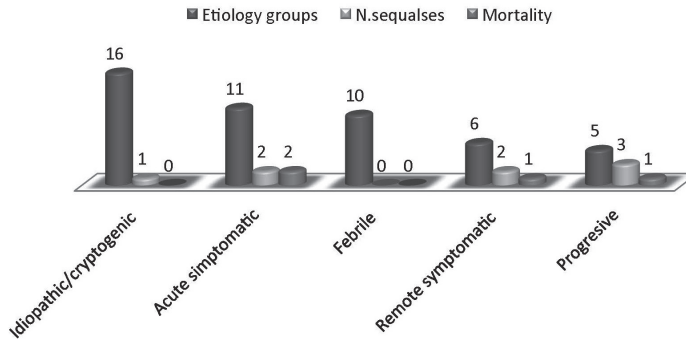
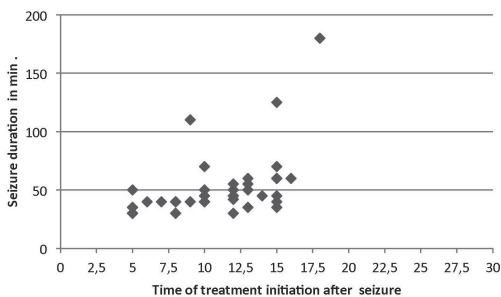


Figure 2. Neurological outcome according to etiology

According to multivariate analysis neurological abnormalities before CSE (4.51-241.28) and recurrent CSE (CI 1.53-52.8) represented significant risk factors for the development of morbidity after CSE ($P < 0.001$).

CSE Treatment and outcome: In pre-hospital setting treatment with one dose of BZD occurred in 31 (64.5%) patients and more than one dose BZD in 17(35.5) % cases. “Appropriate” hospital treatment with one dose of BZD was carried out in 21 (43,7%) and “inappropriate” hospital treatment with 2 and more dose of BDZ in 27 (56.3%) cases). In case of appropriate pre-hospital treatment (using one dose of BZD), seizure duration ranged from 30 - 70 min (median 40,65min). In case of “inappropriate” (using more than one dose BZD) treatment seizures lasted from 30 - 180 (median time 65.8min). Median time of treatment initiation from clinically manifested seizure were 10.38 minutes (ranged from 5 to 18 minutes), when median duration of CSE were 49, 58 minutes (ranged from 60 to 180 minutes).



GLM Univariate analysis showed high correlation between timely initiation of treatment ($P < 0.05$), “appropriate” pre-hospital treatment ($P < 0.05$) with the short duration of CSE. 13 (27%) patients needed artificial ventilation. All these patients had received more than two doses of BZD in the pre-hospital setting. We identified a statistically significant increase of incidence of artificial ventilation ($p < 0.001$) in patients receiving more than one dose of BZD in pre-hospital.

Figure 3. Correlation between CSE treatment initiation and seizure duration.

Discussion

A synthesis of available data on the outcome of CSE is important for clinicians and careers as such review gives prognostic information that can guide management and can indicate significant issues for future research. Unfortunately still there are not many high quality studies about mortality and morbidity of CSE and risk factors influencing the outcome. According to systematic review of available studies on outcome (Raspall-Chaure et al. 2006), short-term mortality after CSE was 2.7–5.2% if studies with the highest quality scores are considered. If only children admitted to ICU are included, mortality is estimated between 5% and 8%.¹⁰ According to our study; short term mortality rate is 8.3% similar to those studies where only children who needed ICU were included. Reported data on the sequelae of SE are difficult to interpret because they may be related to an underlying disorder rather than SE itself. Based on prospective population-based studies, neurologic sequels are reported in up to 15% of children. Young age, female sex, and a long duration of SE is associated with worse outcome.¹¹ In our study new neurological deficit was found in only eight (16.7%) cases. A high correlation was found between recurrence of CSE and existence of neurological abnormality before CSE and increased incidence of new neurological deficit after CSE.

In recent studies most of authors agreed that timely and adequate treatment of CSE influenced seizure duration, and multiple uses of benzodiazepines in pre-hospital setting are associated with more frequent respiratory depression. A study from Chin, et al (2004) demonstrates that the risk of respiratory depression is greater with more than two doses of benzodiazepines in pre-hospital setting, treatment delays also contribute to respiratory failure.¹² Our study identified statistically significant increase of incidence of artificial ventilation ($p < 0.001$) in patients receiving more than one dose of BZD in pre-hospital setting, additionally we found a statistically strong relationship between timely initiation of treatment ($P < 0.05$) and appropriate pre-hospital treatment ($P < 0.05$) with a short duration of CSE.

Conclusion

In our study existence of neurological abnormality before CSE, recurrent CSE, and progressive encephalopathy were the main determinants of morbidity.

Duration of CSE was significantly dependent on timely treatment and adequate pre hospital care. There was statistically significant increased incidence of artificial ventilation ($p > 0.001$) in patients receiving more than one dose of BZD in pre-hospital setting.

Timely and appropriate pre-hospital treatment will significantly shorten seizure duration.

Reference:

1. Novorol CL, Chin RF, Scott RC. Outcome of convulsive status epilepticus: a review. *Arch Dis Child.* 2007; 92(11): 948–951.
2. Raspall-Chaure M, Chin R F, Neville B G. et al Outcome of paediatric convulsive status epilepticus: a systematic review. *Lancet Neurol* 2006. 5(9)769–779.779.
3. Kravljanac R, Jovic N, Djuric M, et al. Outcome of status epilepticus in children treated in the intensive care unit: A study of 302 cases. *Epilepsia* 2011; 52(2): 358–363
4. Dunn DW. StatusEpilepticus in Children: Etiology, Clinical Features, and Outcome. *J Child Neurol* 1988; 3(3): 167-73.
5. Kang DC, Lee YM, Lee J, et al. Prognostic Factors of Status Epilepticus in Children. *Yonsei Med J.* 2005 28; 46(1): 27-33.
6. Chin RF, Neville BG, Peckham C, et al. Incidence, cause, and short-term outcome of convulsive status epilepticus in childhood: prospective population based study. *Lancet* 2006; 368(9531): 222–9.
7. Shinnar S. Epidemiology of childhood status epilepticus. In Wasterlain CG, Treiman DM (Eds) *Status epilepticus: mechanisms and management.* The MIT Press, Cambridge, MA 2006; pp. 39–51.

8. Squires, J., & Bricker, D. (2009). *Ages & Stages Questionnaires, Third Edition (ASQ-3)*. Baltimore, MD: Brookes Publishing. www.agesandstages.com
www.brookespublishing.com/store/books/squires-asqse/
9. Msall ME, Braun S, Granger CV. Use of the Functional Independence Measure for Children (WeeFIM): an interdisciplinary training tape. *Dev Med Child Neurol* 1990; 62:46.
10. Arzimanoglou A. Outcome of status epilepticus in children. *Epilepsia* 2007; 48(8): 91–93.
11. Chevrie JJ, Aicardi J. Convulsive disorders in the first year of life: Neurological and mental outcome and mortality. *Epilepsia* 1978; 19: 67-74.
12. Chin RF, Verhulst L, Neville BG, et al. Inappropriate emergency management of status epilepticus in children contributes to need for intensive care. *J Neurol Neurosurg Psychiatry* 2004, 75: 1584-1588.
13. North Central London Epilepsy Network for Children & Young People Guidelines April 2005. www.ich.ucl.ac.uk/nclchildresepilepsy/NCL_network_guidelines.pdf

EFFECTS AND MECHANISMS OF INTRINSIC AND EXTRINSIC VARIABLE ASSISTED MECHANICAL VENTILATION IN THE EXPERIMENTAL ACUTE RESPIRATORY DISTRESS SYNDROME (ARDS)

Martin Scharffenberg

E-mail: martin.scharffenberg@mailbox.tu-dresden.de

Pulmonary Engineering Group,
Dept. of Anesthesiology and Intensive Therapy,
University Hospital Carl Gustav Carus Dresden
Technical University Dresden, Germany

Co-authors: Dr. med. A. Güldner, Dr. med. Thomas Kiss, DSc. Lillian Moraes,
Claudia Becker, Prof. Dr. med. T. Koch
Tutor: Prof. Dr. med. M. Gama de Abreu

Introduction

The acute respiratory distress syndrome (ARDS) is a potentially life-threatening condition in intensive care medicine, which is associated with relatively high mortality¹. Although mechanical ventilation (MV) is usually required to avoid severe hypoxemia and to reduce the work of breathing, it can further damage the lungs (ventilator-associated lung injury - VALI)². Variable pressure support ventilation (noisy PSV), which leads to extrinsic breath-to-breath variability of tidal volume (V_T) improves lung function and reduces the severity of VALI compared to protective pressure controlled MV (PCV) in the mid-term³. So does the neurally adjusted ventilator assist (NAVA), which requires a gastric tube and is triggered by the electrical activity of the diaphragm, leading to intrinsic variability of V_T ⁴. The aim of this study was to characterize the effects of long term noisy PSV and NAVA on lung function and damage, and to investigate their mechanisms.

Methods

Experimental severe ARDS was induced in 24 anesthetized pigs by repetitive bronchoalveolar lavages followed by injurious ventilation. Afterwards, animals were randomly assigned to 24 hours of mechanical ventilation with one of the following three ventilation modes: 1) NAVA, 2) noisy PSV or 3) PCV. In all groups, the ventilator was set to achieve a mean V_T of 6 ml/kg BW; the fraction of inspired oxygen (FiO_2) and positive end-expiratory pressure (PEEP) were adjusted according to the ARDS Network table. Hemodynamics, lung function and respiratory parameters were measured every 6 hours. After killing the animals by anesthesia overdose, lung tissue samples were immediately removed for analyses of inflammatory and fibrotic protein and transcript markers and histological examination. The lung tissue wet to dry ratio was assessed in the right middle lobe. Statistical analyses were performed using parametric and non-parametric methods, as appropriate. Statistical significance was accepted $\alpha < 0.05$.

Results

Hemodynamics, oxygenation, blood gases, minute ventilation, V_T and PEEP were comparable among groups. Mean airway and mean transpulmonary pressures were lower in the NAVA- and noisy PSV- compared to the PCV-group (*Fig. 1*). NAVA exhibited the highest variability in VT and respiratory rate (RR) followed by noisy PSV and PCV. Furthermore, NAVA and noisy PSV showed a higher variability of the pressure support level (P_{ASB}) than PCV (*Table 1*). Compared to PCV, NAVA yielded lower concentrations of interleukin 8 (IL-8) both in ventral and dorsal lung tissue samples (*Fig. 2*). Furthermore, NAVA resulted in lower concentration of tumor necrosis factor alpha (TNF α)

in the bronchoalveolar lavage fluid compared with noisy PSV. Compared to PCV, the expression of procollagen III was reduced in Noisy PSV, but not NAVA. Histological analyses demonstrated a more severe damage to the lung epithelium in noisy PSV compared to the other groups and additionally more interstitial edema in dorsal lung regions. However, both the overall cumulative alveolar damage score (DAD score) and the wet to dry ratio analysis uncovered no differences between all groups.

Discussion

Compared to traditional controlled protective ventilation and in addition to low tidal volumes, NAVA and noisy PSV offer further lung protection by reducing mean airway and transpulmonary pressures. Noisy PSV generated similar coefficients of variation (CV) of P_{ASB} as in NAVA. Both the CV of VT and RR in NAVA and noisy PSV were in the range corresponding values in young healthy humans ⁵, whereas PCV exhibited negligible variability. The reduction of airway and transpulmonary pressures during NAVA was associated with diminished inflammatory response compared to PCV. This is in agreement with the work of Brander et al. ⁴. The elevated concentration of TNF α and the higher lung epithelium damage and interstitial edema in Noisy PSV might be due to differences in animal-ventilator synchrony, but this issue deserves further evaluation. However, the cumulative DAD score, which consisted of five additional criteria, did not differ among groups. According to the work of Carvalho et al., noisy PSV causes less re-aeration and hyperinflation compared to PCV ⁶. This could avoid high stress to lung tissue and prevent fibrotic remodeling, and might explain a lower procollagen III expression in noisy PSV. As mentioned above, further examinations of ventilator-asynchrony, breathing comfort and biological and histological analyses of the diaphragm need to be performed or are in progress, respectively.

Conclusions

In the present model of severe ARDS in pigs, long term mechanical ventilation with NAVA reduced lung epithelium damage and interstitial edema, compared to noisy PSV and PCV, while noisy PSV reduced the pro-fibrotic lung response compared to PCV. Extrinsic and intrinsic variability of pressure support were not associated with major effects on lung function, compared to conventional protective mechanical ventilation.

Summary

The acute respiratory distress syndrome (ARDS) is potentially life-threatening and usually requires mechanical ventilation (MV). Although MV is essential to avoid severe hypoxemia, it can further damage the lung. Variable MV modes, for example variable pressure support ventilation (noisy PSV) and neurally adjusted ventilatory assist (NAVA), reduce the ventilator-associated lung damage in the mid-term. It is not clear whether both modes exhibit different effects on lung function and damage in the long term. In this experimental study with 24 anesthetized pigs, long-term NAVA and noisy PSV reduced airway and transpulmonary pressures and restored variability of respiratory patterns compared to conventional protective ventilation. NAVA reduced lung inflammation and lung epithelium damage and interstitial edema compared to noisy PSV and PCV, while noisy PSV reduced the pro-fibrotic lung response compared to PCV. Both extrinsic and intrinsic variability of pressure support were advantageous compared to conventional protective ventilation.

References

1. Matthay MA, Ware LB, Zimmerman GA: The acute respiratory distress syndrome. *J Clin Invest.* 2012; 122(8): 2731–2740.
2. The Acute Respiratory Distress Syndrome Network: Ventilation with lower tidal volumes as compared with traditional tidal volumes for acute lung injury and the acute respiratory distress syndrome. *N Engl J Med* 2000; 342: 1301-8.

3. Spieth PM, Carvalho AR, Güldner A et al.: Pressure support improves oxygenation and lung protection compared to pressure-controlled ventilation and is further improved by random variation of pressure support. Crit Care Med 2011; 39: 746–755.
4. Brander L, Sinderby C, Lecomte F et al.: Neurally adjusted ventilatory assist decreases ventilator-induced lung injury and non-pulmonary organ dysfunction in rabbits with acute lung injury. Intensive Care Med 2009; 35: 1979–1989.
5. Tobin MJ, Mador MJ, Guenther SM et al.: Variability of resting respiratory drive and timing in healthy subjects. J Appl Physiol 1988; 65: 309-317.
6. Carvalho AR, Spieth PM, Güldner A, et al. Distribution of regional lung aeration and perfusion during conventional and noisy pressure support ventilation in experimental lung injury. J Appl Physiol 2011; 110: 1083–1092.

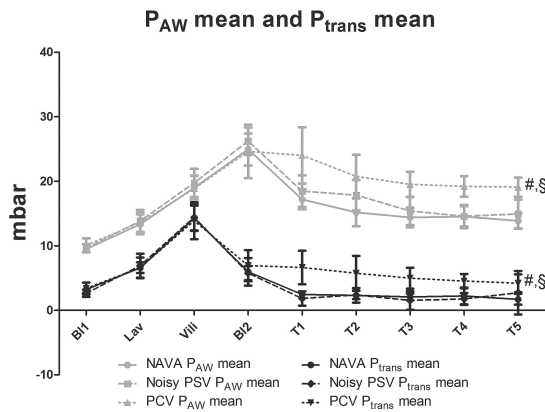


Fig. 1. Mean airway pressure and mean transpulmonary pressure in [mbar]. B11: Baseline 1; Lav: Lavage; Vili: Ventilator-induced lung injury; B12: Baseline 2; T1 – T5: Measurements every 6 hours. # vs. Noisy PSV $p < 0.05$; § vs. NAVA $p < 0.05$

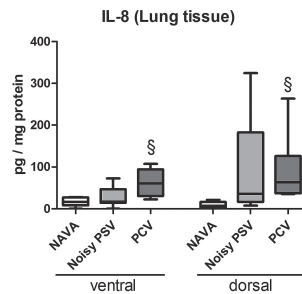


Fig. 2. Concentrations of interleukin 8 (IL-8) in [pg/mg protein] in ventral and dorsal lung tissue samples. B11: Baseline 1; Lav: Lavage; Vili: Ventilator-induced lung injury; B12: Baseline 2; T1 – T5: Measurements every 6 hours. § vs. NAVA $p < 0.05$

		T1	T2	T3	T4	T5	p-value
CV VT	NAVA	28,76 ± 12,78	29,42 ± 6,50	28,69 ± 8,74	17,14 ± 7,33	19,48 ± 7,68	\$ 0,025 § 0,000
	Noisy PSV	18,98 ± 6,25	19,61 ± 2,33	17,44 ± 4,15	17,02 ± 5,28	16,20 ± 8,53	\$ 0,025 # 0,000
	PCV	1,19 ± 0,68	1,32 ± 0,69	2,44 ± 1,88	1,80 ± 1,41	1,13 ± 0,46	§ 0,000 # 0,000
CV RR	NAVA	23,19 ± 10,72	30,33 ± 10,38	30,64 ± 11,16	27,29 ± 10,65	32,53 ± 5,96	\$ 0,003 § 0,000
	Noisy PSV	12,94 ± 4,02	13,19 ± 4,75	12,50 ± 7,05	20,31 ± 8,50	17,61 ± 13,05	\$ 0,003 # 0,001
	PCV	0,93 ± 0,99	0,52 ± 0,25	0,46 ± 0,16	0,79 ± 0,87	0,52 ± 0,33	§ 0,000 # 0,001
CV P _{ASB}	NAVA	33,48 ± 17,53	33,79 ± 6,64	34,74 ± 9,21	21,25 ± 10,23	25,37 ± 13,31	\$ 0,121 § 0,000
	Noisy PSV	23,70 ± 5,36	25,69 ± 2,49	24,64 ± 3,81	24,06 ± 4,22	24,54 ± 12,50	\$ 0,121 # 0,000
	PCV	1,02 ± 0,91	0,77 ± 0,28	1,76 ± 1,52	1,73 ± 1,19	1,56 ± 1,50	§ 0,000 # 0,000

Table 1. Coefficients of variation (CV) in [%]. Values represent means and SD. VT: Tidal volume; RR: Respiratory Rate; P_{ASB}: Level of pressure support; T1 – T5: Measurements every 6 hours. \$: NAVA vs. Noisy PSV; §: NAVA vs. PCV; #: Noisy PSV vs. PCV

THE IMPACT OF NEUROPILIN-2 ON THE CXCR4/CXCL12 AXIS IN THE FORMATION OF LYMPH NODE METASTASIS IN COLON CANCER

Hannah Schneider

E-Mail: Hannah.Schneider@uniklinikum-dresden.de

Faculty of Medicine Carl Gustav Carus, Technical University Dresden/ Institute of Pathology,
Dresden, Germany

Co-Author: P. Hönscheid

Tutor: Dr. med. habil. M.H. Muders, Associate Professor

Introduction

The presence of lymph node metastases is an important prognostic factor in colorectal cancer (CRC). To be able to form lymph node metastases disseminating tumor cells have to meet a supportive microenvironment called the metastatic niche. An essential part of this niche are lymph vessels that are located in lymph nodes prior to metastasis. The function of these intranodal lymph vessels might be the production of chemoattractant factors like CXCL12 that can bind to CXCR4-positive tumor cells.

Aims

In the first part, we have investigated the hypothesis that intranodal lymph vessels are a prognostic factor for node negative colon cancer patients. In the second part, we evaluated the role of Neuropilin-2 (NRP2) in mediating lymph node metastasis by modulating the chemoattractant CXCR4/CXCL12 signaling pathway.

Methods

A cohort of 113 patients with node negative colon cancer (pT3 pN0) was analyzed by D2-40-staining, which is specific for lymphatic endothelium, for intranodal lymph vessel density in regional lymph nodes. In the colorectal cancer cell lines SW 480 and SW 620 protein and mRNA levels were assessed by Western blot and quantitative real time PCR. Boyden Chamber Migration assays were performed after stimulation with human recombinant CXCL12 and RNAi mediated depletion of NRP2 and CXCR4 via or NRP2 inhibition by addition of Semaphorin 3F (Sema3F). To confirm our results in human tissue 78 Patients with advanced colon cancer (pT3-4, pN1, pM0) were analyzed for NRP2- and CXCR4-expression in primary tumors and corresponding lymph node metastases by immunohistochemistry.

Results

Intranodal lymphangiogenesis is significantly correlated with disease-free survival in patients with node negative colon cancer. In the colorectal cancer cell line SW480 blockade of NRP2 via siRNA and Sema3F decreased CXCR4-expression and abrogated phosphorylation of Akt after stimulation with CXCL12. Furthermore, CXCL12 triggered up-regulation of CXCR4 mRNA ("feed forward loop") was blocked after NRP2 depletion via siRNA and Sema3F. In contrast, RNAi mediated inhibition of CXCR4 expression had no influence on NRP2-expression. Inhibition of NRP2 via siRNA and Sema3F significantly abrogated CXCL12-induced migration ($P < 0,001$). Interestingly, the metastatic cell line SW 620 expressed decreased levels of CXCR4 but highly increased Sema3F-Expression. Significant upregulation of NRP2 in lymph node metastasis of colon carcinoma patients confirmed our in vitro results. Interestingly, CXCR4 protein levels were significantly downregulated compared to the primary tumor.

Discussion

Sentinel node lymphangiogenesis has been shown to be an important factor in developing not only lymph node metastasis but also distant metastasis (Hirakawa et al. 2005, Hirakawa et al. 2007). Our laboratory has also shown the contribution of intranodal lymphangiogenesis in a rectal cancer cohort after neoadjuvant treatment (Jakob et al. 2011). In line with these results this study also demonstrates that in node negative colon cancer patients lymphangiogenesis located in regional lymph nodes is an adverse prognostic factor. These results might have some clinical impact because in node negative colon cancer patients there are no clear cut criteria for the use of adjuvant therapy. The present study suggests, that in patients with intranodal lymphangiogenesis a more aggressive adjuvant treatment is indicated than in patients without any lymph vessels in regional lymph nodes.

The essential role of intranodal lymph vessels in the formation of the metastasis can be attributed to the fact, that lymphatic endothelial cells produce CXCL12 (Kim et al. 2010) and this attracts CXCR4 positive primary tumor cells. Therefore, high CXCR4 expression in the primary tumor correlates with lymph node involvement (Silinsky et al. 2013). Because NRP2 has already been shown to be important in distant metastasis in colorectal cancer (Gray et al. 2008) and Yasuoka et al. have demonstrated an association between NRP2 and CXCR4 expression in breast cancer (Yasuoka et al. 2009) the role of NRP2 in the regulation of the CXCR4/CXCL12 axis has been investigated in colon cancer. In vitro, RNAi mediated depletion of NRP2 downregulated CXCR4 protein and messenger expression and inhibited CXCL12 induced intracellular signaling. Heckmann et al. have already demonstrated that CXCR4 depletion inhibits the migration of colorectal cancer cells (Heckmann et al. 2013). Accordingly, NRP2 inhibition via siRNA and Sema3F reduced the migration in a CXCL12 chemoattractant assay. The in vitro study results have been confirmed in patient tissue that demonstrated a significant increase in NRP2 expression compared to the primary tumor. Interestingly, in the metastatic situation the CXCR4/CXCL12 axis seems to have minor importance as demonstrated by the decreased CXCR4 levels in the lymph node metastases. What is more, our in vitro results in a metastatic colon cancer cell line demonstrated a significantly increased Sema3F expression suggesting the CXCR4/CXCL12 axis is even blocked.

Conclusion

In conclusion, NRP2 regulated CXCR4/CXCL12 signaling and influenced the migration of primary colorectal cancer cells. Thus, the expression and functionality of both receptors may have an impact on the metastatic potential of colorectal cancer cells. Therefore, NRP2 may be an interesting therapeutic target to block the CXCR4/CXCL12 axis and by this way to avoid metastatic spreading of colorectal cancer cells.

Summary

- CXCL12 producing intranodal lymph vessels correlate with disease free survival in node negative colon cancer patients.
- NRP2 is significantly higher expressed in lymph node metastasis compared to the primary tumor.
- In vitro, NRP2 is essential for the function of CXCR4/CXCL12 signaling axis that is important to attract cancer cells to the lymph nodes.
- In vitro, inhibition of NRP2 reduces CXCL12 induced cancer cell migration.

References

1. Gray MJ, Van Buren G, Dallas NA et al.: Therapeutic targeting of neuropilin-2 on colorectal carcinoma cells implanted in the murine liver. *J Natl Cancer Inst* 2008; 100, 109-120.
2. Heckmann D, Maier P, Laufs S et al.: CXCR4 Expression and Treatment with SDF-1alpha or Plerixafor Modulate Proliferation and Chemosensitivity of Colon Cancer Cells. *Transl Oncol* 2013; 6, 124-132.

3. Hirakawa S, Brown LF, Kodama S et al.: VEGF-C-induced lymphangiogenesis in sentinel lymph nodes promotes tumor metastasis to distant sites. *Blood* 2007; 109, 1010-1017.
4. Hirakawa S, Kodama S, Kunstfeld R et al.: VEGF-A induces tumor and sentinel lymph node lymphangiogenesis and promotes lymphatic metastasis. *J Exp Med* 2005; 201, 1089-1099.
5. Jakob C, Aust DE, Liebscher B et al.: Lymphangiogenesis in regional lymph nodes is an independent prognostic marker in rectal cancer patients after neoadjuvant treatment. *PLoS One* 2011; 6, e27402.
6. Kim M, Koh YJ, Kim KE et al.: CXCR4 signaling regulates metastasis of chemoresistant melanoma cells by a lymphatic metastatic niche. *Cancer Res* 2010; 70, 10411-10421.
7. Silinsky J, Grimes C, Driscoll T et al.: CD 133 and CXCR4 colon cancer cells as a marker for lymph node metastasis. *J Surg Res* , (Epub Ahead of Print) 2013 .
8. Yasuoka H, Kodama R, Tsujimoto M et al.: Neuropilin-2 expression in breast cancer: correlation with lymph node metastasis, poor prognosis, and regulation of CXCR4 expression. *BMC Cancer* 2009; 9.

ELECTROPHYSIOLOGICAL PROPERTIES OF THE PRONOCICEPTIVE DORSAL RETICULAR NUCLEUS

Maria Mafalda Sousa

E-mail: mafsousa@ibmc.up.pt

Department of Experimental Biology, Faculty of Medicine of University of Porto,
Porto, Portugal

Co-authors: D. Lima, P. Szucs and P. Aguiar

Tutors: Paulo Aguiar, PhD, Peter Szucs, MD, PhD, Deolinda Lima, MD, PhD

Introduction

The dorsal reticular nucleus (DRt) is located in the dorsolateral quadrant of the medulla oblongata, surrounded by the cuneate nucleus (Cu), the nucleus tractus solitarius (Sol), motor nuclei of the vagal (10N) and hypoglossal (12N) nerves, the spinal trigeminal nucleus and the caudal ventrolateral reticular formation. DRt neurons were shown to be preferentially or exclusively activated by noxious stimulation conveyed by A δ - and C-fibres from the entire body [1, 2]. They receive projections from spinal dorsal horn nociceptive neurons that establish asymmetrical, potentially excitatory, synaptic contacts, and project back to the dorsal horn [3-7]. DRt neurons were also shown to encode the intensity of noxious stimuli and to be associated with diffuse noxious inhibitory controls [2, 8].

While the functional importance of DRt in nociception is well established, very little is known about the basic electrophysiological properties of DRt neurons. It is also not known whether electrophysiological properties of DRt neurons are distinct from that of neurons in the adjacent brainstem areas, such as the parvocellular reticular nucleus (PCRt). While these two adjacent regions are both part of the mesh-like neuronal column of the reticular formation, their input is clearly different: ascending axons from the spinal dorsal horn to the reticular formation cannot not be traced further than the rostral border of DRt [5], while PCRt receives projections from the trigeminal mesencephalic nuclei neurons and contains the dorsal group of interneurons that integrate and coordinate activity of the oral motor nuclei [9].

The aim of this work was to 1) characterize the electrophysiological properties of DRt neurons in the rat using intracellular recordings; 2) establish functional neuronal classes; and 3) identify electrophysiological features that would distinguish DRt neurons from neurons in adjacent reticular formation and neighbouring brainstem regions.

Methods

Laboratory Wistar rats (P14-P18) were killed in accordance with the national guidelines after anaesthesia by intraperitoneal injection of Na⁺-pentobarbital (30mg/Kg). The brainstem was exposed by removing the cranial bone, the brain and the cerebellum. In order to achieve maximally preserved reticular neurons, a transverse cut in the brainstem was done, at the level corresponding to Plates 147-152 from Paxinos. Reticular neurons on the cut surface were visualized using the oblique infrared (IR-LED) illumination technique [10].

Recordings were made with an EPC-10 amplifier. In whole-cell mode, neurons were filled, by passive diffusion of biocytin, from the pipette. Incrementing current and voltage step protocols were applied to assess passive membrane properties along with firing pattern responses. To determine the local network contribution to spontaneous activity, synaptic transmission was blocked by bath application of a cocktail of postsynaptic receptor antagonists (CNQX, Strychnine and Picrotoxin).

To reveal the biocytin, the free floating brainstem sections were treated according the avidin-biotinylated horseradish peroxidase method and the histochemical reaction was completed with a diaminobenzidine chromogen reaction. Complete 3-D reconstruction of the labelled cell along with

contours of the brainstem and borders of landmark structures was performed in one case with a 40x objective, using NeuroLucida.

Model construction and computer simulations were performed in NEURON simulation environment. Spontaneous activity data, acquired in current-clamp mode, was analysed using scripts developed in MATLAB. Excitatory post-synaptic currents (EPSC) and inhibitory post-synaptic currents (IPSC) were detected using the Mini Analysis software and analysed in MATLAB.

Results

After removing cells that did not remain stable for sufficient time to perform adequate electrophysiological characterization, 43 (from a total of 100 cells) were morphologically recovered, allowing their identification or their location. Passive and active membrane properties of the recorded neurons were analysed and distinguished between four regions. Passive membrane properties (E_m , R_m and τ_m) between these neurons did not show any significant difference, although the combination of smallest τ_m and a high R_m in case of DRt neurons suggests somewhat smaller somata in this group. Action potential amplitude and overshoot, measured on voltage traces corresponding to the first suprathreshold depolarizing current step, was the highest in DRt neurons. Interestingly, nonRt neurons had the slowest spikes, which was evident from the significantly larger half-width of the action potentials. Neurons in the reticular formation (DRt and PCRt) responded, almost exclusively, with tonic firing profiles to depolarizing current steps; the single exception being a DRt neuron that showed gap-firing. Neurons outside the reticular formation presented a larger repertoire of firing patterns: tonic, gap-firing, and single-spike.

Our experimental data revealed that about 62% of the neurons showed network driven spontaneous activity (SA). About 30% ($n = 15$) of the neurons showing SA were strongly modulated by frequencies within the range from 2 to 11 Hz. However many neurons also showed irregular spontaneous activity. As an in-depth analysis of electrophysiological properties, membrane potential distributions were calculated for neurons exhibiting spontaneous activity to provide information about membrane current dynamics, presence of plateaus and balance between excitation and inhibition. Sub-threshold membrane potential distributions showed several distinct histogram profiles that could be grouped in two major classes and were present in all three neuronal populations.

Apart from intrinsic conductances, rhythmic excitatory synaptic input could also drive spontaneous firing in neurons. Thus, we assessed the synaptic input pattern of the recorded neurons and concluded that EPSCs were randomly distributed in all investigated cell groups. Therefore it is not likely that the observed rhythmic spontaneous firing is driven by suprathreshold rhythmic synaptic input. This suggests that irregular spontaneous firing is most likely network driven while rhythmic activity could be intrinsic.

Discussion and conclusions

Although the reticular formation is considered a mesh of multiple functional neurons, their electrophysiological properties are not as heterogeneous as expected. Namely, in terms of electrophysiology, there are no relevant differences between neurons in DRt and PCRt with both regions showing a very high incidence of tonic neurons. These results have strong implications given the pronociceptive role of the DRt, and they point to the possibility that neurons on the reticular formation are functionally similar differing only in their connectivity profiles (input sources and output targets). Also of great importance is the high prevalence of spontaneous activity (regular and irregular) in DRt neurons which certainly affects, and shapes, the nociceptive information modulation provided by these neurons.

Summary

In this work we performed whole-cell patch-clamp recording in rat brainstem blocks to characterize the electrophysiological properties of neurons in the dorsal reticular nucleus (DRt), a region known to be involved in pronociceptive modulation. We also compared properties of DRt neurons with those in the adjacent (PCRt) and in neighbouring regions outside the reticular formation. We found that neurons in the DRt and PCRt had similar electrophysiological properties and exhibited mostly tonic-like firing patterns, whereas neurons outside the reticular formation showed a larger diversity of firing-patterns. Interestingly, more than half of the neurons also showed spontaneous activity. Our results indicate that functional difference of neurons in the reticular formation may mostly be determined by their connectivity profiles and not by their intrinsic electrophysiological properties. The dominance of tonic neurons in the DRt supports previous conclusions that these neurons encode stimulus intensity through their firing frequency, while the high prevalence of spontaneous activity most likely shapes nociceptive modulation by this brainstem region.

References

1. Lima, D. and A. Almeida, The medullary dorsal reticular nucleus as a pronociceptive centre of the pain control system. *Prog Neurobiol*, 2002. 66(2): 81-108.
2. Villanueva, L., et al., Encoding of electrical, thermal, and mechanical noxious stimuli by subnucleus reticularis dorsalis neurons in the rat medulla. *J Neurophysiol*, 1989. 61(2): 391-402.
3. Almeida, A., I. Tavares, and D. Lima, Reciprocal connections between the medullary dorsal reticular nucleus and the spinal dorsal horn in the rat. *Eur J Pain*, 2000. 4(4): 373-387.
4. Lima, D., A spinomedullary projection terminating in the dorsal reticular nucleus of the rat. *J Neurosci.*, 1990. 34(3): 577-589.
5. Raboisson, P., et al., Organization of efferent projections from the spinal cervical enlargement to the medullary subnucleus reticularis dorsalis and the adjacent cuneate nucleus: a PHA-L study in the rat. *J Comp Neurol*, 1996. 367(4): 503-517.
6. Soto, C. and A. Canedo, Intracellular recordings of subnucleus reticularis dorsalis neurones revealed novel electrophysiological properties and windup mechanisms. *J Physiol*, 2011. 589(Pt 17): 4383-4401.
7. Villanueva, L. and D. Le Bars, The activation of bulbo-spinal controls by peripheral nociceptive inputs: diffuse noxious inhibitory controls. *Biol. Res.*, 1995. 28(1): 113-125.
8. Le Bars, D., The whole body receptive field of dorsal horn multireceptive neurones. *Brain Res. Rev.*, 2002. 40(1-3): 29-44.
9. Zhang, J. and P. Luo, Ultrastructural features of synapse from dorsal parvocellular reticular formation neurons to hypoglossal motoneurons of the rat. *Brain Res.*, 2003. 963: 262-273.
10. Szucs, P., V. Pinto, and B.V. Safronov, Advanced technique of infrared LED imaging of unstained cells and intracellular structures in isolated spinal cord, brainstem, ganglia and cerebellum. *J Neurosci Methods*, 2009. 177(2): 369-380.

VITAMIN D DEFICIENCY AND ITS POTENTIAL IMPLICATIONS IN RENAL TRANSPLANTATION

Ursula Thiem

E-mail: ursula.thiem@meduniwien.ac.at

Division of Nephrology and Dialysis, Medical University of Vienna, Vienna, Austria

Co-authors: B. Olbramski, A. Gessler, R. Marculescu, E. Kállay, S. Winkler,
T. Perkmann, U. Gössler, T. Wekerle, F. Kainberger, M. Schemper,
F. Mühlbacher, W. Druml, K. Borchhardt
Tutor: Priv.-Doz. Dr. Kyra Borchhardt

Introduction

Low calcidiol levels are a common finding in kidney transplant recipients. Only about 5 - 25% of prevalent kidney transplant recipients were reported to have sufficient calcidiol levels, i.e. > 75 nmol/l [1-3]. Despite the high prevalence of vitamin D deficiency (calcidiol ≤ 50 nmol/l) and insufficiency (calcidiol 51 - 75 nmol/l) among kidney transplant recipients, there is no general consensus on the management of vitamin D deficiency after kidney transplantation [4].

Calcitriol, the active metabolite of vitamin D, does not only play an important role in the regulation of mineral and bone metabolism, but has known immunomodulatory and renoprotective properties [5]. In the transplant setting, these immunomodulatory and renoprotective properties could be exploited to enhance graft tolerance and survival as demonstrated in different animal models of transplantation [6-8]. It is believed that vitamin D deficiency might impair these potential beneficial actions.

Aims

On the one hand, we aimed to determine the prevalence of vitamin D deficiency/insufficiency in kidney transplant recipients attending the outpatient department for renal transplantation at the Medical University of Vienna and to study the course of vitamin D levels over time. On the other hand, we investigate in a randomized, controlled trial whether treatment of vitamin D deficiency in de-novo kidney transplant recipients affects the outcome one year after kidney transplantation.

Methods

Out of 1046 prevalent kidney transplant recipients who attended the outpatient department for renal transplantation at the Medical University of Vienna in 2010, 879 underwent renal transplantation more than 6 months ago and had their calcidiol levels measured within the yearly check-up and were thus included in the cross-sectional analysis. Moreover, we retrospectively analyzed the course of calcidiol levels in a seasonally-matched subgroup of 208 kidney transplant recipients who had their calcidiol levels measured between 2005 and 2007 as well as in 2010. At our institution, vitamin D supplements are not routinely prescribed to kidney transplant recipients with vitamin D deficiency.

Furthermore, in a currently ongoing randomized, placebo-controlled study (VITA-D study), we investigate whether correction of vitamin D deficiency in de-novo kidney transplant recipients improves the post-transplant outcome [9]. As primary endpoints graft function, the occurrence of allograft rejections and infections are assessed one year after transplantation. 202 adult de-novo kidney transplant recipients with vitamin D deficiency (calcidiol ≤ 50 nmol/l) were stratified by calcidiol levels (< 25 or $25 - 50$ nmol/l) and randomized in a 1:1 ratio to 6800 International Units vitamin D₃ per day or placebo. The participants are treated for one year. We excluded patients who underwent re-transplantation more than twice or were highly immunized as well as those who had a history of gastrointestinal diseases that lead to impaired intestinal vitamin D absorption.

Results

The cross-sectional study of 879 prevalent kidney transplant recipients [63% male, median (range) age of 58 (19 - 87) years] revealed that only 4% of the patients have sufficient calcidiol levels (> 75 nmol/l) after a median period of 7.1 (0.5 to 36.8) years after transplantation. The median calcidiol was 38.9 (5.0 - 166.0) nmol/l and was significantly higher in summer as compared with all other seasons ($p < 0.0001$). 21% of patients were vitamin D insufficient (51 - 75 nmol/l), 41% were deficient (26 - 50 nmol/l), and 34% were severely deficient (≤ 25 nmol/l). In a seasonally-matched subgroup of 208 patients, calcidiol significantly decreased over a median period of 4 (2 - 5) years [54.7 (10.4 - 140.3) nmol/l between 2005 and 2007 to 32.8 (5 to 91.2) nmol/l in 2010 ($p < 0.0001$)]. The percentage of patients with sufficient calcidiol levels decreased from 21% to 4%, while the percentage of patients with severe vitamin D deficiency increased from 14% to 34% over this period.

Considering the high prevalence of vitamin D deficiency and insufficiency in kidney transplant recipients and the lack of general treatment guidelines for these patients, we are currently performing a randomized, controlled trial to investigate the effects of vitamin D supplementation on the outcome after transplantation. Between May 2009 and August 2013 we screened 605 de-novo kidney transplant recipients, 73% of whom had calcidiol levels below 50 nmol/l. Out of the 202 randomized patients, 42% were severely vitamin D deficient (< 25 nmol/l). Baseline characteristics of the study population will be presented. The study will be completed in one year and the final results are expected for the autumn of 2014.

Conclusions

At our transplant center, three quarter of the prevalent kidney transplant recipients are vitamin D deficient. The circannual rhythm of vitamin D seems to be preserved in these patients. However, vitamin D deficiency does not resolve spontaneously over time. Today, there are no general recommendations on how to manage vitamin D deficiency after kidney transplantation; neither do we know whether correction of vitamin D deficiency would affect the post-transplant outcome. Therefore, our currently ongoing VITA-D randomized controlled study should help to determine the potential beneficial effects of vitamin D₃ on the post-transplant outcome as well as its safety in vitamin D deficient kidney transplant recipients.

Acknowledgement

U.T. is a recipient of a DOC-fFORTE fellowship of the Austrian Academy of Sciences at the Department of Medicine III in cooperation with the Institute of Pathophysiology and Allergy Research, Medical University of Vienna.

References

1. Querings K, Girndt M, Geisel J, Georg T, Tilgen W, Reichrath J. 25-hydroxyvitamin D deficiency in renal transplant recipients. *J Clin Endocrinol Metab* 2006; 91 (2), 526.
2. Ewers B, Gasbjerg A, Moelgaard C, Frederiksen AM, Marckmann P. Vitamin D status in kidney transplant patients: need for intensified routine supplementation. *Am J Clin Nutr* 2008; 87 (2), 431.
3. Penny H, Frame S, Dickinson F, et al.: Determinants of vitamin D status in long-term renal transplant patients. *Clin Transplant* 2012; 26 (6), E617.
4. Thiem U, Olbramski B, Borchhardt K. Calcidiol deficiency in end-stage organ failure and after solid organ transplantation: status quo. *Nutrients* 2013; 5 (7), 2352.
5. Thiem U, Borchhardt K. Vitamin D in solid organ transplantation with special emphasis on kidney transplantation. *Vitam Horm*, vol 86. United States: 2011 Elsevier Inc, 2011: 429.
6. Redaelli CA, Wagner M, Gunter-Duwe D, et al.: 1alpha,25-dihydroxyvitamin D₃ shows strong and additive immunomodulatory effects with cyclosporine A in rat renal allotransplants. *Kidney Int* 2002; 61 (1), 288.

7. Redaelli CA, Wagner M, Tien YH, et al.: 1 alpha,25-Dihydroxycholecalciferol reduces rejection and improves survival in rat liver allografts. *Hepatology* 2001; 34 (5), 926.
8. Gregori S, Casorati M, Amuchastegui S, Smiroldo S, Davalli AM, Adorini L. Regulatory T cells induced by 1 alpha,25-dihydroxyvitamin D3 and mycophenolate mofetil treatment mediate transplantation tolerance. *J Immunol* 2001; 167 (4), 1945.
9. Thiem U, Heinze G, Segel R, et al.: VITA-D: cholecalciferol substitution in vitamin D deficient kidney transplant recipients: a randomized, placebo-controlled study to evaluate the post-transplant outcome. *Trials* 2009; 10, 36.

TRANSLATION OF BIOMECHANICAL STIMULI IN TO MORPHOLOGICAL AND MICROSCOPIC RESPONSE IN THE RAT TIBIA

Paula Vickerton

E-mail: p.vickerton@student.liv.ac.uk

Department of Musculoskeletal Biology II, Institute of Ageing and Chronic Disease,
University of Liverpool

Co-authors and tutors: Dr. Nathan Jeffery, Dr. Jonathan Jarvis, Professor Jim Gallagher

Introduction

It is well-established that the musculoskeletal system responds to mechanical stimuli. The precise mechanisms guiding this response are not fully understood, and the functional nature of the adapted morphology produced is usually assumed, and rarely tested. The aims of this study are to:

- Test miniature neuromuscular stimulators as an appropriate method for musculoskeletal loading.
- Quantify the change in bone and muscle morphology and histology.
- Replicate the loading caused by muscle stimulation *in silico* to establish the forces acting upon the bone.

Methods

Rats underwent surgical implantation of miniature neuromuscular stimulators. The stimulators caused contraction of muscles in the left limb only, indirectly loading the tibia. The right limb was used as a contra-lateral control. The stimulators were set on a burst pattern of 100Hz every 30 seconds, for 28 days. All experiments were carried out in strict accordance with the Animals (Scientific Procedures) Act of 1986, which governs animal experimentation in the UK.

Hindlimbs were imaged using microCT, and iodine-enhanced microCT, (Jeffery et al., 2011) at the EPSRC funded Henry Moseley X-ray Imaging Facility, University of Manchester. The microCT data were used to quantify muscle volume, create global BMD maps, and for more focused sampling of BMD and cortical thickness. All tibias were analysed using geometric morphometrics to determine which sample had the geometry closest to the mean shape. These tibias were used for further analysis.

For cellular detail bone and muscle samples were sectioned for histology. Bones were fixed and decalcified, then routinely processed for histology and paraffin embedded. Paraffin blocks were sectioned, mounted and stained with Haematoxylin and Eosin. Muscle samples were snap frozen in liquid nitrogen, sectioned and stained for myofibrillar ATPase and NADH reductase. Images obtained by light microscopy.

Finite element (FE) models of both tibias were constructed. Tetrahedral meshes were created in Amira 5.4.1. The model included cortical and trabecular bone, cartilage, fat, femoral head, and a platform. Material properties were taken from the literature. Muscle was modelled based on Blemker et al's contractile material (Blemker et al., 2005). This produces a more realistic pattern of muscular loading than other methods. The model was found to reach equilibrium at 1.1 seconds, and to converge between 100000 and 155000 tetra. Models were validated against previously published data (Torcasio et al., 2012). Analysis was run in FEBio 1.5 software.

Results

Stimulated muscle showed a decrease in type 2b fibres and an increase in oxidative potential. This was accompanied by a 20% reduction in muscle volume. The tibias showed significantly lower BMD, and higher cortical thickness in the anterior-distal region of the tibia compared with their contra lateral control (Fig.1). Histological analysis of the antero-distal region of the tibia showed that the stimulated

limb had a large degree of primary osteon formation (Fig.2).

FE analysis established that during contraction of tibialis anterior there was high compressive and effective strain in the antero-distal region of the tibia. The geometry of the stimulated tibia was modelled and showed significantly reduced ($p < 0.05$) strain in this region (Fig.3).

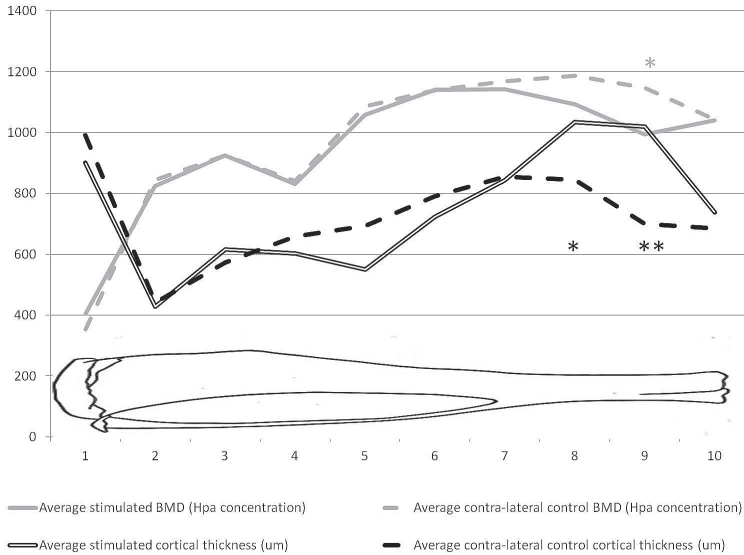


Figure 1. BMD (grey lines) and cortical thickness (black lines) of the stimulated (continuous lines) and contra-lateral control (dashed lines) tibias, sampled along the anterior aspect of the tibia. At sample point 9 the cortex is significantly thicker ($p < 0.05$) and the BMD is significantly lower ($p < 0.05$) in the stimulated tibia than in the contra-lateral control. Diagram of tibia represents the approximate position of the sample site along the tibia.

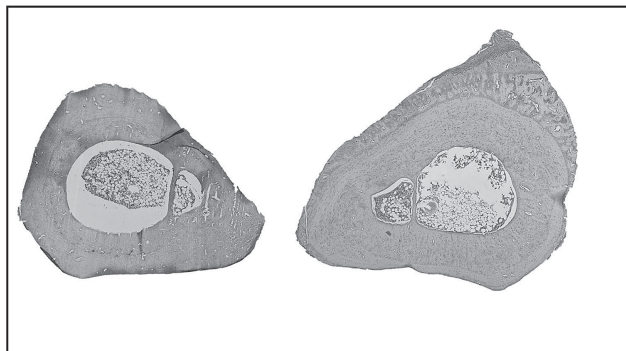


Figure 2. histological sectioning of the contra-lateral control (left) and stimulated (right) tibias.

Figure 3. FE models, showing compressive strain across the unstimulated geometry (left) and the stimulated geometry (right) under identical loading conditions. White indicates highest strain, black the lowest.



Discussion

Previously the implantation of miniature neuromuscular stimulators has been used to study the transformation in muscle (Sutherland et al., 1998). Here we show that they are also capable of altering the morphology of the bones the muscles load in a highly localised manner. The stimulated muscles showed a transformation to a smaller more oxidative muscle than the contra-lateral controls. The increase in mitochondria in muscle fibres is characteristic of muscle training and help resistance to fatigue. Volume reduction in the stimulated muscles may be due to the decrease in thick type 2b fibres and increase in thinner type 2a fibres (Pullen, 1977).

Histological analysis of the antero-distal region of the tibia showed primary osteon formation, a number of chondrocytes, and a reactive periosteum, which are features more commonly associated with fracture repair than bone modelling (Tomlinson et al., 2012). Histological analysis showed no evidence of stress fractures present or repaired within the bone.

FEA reveals that the muscular contraction of tibialis anterior showed peak compressive strains at the muscle attachment site and another region of high strain in the antero-distal region of the tibia. It is interesting to note that there was no change in geometry or BMD measured in this region. Previous work has found that compressive strain, and strain energy density correlate very well with bone apposition (Webster et al., 2012). The difference between results almost certainly arises from the mechanism of loading. In our study we loaded our bones using muscle contraction, as opposed to a compressive

rig. Muscular contraction clearly detracts from the simplicity of the bone response. Previous studies have found that increased muscular activity does not alter the morphology of muscular attachment sites (Zumwalt, 2006). This discrepancy may be caused by bone being “tuned” to particular forces, so habitual loading, such as muscular contraction at a muscle origin, does not stimulate adaptive responses. It is well documented that “novel” loading regimes are more osteogenic than habitual regimes (Lanyon, 1996).

Conclusions

Implantable miniature neuromuscular stimulators are capable of transforming muscle and bone. The region of bone growth was found to be under high compressive strain during tibialis anterior contraction, but this was not the region of peak strain, which was the un-altered muscle attachment site. The altered tibial geometry significantly decreased strain within the antero-distal region of the tibia.

Summary

Here we present an *in vivo* model of musculoskeletal loading, and correlate it with a complex FE model, which acknowledges the contractile nature of muscular loading. No morphological change was observed at the muscle attachment site, despite it being the region of peak strain. A highly localised change in morphology was observed in the antero-distal region of the tibia, which was a region of high compressive strain. The observed change in morphology significantly reduces strains within this region, implying that it is a functional response. This region shows many cellular characteristics of fracture repair as opposed to bone modelling, despite a lack of visible damage in bone. Taken together this suggests that the morphological change observed fulfils a biomechanical role and effectively reduces strain within this region.

References

1. Blemker SS, Pinsky PM, Delp SL. 2005. A 3D model of muscle reveals the causes of nonuniform strains in the biceps brachii. *Journal of Biomechanics* 38: 657-665.
2. Jeffery NS, Stephenson RS, Gallagher JA, Jarvis JC, Cox PG. 2011. Micro-computed tomography with iodine staining resolves the arrangement of muscle fibres. *Journal of Biomechanics* 44: 189-192.
3. Kidd L, Stephens A, Kuliwaba J, Fazzalari N, Wu A, Forwood M. 2010. Temporal pattern of gene expression and histology of stress fracture healing. *Bone* 46: 369-378.
4. Lanyon LE. 1996. Using functional loading to influence bone mass and architecture: objectives, mechanisms, and relationship with estrogen of the mechanically adaptive process in bone. *Bone* 18: S37-S43.
5. Pullen A. 1977. The distribution and relative sizes of three histochemical fibre types in the rat tibialis anterior muscle. *Journal of Anatomy* 123:1.
6. Sutherland H, Jarvis JC, Kwende M, Gilroy SJ, Salmons S. 1998. The dose-related response of rabbit fast muscle to long-term low-frequency stimulation. *Muscle & Nerve* 21: 1632-1646.
7. Tomlinson RE, McKenzie JA, Schmieder AH, Wohl GR, Lanza GM, Silva MJ. 2012. Angiogenesis is required for stress fracture healing in rats. *Bone*.
8. Torcasio A, Zhang X, Duyck J, van Lenthe GH. 2012. 3D characterization of bone strains in the rat tibia loading model. *Biomech Model Mechanobiol* 11: 403-410.
9. Webster D, Wirth A, van Lenthe G, Müller R. 2012. Experimental and finite element analysis of the mouse caudal vertebrae loading model: prediction of cortical and trabecular bone adaptation. *Biomech Model Mechanobiol* 11: 221-230.
10. Zumwalt A. 2006. The effect of endurance exercise on the morphology of muscle attachment sites. *Journal of Experimental Biology* 209: 444-454.

TUMOR INFILTRATING LYMPHOCYTES AS PROGNOSTIC FACTOR OF EARLY RECCURENCE AND POOR PROGNOSIS OF COLORECTAL CANCER AFTER RADICAL SURGICAL TREATMENT

Ondřej Vyčítal

E-mail: vycitalo@volny.cz

Department of Surgery, Medical School and Teaching Hospital Plzen,
Charles University in Prague

Co-authors: Třeška Vladislav, Daum Ondřej, Novák Petr, Brůha Jan,
Pitule Pavel, Liška Václav

Tutor: MUDr. Václav Liška, Ph.D.

Introduction

Tumor infiltrating lymphocytes (TIL) were described as a good prognostic factor for patients with a high risk of relapse (1,2). The aim of this study was to analyse the relationship of contemporary clinical and histopathological factors and TIL to determine patients with a high risk of poor overall survival and tendency to early.

Methods

We analysed 150 patients who underwent radical surgical procedure for CRC between the years 2004-2007. The following clinical parameters were statistically analysed in relation to the disease free interval (DFI) and the overall survival (OS): staging, grading, preoperative leukocytosis, type of surgical procedure (radical vs. palliative), postoperative complications and postoperative oncological treatment. We evaluated endovascular (VI), endolymphatic (LI) and perineural infiltration (PI) by cancer cells. Lymphocytic infiltration was detected as intratumoral (ITL), intrastromal (ISL), peritumoral (PTL) and Crohn-like reaction (Crohn-like PTL). Reactive histological changes in lymph nodes (LN reactions) were detected as follicular hyperplasia (LN-FH), sinus histiocytosis (LN-SH) and the presence of granulomas (LN-GR). We examined also immunohistochemical positivity of lymphocytes for CD4 and CD8.

Results

The Spearman rank correlation coefficient did not prove any stronger correlation than a moderate correlation at LI and lymph node infiltration by metastatic process (Spearman rank correlation coefficient 0.56, $p < 0.05$). Lymph node infiltration, CD4+ lymphocytic infiltration and VI were proved as negative prognostic factors of shorter overall survival. The presence of PTL, Crohn-like PTL, LN-FH, CD8+ was proved as a positive prognostic factor of OS.

PI and lymph node infiltration were proved as a negative prognostic factor of an earlier recurrence. CD8+ lymphocytic infiltration was proved as a positive prognostic factor enlarging DFI. The Multivariate Cox Regression Hazard Model proved the combination of the severity of the lymph node infiltration by a metastatic process and the severity of CD8 positivity of infiltrating lymphocytes as the best prognostic factors for the prediction of risk of early recurrence and combination of the severity of lymph node infiltration by metastatic process and LN-FH as the best prognostic factors for the prediction of the risk of shorter overall survival.

Discussion

Our outcomes support the hypothesis that the adaptive immunological reaction in tumor tissue and lymph nodes can influence the behavior of CRC CD4 and CD8 positivity of ITL was demonstrated

as a crucial histopathological sign of tumor-specific immune response that could reflect the clinical situation and a tendency to relapse (CD4+) or the larger overall survival (CD8+)(3,4,5).

Conclusion/Summary

Tumor infiltrating lymphocytes seem to be promising prognostic factors that could find their use in colorectal surgery and consecutive oncological treatment (6) as an indicator of the type or combinations of therapies reflecting the risk of patients to early recurrence or poor overall survival.

References

1. Atreya, I., & Neurath, M. F. (2008). Immune cells in colorectal cancer: prognostic relevance and therapeutic strategies. *Expert Review of Anticancer Therapy*, Vol.8, No.4, (April 2008), 561-572, ISSN 1473-7140
2. Galon, J., Costes, A., Sanchez-Cabo, F., Kirilovsky, A., Mlecnik, B., Lagorce-Pagès, C., Tosolini, M., Camus, M., Berger, A., Wind, P., Zinzindohoué, F., Bruneval, P., Cugnenc, P. H., Trajanoski, Z., Fridman, W. H. & Pagès, F. (2006). Type, density, and location of immune cells within human colorectal tumors predict clinical outcome. *Science*, Vol.313, No.5795, (September 2006), 1960-1964, ISSN 0036-8075
3. Chiba, T., Ohtani, H., Mizoi, T., Naito, Y., Sato, E., Nagura, H., Ohuchi, A., Ohuchi, K., Shiiba, K., Kurokawa, Y. & Satomi, S. (2004). Intraepithelial CD8+ T-cell-count becomes a prognostic factor after a longer follow-up period in human colorectal carcinoma: possible association with suppression of micrometastasis. *British Journal of Cancer*, Vol.91, No.9, (November 2004), 1711-1717, ISSN 0007-0920
4. Koch, M., & Beckhove, P. (2006). Op den Winkel J et al. Tumor infiltrating T lymphocytes in colorectal cancer: Tumor-selective activation and cytotoxic activity in situ. *Annals of Surgery*, Vol.244, No.6, (December 2006), 986-992, ISSN 0003-4932
5. Pagès, F., Galon, J., Die-Nosjeanu, M. C., Tartour, E., & Sautes-Fridman, C. (2010). Immune infiltration in human tumors: a prognostic factor that should not be ignored. *Oncogene*, Vol.29, No.8, (February 2010), 1093-1102, ISSN 0950-9232.
6. Zbar, A. P. (2004) The immunology of colorectal cancer. *Surgical Oncology*, Vol.13, No.2-3, (August-November 2004), 45-53, ISSN 0960-7404

Acknowledgement

The project was supported by grants IGA MZ CR 12025 and 14329.

LIPOCALIN-2 DEACTIVATES MACROPHAGES AND WORSENS PNEUMOCOCCAL PNEUMONIA OUTCOMES

Joanna Maria Warszawska

E-mail: joanna.warszawska@meduniwien.ac.at

Dept. of Anaesthesia, General Intensive Care and Pain Management,
Medical University of Vienna

& Research Center for Molecular Medicine (C-e-M-M-), Vienna, Austria

Co-authors: R. Gawish, O. Sharif, S. Sigel, B. Doninger, K. Lakovits, I. Mesteri, M. Nairz,
L. Boon, A. Spiel, V. Fuhrmann, B. Strobl, M. Müller, P. Schenk, G. Weiss
Tutor: Prof. Dr. Sylvia Knapp, PhD

Introduction

Macrophages play a key role in responding to pathogens, and initiate an inflammatory response to combat microbial multiplication [1]. Deactivation of macrophages facilitates the resolution of the inflammatory response. Deactivated macrophages are characterized by an immunosuppressive phenotype, but the lack of unique markers that can reliably identify these cells explains the poorly defined biological role of this macrophage subset [2].

Lipocalin 2 (LCN2)[3], also known as neutrophil gelatinase-associated lipocalin (NGAL), is a mammalian protein expressed by myeloid and epithelial cells in response to Toll like receptor (TLR)-activation during infections. LCN2 scavenges a subset of bacterial siderophores, thereby restricting iron acquisition by bacteria such as *Escherichia coli* [4], *Klebsiella pneumoniae*[5] or mycobacteria[6]. However, *Streptococcus pneumoniae*, the most prevalent respiratory pathogen, does not depend on siderophores for iron acquisition. We and others found that *S. pneumoniae* induced remarkably high LCN2 levels in the respiratory tract [7]. This finding alerted us to the possibility of a siderophore-independent role of LCN2 within the pulmonary compartment. Upon analysis of the published LCN2 promoter [8] we noticed NF κ B binding sites, but also glucocorticoid response elements and several binding sites for transcription factors which are critically involved in the deactivation of macrophages. Considering that LCN2 may modulate inflammation, we hypothesized that LCN2 could play a role in macrophage deactivation and thereby impact host defense against pathogens such as *S. pneumoniae*.

Methods

Human subjects. Sixty-four intubated and mechanically ventilated ICU patients with suspected pneumonia, defined by the presence of new infiltrates in the chest X-ray were examined. Diagnosis of pneumonia was considered confirmed if microbiological assays revealed $>10^4$ CFU/ml of potentially pathogenic bacteria in the bronchoalveolar (BAL)-fluid. BAL samples were obtained via bronchoscopy and blood was withdrawn from ICU patients before bronchoscopy.

Murine pneumonia model. Pathogen-free 8-10 week old female C57BL/6 wild-type (WT) littermate and LCN2 $^{-/-}$ mice were used for experiments. *S. pneumoniae* serotype 3 was inoculated intranasally into anesthetized mice. Six, 24 or 48 hours post infection mice were sacrificed and blood, BAL and lung samples were collected for assessment of bacterial growth and inflammation (cytokine levels, cell influx, histology). IL-10 blocking in vivo: mice were administered 150 μ g of either anti-IL-10 or isotype Ab intranasally 15 min following *S. pneumoniae* infection.

Cell culture and stimulations. Primary cells (ex vivo isolated alveolar, bone marrow derived macrophages and primary epithelial cells) and the murine MH-S cell line were stimulated with cytokines (IFN γ , IL-4, IL-13, IL-10), dexamethasone, LCN2, heat inactivated bacteria and bacterial ligands.

Analysis of Lcn2 and inflammatory mediators. Expression of Lcn2 was assessed by flow cytometry.

Levels of secreted mediators were measured using specific ELISAs. Messenger RNA levels were quantified by RT-PCR.

Luciferase gene reporter assays. RAW264.7 cells overexpressing Lcn2 and GFP control cells were transiently transfected with an IL-10 reporter plasmid and stimulated 24h later with *S. pneumoniae*. Luminescence was assessed after 24h and normalized to renilla.

Results

We found that high LCN2 secretion is a feature of dexamethasone deactivated macrophages and a robust marker of IL-10 polarized alveolar macrophages. Comparing TLR-induced responses of WT and LCN2^{-/-} macrophages we observed that the absence of LCN2 resulted in M1 skewing which is associated with a sustained pro-inflammatory immune response. Concordantly, recombinant mouse Lcn2 dampened macrophage responses to TLR ligands, and overexpression and blocking studies disclosed that Lcn2 mediated these effects via IL-10 induction. In agreement, alveolar macrophages (AM) from WT mice infected with *S. pneumoniae* exhibited increased IL-10 and suppressed KC mRNA expression compared with LCN2^{-/-} AM.

Studying a murine pneumonia model, we found Lcn2^{-/-} mice to exhibit augmented bacterial clearance and consequently, accelerated resolution of lung inflammation and improved survival (Figure 1A), indicating a harmful role for LCN2. As an explanation for the improved host defense in LCN2^{-/-} animals, we found the early inflammatory response (6h after induction of pneumonia) to be exaggerated with a significantly increased neutrophil influx in LCN2^{-/-} animals. Blocking IL-10 in vivo confirmed that LCN2 impairs bacterial clearance in an IL-10 dependent manner.

Analyzing LCN2 concentrations in BAL-fluid and plasma of patients with suspected pneumonia we found significantly enhanced levels in patients with confirmed bacterial pneumonia which were further enhanced by inhaled glucocorticoid therapy. Intriguingly, siderophore-independent pathogens, such as *S. pneumoniae*, induced LCN2 as potently as siderophore-dependent bacteria. Finally, in accordance with murine data, high LCN2 levels in the BAL-fluid of ICU patients suffering from pneumonia caused by Gram-positive bacteria but not by Gram-negative bacteria were indicative for an adverse clinical outcome (Figure 1B).

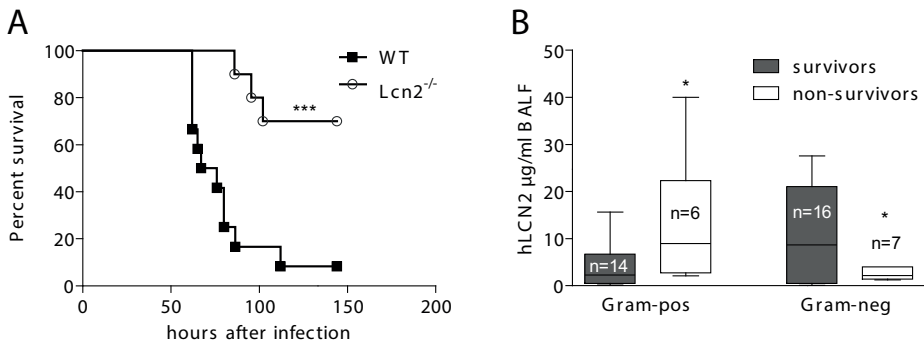


Figure 1. LCN2 exerts detrimental effects during pneumococcal pneumonia in mice and humans [9].

Discussion

The question remains why do host cells induce Lcn2 upon infection with siderophore-independent bacteria, if it is detrimental? Since we discovered a positive LCN2-IL-10 feedback loop in macrophages, we postulate that Lcn2 might provide a means to prevent overwhelming inflammation and promote tissue repair after clearance of infectious pathogens. This pathway might prove safe in uncomplicated infections, which is supported by a report demonstrating a pro-regenerative function for Lcn2 in a model of renal ischemia-reperfusion injury [10]. However, in ICU patients with severe pneumonia, elevated Lcn2 levels may be a result of an exaggerated immune response to higher bacterial concentrations. In this setting, elevated Lcn2 might deactivate macrophages and in turn prevent efficient bacterial clearance and aggravate the disease. In agreement, we report a worse outcome during severe pneumonia with Gram positive bacteria in ICU patients with elevated Lcn2 levels in the BAL. Corticosteroids can further enhance Lcn2 formation and macrophage deactivation, which is undesirable for the clearance of viable bacteria. Thus, the use of these drugs might be harmful during severe infections with siderophore-independent pathogens.

Conclusions

We identified LCN2 as both a marker of deactivated macrophages and a macrophage deactivator. We show that LCN2 attenuated the early inflammatory response and impaired bacterial clearance, leading to impaired survival of mice suffering from pneumococcal pneumonia. LCN2 induced IL-10 formation by macrophages, skewing macrophage polarization in a STAT3-dependent manner. Pulmonary LCN2 levels were tremendously elevated during bacterial pneumonia in humans and high LCN2 levels were indicative of a detrimental outcome from pneumonia with Gram-positive bacteria.

Summary

We postulate that LCN2 modulates the early inflammatory response upon *S. pneumoniae* infection through induction of IL-10 and deactivation of lung macrophages, which ultimately results in impaired bacterial clearance and survival.

References

1. Murray, P.J. and T.A. Wynn: Protective and pathogenic functions of macrophage subsets. *Nat Rev Immunol*; 2011, 723-37.
2. Gordon, S.: Alternative activation of macrophages. *Nat Rev Immunol*; 2003, 23-35.
3. Kjeldsen, L., et al.: Identification of neutrophil gelatinase-associated lipocalin as a novel matrix protein of specific granules in human neutrophils. *Blood*; 1994, 799-807.
4. Flo, T.H., et al.: Lipocalin 2 mediates an innate immune response to bacterial infection by sequestering iron. *Nature*; 2004, 917-21.
5. Chan, Y.R., et al.: Lipocalin 2 is required for pulmonary host defense against *Klebsiella* infection. *J Immunol*; 2009, 4947-56.
6. Saiga, H., et al.: Lipocalin 2- dependent inhibition of mycobacterial growth in alveolar epithelium. *J Immunol*; 2008, 8521-7.
7. Nelson, A.L., et al.: Bacterial colonization of nasal mucosa induces expression of siderocalin, an iron-sequestering component of innate immunity. *Cell Microbiol*; 2005, 1404-17.
8. Park, S., et al.: Identification of 24p3 as a direct target of Foxo3a regulated by interleukin-3 through the phosphoinositide 3-kinase/Akt pathway. *J Biol Chem*; 2009, 2187-93.
9. Warszawska, J.M., et al.: Lipocalin 2 deactivates macrophages and worsens pneumococcal pneumonia outcomes. *J Clin Invest*; 2013.
10. Jung, M., et al.: Infusion of IL-10-expressing cells protects against renal ischemia through induction of lipocalin-2. *Kidney Int*; 2012, 969-82.

PLATELET AND PLATELET-DERIVED MICROPARTICLE STUDIES IN SEVERE SEPSIS

Gábor László Woth

Email:glwoth@gmail.com

Department of Anaesthesiology and Intensive Therapy
and Department of Laboratory Medicine,
University of Pécs, Pécs, Hungary

Tutors: Gábor L. Kovács MD, PhD, DSc., Diana Mühl, MD, PhD

Introduction

Severe sepsis and septic shock are leading causes of in-hospital. We aimed to assess the contribution of platelets and microparticles in the pathophysiology severe sepsis. Platelets are well known contributors of haemostasis and also have an immunomodulatory role. The first description of microparticles (MPs) came from Wolf in 1967, who first noted them as platelet-dust. He proved their procoagulant activity and that this feature is removable by ultracentrifugation. During cell activation, apoptosis or increased shear stress the presence of phosphatidylserine (PS) in the outer leaflet is one of the first signs of this process. According to the “classical” view of MPs production, intracellular Ca^{2+} increase is the main determinant of MP formation. Calcium-induced degradation of cytoskeleton by calpains and the transient mass difference between membrane leaflets support the formation of MPs and Ca^{2+} influx following cell activation may inhibit flippase and activate floppase enzymatic activity. Outer membrane composition of MPs in the circulation of mainly platelet origin consists of cholesterol (about 60%), sphingomyelin, phosphatidylethanolamine and PS.

The aim of our first study was to determine whether spontaneous aggregation of platelets is present in the circulation of severe septic patients and if it may determine the outcome of severe sepsis. As the source pathogen may define the pathophysiology of sepsis our second study aimed to determine if microparticle profiling can help the choice of early antimycotic treatment. In our third study we were interested if microparticles are involved in the development of sepsis-related organ failures.

Methods

Our patient inclusion criteria were recently discovered severe sepsis (within 24 hours) with two or more sepsis-related organ dysfunctions and procalcitonin levels above 2 ng/ml, and 5 ng/ml in the infection source MP study. In our studies patients in moribund state or with any kind of haematological baseline disease such as myeloproliferative disorders like lymphoma or leukaemia, cytostatic treatment in the last 30 days, high dose prolonged steroid medication, patients with disseminated intravascular coagulation score >5 , drugs known to alter platelet functions (i.e. acetylsalicylic acid), platelet transfusion during the study period were excluded. Platelet tests were carried out using the Carat TX4 light transmission aggregometer using adrenaline (ADR, 10 μ mol), ADP (10 μ mol), collagen (COL, 2 μ g/ml) and normal saline (SAL) as inductors. Microparticles were isolated by multiple centrifugation steps. Surface PS was labelled by annexin V, specific antigens were labelled by fluorescent monoclonal antibodies. Constitutively expressed platelet fibrinogen receptor subunits, GPIIb-IIIa were measured by the CD41 and CD61 antibodies respectively. Fibrinogen binding active form was assessed by the PAC1 antibody. Platelet adhesion receptor glycoprotein GPIb-V-IX has been tested with CD42a labelling. For microbiological assessment we used standard blood cultures. Acute sepsis-related kidney injury was defined by the Injury category of the RIFLE criteria (serum creatinine normal $\times 2$, $>50\%$ deteriorated filtration rate, or urine production <0.5 ml/bwkg/h).

Results

Forty-five patients were included in our platelet aggregation study. Fourteen patients deceased during our study and 31 patients built up the survival group. Non-survivors showed no significant deterioration in platelet count ($p > 0.05$). All induced and saline aggregation measurement results, when compared to survivors were not significantly different in non-survivors. The spontaneous aggregation group (14 patients) revealed a non-significant difference in platelet counts compared to the non-spontaneous aggregation group. The non-spontaneous aggregation group showed a significantly higher, but constantly decreasing procalcitonin levels on the 1st, 3rd, 4th consecutive days. Lactate levels were also non-significantly lower in the spontaneous aggregative patients during our study.

During our first microparticle study 33 patients were enrolled. Six patients comprised the mixed fungal septic group and 27 patients were in the non-fungal septic group. Microbiological identification proved *Candida albicans* in all six fungal septic patients. Upon admission annexin V⁺ MPs and CD41⁺ MPs were elevated in both the mixed fungal and in the non-fungal septic group compared to volunteers. While CD42a⁺ MP numbers were negligible in non-fungal and control groups, mixed fungal septic patients showed significantly elevated numbers in all measurements with an elevation until day 5 ($p < 0.05$). Mixed fungal septic patients showed significantly elevated numbers of PAC1⁺ MPs in the 1st and 5th study days compared to non-fungal septic patients ($p < 0.05$).

In our second study ($n = 37$) we focused on the presence of various organ dysfunctions and the connection with microparticle profile. Although patients presented a wide variety of total MP numbers, patients with renal injury showed significantly increased MP numbers on inclusion and a slight decrease of MP numbers on day 3. Patients without renal injury had a continuous elevation of MP numbers during our study period ($p < 0.05$). Patients without renal injury showed a steady non-significant increase of CD41⁺ particles, while sepsis-related renal injury patients had elevated CD41⁺ MP numbers on admission already. Also, CD13⁺ particles were significantly elevated on admission in patients with renal impairment ($p < 0.05$) and patients without renal failure showed elevating MP numbers.

Discussion and conclusions

Studies have not assessed the use of saline as an alternative for the measurement of spontaneous aggregation in severely septic patients. Increased procalcitonin and increased lactate levels in the non-spontaneous group hypothesise that members of this group may have a more severe state compared to the spontaneous group. Our data support the model of increased numbers of platelet MPs compared to volunteers in sepsis. We have shown that compared to severe bacterial sepsis, severe sepsis with fungal infection contributes to more increased platelet MP levels in our multidisciplinary intensive care unit setting. We believe our MP measurement based on PAC1⁺ and CD42a⁺ PMP measurements can provide valuable additional information on mixed fungal sepsis prone patients following the admission to the intensive care unit. After the assessment on the effect of various organ failures on MPs, patients with renal dysfunction on study inclusion showed overall MP, platelet MP and myeloid MP increase. The activation of the innate immune system and infiltration of the kidney by monocytes and macrophages contributes to sepsis-related renal failure. Monocyte-derived microparticles are a main source of blood-born tissue factor and carry high amounts of PS. Elevation of these microparticles can cause increased clot formation and obstructions in kidney vessels.

Summary

Our study was the first to provide evidence on the presence of increased spontaneous platelet aggregation in severe septic patients. We provided further evidence on increased MP levels in severe sepsis. Our clinical study was the first which showed the MP profile difference in patients with severe sepsis complicated with fungal (*C. albicans*) infection. This finding could help the development of a future early diagnostic test based on MPs. Our novel approach revealed that there is no direct connection between the number of organ failures and MP numbers. Data from our second study support the contribution of MPs in the development of sepsis-related acute kidney injury.

References

1. Tőkés-Füzesi M, Woth G, Emyey B, et al.: Microparticles and acute renal dysfunction in septic patients. *J Crit Care.* 2013; 28(2), 141-147.
2. Woth G, Tőkés-Füzesi M, Magyarlaki T, et al.: Activated platelet-derived microparticle numbers are elevated in patients with severe fungal (*Candida albicans*) sepsis. *Ann Clin Biochem.* 2012; 49(Pt 6), 554-560.

INDEX

Agrawal Khushboo	12
Blekic Mario	16
Erjavec Igor	20
Farkašová Anna	24
Fontana Josef	25
Heřmanová Ivana	29
Horváth Gabor	33
Janoušová Eva	37
Jedličková Lucia	41
Kratochvílová Hana	43
Křivánek Jan	45
Kupsa Tomáš	49
Láníková Lucie	52
Mezera Vojtěch	55
Paulů Petra	57
Pawlica-Gosiewska Dorota	60
Pejchal Jaroslav	64
Pereira Bruno Miguel Correia	70
Pöpperlová Anna	74
Richardson Siân Helen Rose	77
Šalovská Barbora	82
Shatirishvili Teona	85
Scharffenberg Martin	90
Schneider Hannah	94
Sousa Maria Mafalda	97
Thiem Ursula	100
Vickerton Paula	103
Vyčítal Ondřej	107
Warszawska Joanna Maria	109
Woth Gábor László	112

Vydala: Univerzita Karlova v Praze, Lékařská fakulta v Hradci Králové
prof. MUDr. RNDr. Miroslav Červinka, CSc., Ing. Miloslava Paterová
Sazba: TAH reklamní agentura, s.r.o. Hradec Králové, Jiří Vecheta

2013